UNIVERSITÄT PADERBORN

Die Universität der Informationsgesellschaft

Stimuli-responsive self-accelerating polymers for drug delivery systems

---

Dissertation

Zur Erlangung des akademischen Grades

Doktor rerum naturalium

(Dr. rer. nat.)

---

vorgelegt

der Fakultät der Naturwissenschaften

der Universität Paderborn

eingereicht von

M. Sc. Dimitri Jung

geboren am 13. Oktober 1991 in Talas

Abstract

One of the most crucial factors in an efficient and effective therapy is the application of highly potent drugs at the target site while reducing the drug concentration in the rest of the body. Many potent drugs have severe adverse side-effects at non-targeted sites. To overcome this challenge, the drugs can be encapsulated in a polymeric nanoparticle. By introducing a stimuli-responsive moiety into the polymers, the nanoparticles can react to their environment and even release their cargo by degradation upon a suitable stimulus. In this work, polymers were synthesized which degrade after the application of the chosen stimuli: light-irradiation, redox-environment and drop in environmental pH-value. The last two triggers are present in tumor environment. A polyester, a polycarbonate and two polyurethanes were synthesized to address the external trigger light. Three polyurethanes were synthesized to address the overexpression of glutathione and two polyurethanes were synthesized to address the drop in the environmental pH-value. The monomers, polymers and their degradation were characterized by NMR spectroscopy, UV/Vis spectroscopy and SEC. Nanoparticles were formulated of one of the light-responsive polymers and their application in an drug delivery system for cancer treatment was evaluated by photon correlation spectroscopy, HPLC and different cell viability assays.

Kurzzusammenfassung

Einer der wichtigsten Faktoren für eine effiziente und effektive Therapie ist die Anwendung hochpotenter Medikamente am Zielort bei gleichzeitiger Reduzierung der Medikamentenkonzentration im restlichen Körper. Viele hochwirksame Medikamente haben schwere Nebenwirkungen an nicht zielgerichteten Stellen. Um diese Herausforderung zu überwinden, können die Medikamente in einem Polymernanopartikel eingekapselt werden. Durch das Einfügen einer stimuli-responsiven Gruppe in die Polymerseitenkette können die Nanopartikel auf ihre Umgebung reagieren und sogar ihre Ladung durch Abbau bei einem geeigneten Stimulus freisetzen. In dieser Arbeit wurden Polymere synthetisiert, die sich nach Einwirkung der gewählten Stimuli abbauen: Lichtbestrahlung, Redox-Umgebung und Absinken des pH-Wertes in der Umgebung. Die letzten beiden Auslöser sind in der Tumorumgebung vorhanden. Ein Polyester, ein Polycarbonat und zwei Polyurethane wurden synthetisiert, um den externen Reiz Licht anzusprechen. Drei Polyurethane wurden synthetisiert, um auf die Überexpression von Glutathion zu reagieren und zwei Polyurethane wurden synthetisiert, um auf den Abfall des pH-Wertes in der Umgebung zu reagieren. Die Monomere, Polymere und deren Abbau wurden mittels NMR-Spektroskopie, UV/Vis-Spektroskopie und SEC charakterisiert. Aus einem der lichtempfindlichen Polymere wurden Nanopartikel formuliert und ihre Eignung als Drug-Delivery-System zur Krebsbehandlung mit Hilfe von Photonen-korrelationsspektroskopie, HPLC und verschiedene Zellviabilitätsassays evaluiert.

Table of contents

1 Introduction

1.1 Statement of the problem

For several decades one of the major death causes in developed countries and the second leading cause of death in developing countries is cancer.[1] Since 1999, the number of yearly cases of cancer is steadily increasing from 8.1 million estimated cases (1999) to 19.3 million estimated cases (2020).[2–5] The first publication of "cancer statistics" in the "CA: A Cancer Journal for Clinicians" from American Cancer Society (Wiley) presents cancer statistics in the USA and dates back to 1970.[6] Cancer poses a steadily increasing threat in both economically developed countries and developing countries. The death rate of the global cancer cases of 2020 is 51.6%, compared to the death rate of 64.1% in1999.[2,5] Although the death rate was lowered, the impact of 20 years of cancer studies is still small.

The most common cancer treatment methods are radiation therapy,[7] chemotherapy,[8] radiochemotherapy,[9,10] photodynamic therapy (PDT),[11,12] immunotherapy[13–15] and stem cell transplantation.[16,17] Often, a combination of these methods is needed to provide a curative healing. If chemical agents are used as in chemotherapy or PDT, a new challenge arises.[18–20] The therapeutic agent needs to be present at the tumor site in a high concentration to have the highest efficiency. However, most therapeutic agents distribute through the body due to their physicochemical properties like charge, hydrophobicity and size.[21] Even with this passive distribution a higher accumulation of therapeutic agents in cancerous tissue is achieved due to the enhanced permeability and retention (EPR) effect.[22]

To further increase the concentration of the therapeutic agent in cancerous tissue and simultaneously lower the concentration outside of the target site, the use of nanoparticular drug delivery systems (DDS) is necessary.[23] By utilizing DDS, it is possible to deliver a therapeutic agent, which can also be a highly toxic substance like doxorubicin, into cancerous tissue without releasing it into healthy tissue to prevent adverse drug effects.[24–26] DDS can be based on different materials in the range of several nanometers to 100 µm.[27] The nano- or micro-sized architectures that can be used as DDS are amongst others inorganic nanoparticles (NPs),[28–30] polymeric NPs,[31–33] vesicles,[34–36] micelles[37–39] and nano- and microgels.[40–43]

Some properties of the cancer tissue can be used for a targeted release. The cancer cells overexpress glutathione to protect themselves against oxidation and cell damage.[44,45] Another characteristic of cancer tissue is the lower pH (5.8-7.4, or even lower) compared to the healthy environment (7.4).[46–48] These and other characteristics can be used for targeted drug delivery as long as they differ from the healthy tissue.

1.2 Motivation and goal of the present work

The aim of the work is the synthesis of a polymer that is the base for polymeric DDS having the potential to carry an anticancer drug to the desired site and release the drug in a controlled fashion. Furthermore, the polymeric DDS needs to degrade into smaller polymeric or oligomeric molecules (in the best case into small molecules). Many DDS release the drug without decomposing the DDS itself. The empty nanoparticular DDS will travel through the body and has the potential to accumulate in the liver, spleen, kidney and many more organs. To prevent this, the desired DDS needs to decompose and release the cargo at a desired time and location. This can be achieved by a self-accelerating stimuli-responsive polymer as a base for the polymeric DDS. After the application of the corresponding trigger, the polymer can degrade and release the cargo.

One method to introduce a chemical or physical handle into a polymer is the implementation of a responsive group into the repeating unit. There are two sites, where the responsive unit can be implemented: the side-chain of a polymerizable unit or in the backbone as the polymerizable unit.

A facile way to obtain a monomer with a responsive group is to modify and activate the responsive group to subsequently couple it to a polymerizable unit (diol for polyadditions and polycondensations or e.g., a six-membered cyclic carbonate for ring opening polymerization). That polymerizable unit bears an additional nucleophile (amine, thiol or alcohol). The activated responsive unit is coupled to the nucleophile of the polymerizable unit resulting in the synthesis of the monomer. The strategy for this work was the protection of a nucleophile in the side chain with a stimuli-responsive protecting group. After the application of the corresponding trigger and the subsequent deprotection of the nucleophile, the nucleophile can backbite into polymer backbone and cleave a bond in the

main chain resulting in the reduction of the polymer mass. This only takes place, if the polymer is a polycarbonate, polyester or polyurethane. The electrophilic carbon in the ester, carbonate, urethane or carbamate group is an appropriate site where the liberated nucleophile can attack and replace an aliphatic alcohol or amine group leading to the cleavage of the polymer.

Dependent on the manner of the responsive group, suitable polymerizable units are serinol (two alcohol groups, one amine group), pentaerythritol (four alcohol groups), trimethylolethane (three alcohol groups) and thioglycerol (two alcohol groups, one thiol group). The protecting groups were chosen to respond to one of two internal triggers (acidic pH-value or reductive molecules like glutathione) or an external trigger that can be precisely controlled (light). After monomer synthesis and polymerization, the polymer is analyzed by ultraviolet/visible (UV/Vis) spectroscopy, size exclusion chromatography (SEC) and nuclear magnetic resonance (NMR) spectroscopy. NPs were formulated out of one polymer and were analyzed by photon correlation spectroscopy (PCS) to obtain the hydrodynamic radius. The polymers were then triggered and the degradation was analyzed by the same methods. The anticancer properties of the NPs were evaluated by HPLC and cell viability assays.

2 Theoretical background

2.1 Smart drug delivery systems

Drug delivery describes the method or process that facilitates the administration of pharmaceutical compounds to achieve or enhance the therapeutic effect in living beings.[49,50] This major research field emerged in the late 1980s.[51] In a publication by *R. Langer*, the five biggest advantages of drug delivery are described, namely the improvement, safety and efficacy of drugs, delivery of complex drugs and proteins, awareness of different release patterns on efficacy, cost-saving of drug delivery systems, versatility and new methods of drug delivery. DDS are predominantly based on polymeric nanoparticles (NPs), liposomes, organic-inorganic hybrid NPs and exosomes.[52–54] If a DDS can react to a certain stimulus leading to the release of the cargo, the type of DDS can be summarized as responsive or smart DDS.[55–57] There are a number of smart polymeric DDS that react to different stimuli like a change in the pH,[58–60] redox-conditions,[61–63] temperature,[64–66] light,[67–69] electrical field,[70–72] magnetic field[73–75] and ultrasound.[76–78] These externally triggered polymeric DDS are one of the three major DDS categories that are diffusion-controlled DDS, solvent-activated DDS and chemically controlled DDS.[79,80]

By choosing the right DDS architecture, problems that arise because of the physicochemical properties of therapeutical drugs can be overcome. To these problems count poor drug solubility, damage due to cytotoxic drugs, rapid *in vivo* breakdown of the drug, poor biodistribution and the lack of selectivity for the targeted site.[81] Possible polymeric DDS architectures to address these problems include liposomes,[82,83] vesicles,[84,85] micelles,[86,87] condensed NPs.[88,89] A scheme of a micelle, a vesicle and a condensed NP is shown in *Figure 1*.
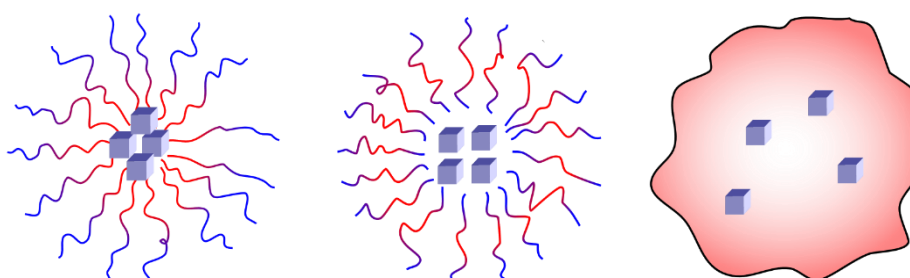
Figure 1: Scheme of a micelle (left), vesicle (middle) and condensed NP (right).

There are only few U.S. Food and Drug Administration (FDA) approved DDS based on vesicles, micelles and NPs. Some examples with the date of approval are Genexol-PM® (paclitaxel-loaded polymeric micelle, already marketed in Europe and South Korea, 2006), DaunoXome® (liposome-encapsulated doxorubicin, 2000), Amphotec® (Amphotericin B loaded lipid NP, 1996) and Myocet® (liposomal doxorubicin, 2000).[90–92] However, these DDS are not stimuli-responsive. There are different kinds of molecular changes in a stimuli-responsive polymeric material. A stimulus can induce two major kinds of responses , a conformational change and an environmental change.[93]

The biggest group of polymers that undergo environmental changes (hydrophilic to hydrophobic) are temperature-responsive polymers. The main thermo-responsive polymers with a lower critical solution temperature (LCST) are poly(vinyl methyl ether) (PVME), poly(*N*-isopropylacrylamide) (PNIPAAM) and poly(N-vinyl caprolactam) (PVCL) (*Scheme 1*).[94,95]
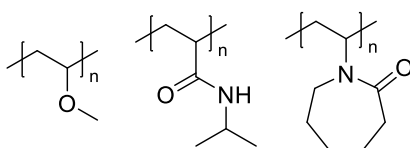
Scheme 1: Examples of polymers with an LCST: poly(vinyl methyl ether) (left), poly(N-isopropylacrylamide) (middle) and poly(N-vinyl caprolactam) (right).

Polymers with thermo-responsive groups can either dissolve (or mix from a two-phase system to one phase) with a rise in temperature due to the upper critical solution temperature (UCST) or undergo the same change, but after lowering the temperature (LCST). Thermo-responsive DDS that carry cargo will release the cargo at the moment the critical solution temperature is overcome and by the dissolution or precipitation of the DDS, the cargo is released. Temperature is a suitable trigger for a DDS to treat cancer as hyperthermia is one of the methods in cancer therapy.[96,97] In this method, the tissue is heated to over 40 °C. At this temperature the cancer cell gets damaged, but the normal tissue survives. By applying thermo-responsive DDS this effect can be enhanced, because the cancer tissue is additionally attacked by the released drug.[98,99]

In this work, the other main group of stimuli-response is utilized; polymers that undergo conformational change after applying a stimulus. Suitable triggers for these conformational changes are light, redox conditions, pH-value, temperature,

mechanical stress and others.[100–107] Typical responsive groups are: *ortho*-nitrobenzyl alcohols (light), disulfide bonds (redox), *para*-nitrobenzyl alcohols (redox), imines (pH), acetals (pH) and silyl ethers (pH). Examples are given in *Scheme 2*.[108]
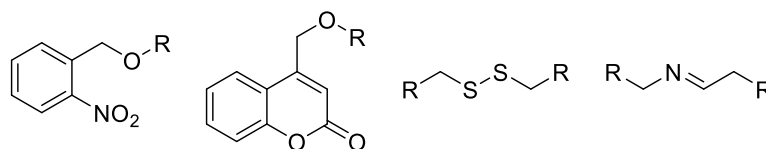
Scheme 2: Stimuli-responsive groups: a) ortho-nitrobenzyl alcohol, b) coumarin, c) disulfide bond, d) imine.

Polymers in which these groups or similarly modified groups are incorporated undergo bond cleavage upon the application of the corresponding stimulus. This cleavage leads directly or indirectly to the cleavage in the polymer backbone, thus the reduction of the polymer molar mass. When a DDS (e.g., a polymeric NP) is consists of these polymers, the application of the stimulus triggers the degradation of the DDS, leading to the release of the cargo (*Figure 2*).
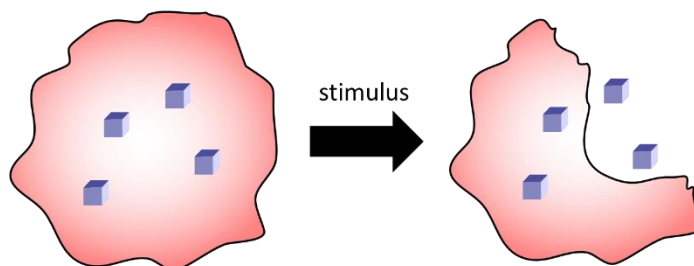
Figure 2: Drug release of a responsive polymeric NP.

The particle can enter the cancerous tissue due to the EPR effect and the released cargo is not spread throughout the whole body.[109] The drug concentration inside the cancer tissue is elevated and the therapy can be more efficient.

2.2 Polymerization methods

To achieve a DDS that is based on a stimuli-responsive polymer, different monomer architectures can be used. There are a handful of different types of polymers (homopolymers, copolymers: random, alternating and block copolymers) that can be achieved by different types of monomers.[110,111] Two major types of polymerization techniques exist; step-growth polymerization and

chain growth polymerization which will be described in the following chapters.[112,113]

2.2.1 Chain-growth polymerization

Chain-growth polymerization is made up of five major classes: radical polymerization,[114] living polymerization,[115] ring-opening polymerization,[116] ionic polymerization[117] and reversible deactivation polymerization.[118] In the chain-growth polymerization the polymerization mechanism can be summarized in three steps: chain initiation, chain propagation and chain termination. The chain initiation describes the generation of a chain carrier (e.g., a radical, an ion) that can undergo chain propagation. In the chain propagation the active center adds a monomer which results in the growing of the polymer chain and the propagation of the radical or charge to the newly added group. The propagation continuous until the whole monomer is consumed or the polymerization is terminated. The chain termination describes the disappearance of active centers due to e.g., combination reactions. With certain methods it is possible to gain a high degree of control over the polymerization. Generally, controlled radical polymerizations (CRP) include atom transfer radical polymerization (ATRP),[119,120] nitroxide-mediated radical polymerization (NMP),[121,122] reversible addition-fragmentation chain transfer polymerization (RAFT)[123,124] and ring-opening polymerization (ROP).[125,126] Classic examples of monomers for chain-growth polymerizations are depicted in *Scheme 3*.
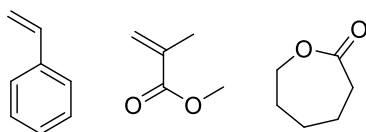
Scheme 3: Monomers for chain-growth polymerizations: styrene (left), methyl methacrylate (middle) and ε-caprolactone (right).

The first two examples depict vinyl compounds that are polymerized by the addition of another molecule and yield aliphatic polymers without functional groups in the backbone and the last example depicts a cyclic ester that opens up during the polymerization (ROP) and yields a polyester.

2.2.2 Step-growth polymerization

In contrast to the chain-growth polymerization, the step-growth polymerization involves bi- or multifunctional monomers. For a linear polymer it is necessary to have monomers which have only two different active groups that react to each other (e.g., acids and amines). Therefore, two different monomers bearing one kind of reactive group can be used to form an AB-type polymer. Normally, reactions occur between nucleophilic groups (e.g., alcohols and amines) with electrophilic groups (e.g., acids, acid chlorides, isocyanates). Examples of monomers with these groups are depicted in *Scheme 4*.
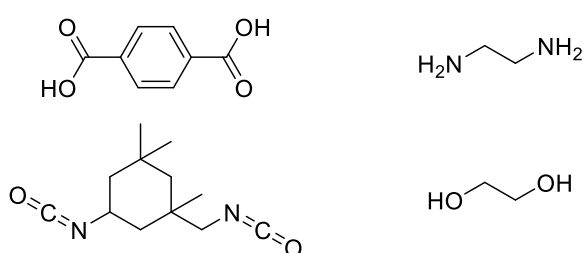
Scheme 4:   Electrophilic   and   nucleophilic   monomers   for   step-growth polymerizations: terephthalic acid (top left) and isophorone diisocyanate (bottom left), ethylene diamine (top right) and ethylene glycol (bottom right).

The main polymerization types for step-growth polymerizations are polyadditions (e.g., with isocyanates and diols) and polycondensations (e.g., with acids or acid halides and diols). Polyurethanes are generally prepared by polyaddition reactions between diisocyanates and diamines (polyurea) or diols. Polyesters, polyamides and polycarbonates are usually prepared by polycondensation reactions with either diols or diamines and acid halides or triphosgene. Typical examples of polyurethanes, polyamides, polyesters and polycarbonates are given in *Scheme 5*.
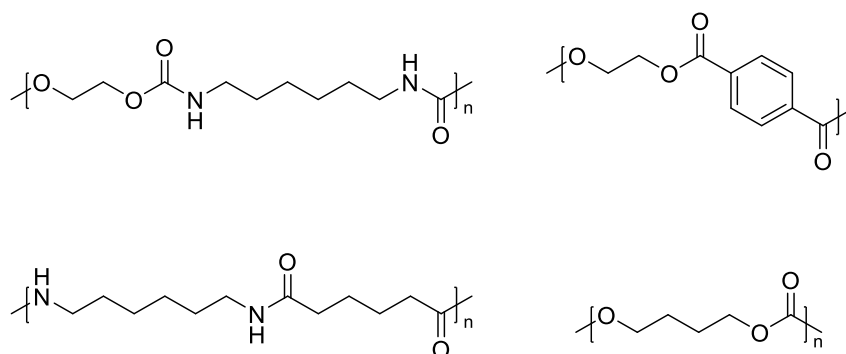
Scheme 5: Examples of polymers obtained via step-growth polymerization: polyurethane (top left), polyester (top right), polyamide (bottom left) and polycarbonate (bottom right).

However, polycarbonates, polyesters and polyamides can also be synthesized by chain-growth polymerization by using cyclic monomers e.g., trimethylene carbonate, lactones and lactames.

2.3   Light-degradable polymers

Light is a widely used trigger due to its extraordinary spatial and temporal precision.[106] Combined with the photodynamic therapy, light can be an attractive trigger for stimuli-accelerated polymeric drug delivery systems in the therapy of e.g., cancer. However, there are some difficulties regarding the application of light-responsive polymers like the wavelength dependency of the light penetration depth. Light of a higher wavelength can penetrate deeper into the tissue compared to light of a smaller wavelength while causing less tissue damage. To address this, small endoscopic light sources can be used locally at the disease-site to employ light of smaller wavelength. Among the many different light-responsive protecting groups, there are two major systems that are primarily used: coumarins as well as *ortho*-nitrobenzyl alcohols (*o*NB) and their derivatives (*Scheme 2*).

By modifying the available sites, it is possible to change the absorbance maxima, quantum yield and insert additional chemical handles. These moieties can be built into the backbone to achieve direct cleavage of the polymer backbone, or they can be implemented as a side group to liberate a backbiting functionality and subsequently degrade the polymer. Another possibility is the implementation as a light-responsive end-cap for self-accelerated depolymerization of polymers. In

this case, the polymer will degrade in a domino-like cascade reaction after the deprotection of the end-cap. Self-accelerated stimuli-responsive polymeric drug delivery is a recent field and therefore only few systems made it into *in vivo* or *in vitro* applications. DiLauro *et al.* had an interesting attempt for a trigger-induced self-immolative polymer.[127] They prepared a poly(phthalaldehyde) out of 1,2-benzenedicarboxyaldehyde with *ortho*-nitrobenzyl alcohol as an initiator leading to an *o*NB end-capped polymer. Upon irradiation with a UV floodlight for 10 min, the degradation took place in solution as well as in solid state. After submerging the film in ethyl acetate, the previously insoluble film quickly dissolved indicating the complete degradation to 1,2-benzene dicarboxyaldehyde. As a proof of principle, a silane-end-capped poly(phthalaldehyde) was treated in the same way and was still insoluble in ethyl acetate, suggesting that the photochemical cleavage was due to the *o*NB-moiety. However, this promising attempt was not used for drug delivery. Sun *et al.* produced a number of stimuli-accelerated polycarbonates, polyesters and polyurethanes.[128–130] Upon irradiation, the photoresponsive unit was removed and a nucleophile was liberated that subsequently backbit into the backbone degrading the polymer into small molecules. The monomers were designed starting from small molecules like 2-(hydroxymethyl)-2-methylpropane-1,3-diol. After substituting one of the hydroxy groups with an amine, the activated light-responsive unit was coupled to the polymerizable unit *via* a carbamate function (*Scheme 6*).
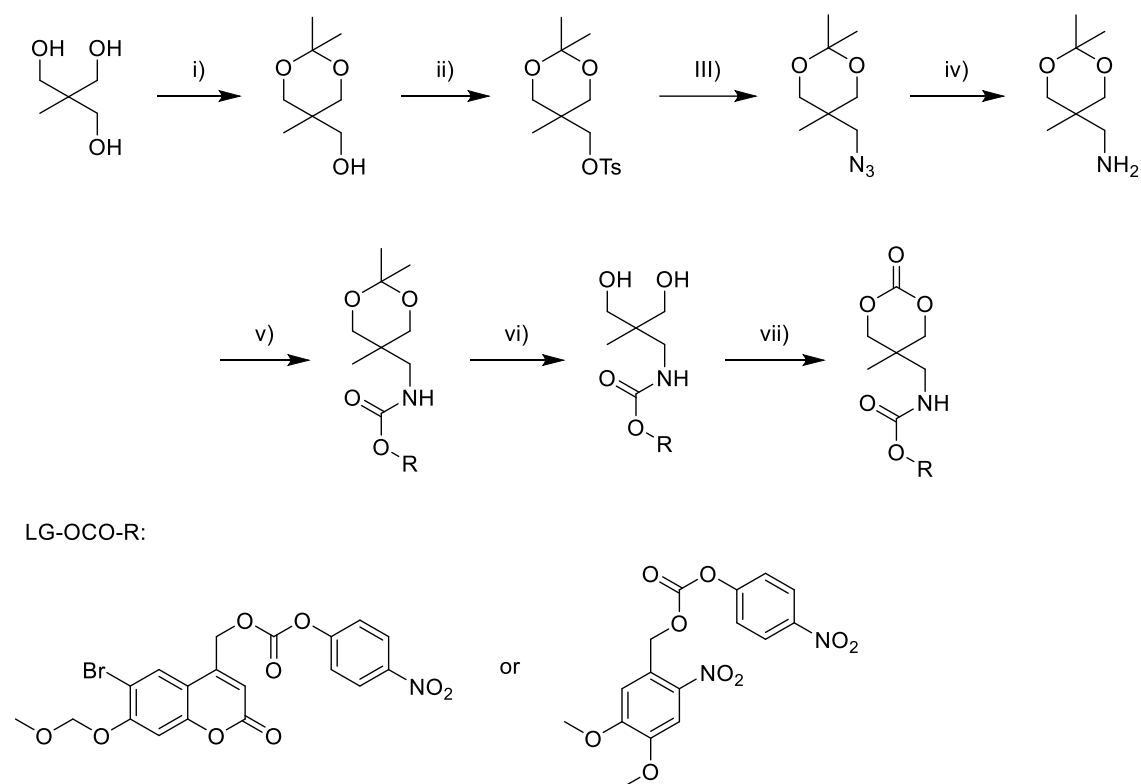
Scheme 6: Synthetic route for a light-responsive monomer: (i) acetone, TsOH, rt, 20 h; (ii) TsCl, pyridine, rt, 30 min → 100 °C, 40 min; (iii) NaN3, DMF/H2O (10/1), 68 h, 100 °C; (iv) ammonium formate, Pd/C, MeOH, rt, 4 h; (v) LG-OCO-R, TEA, MeCN, rt, overnight; (vi) THF/1 N HCl (1/1), rt, overnight; (vii) ethyl chloroformate, TEA, THF, 0 °C → rt, overnight.

In later studies, the extensive monomer synthesis was drastically shortened to two steps using the amine diol serinol, which is based on the amino-acid serine (*Scheme 7*).
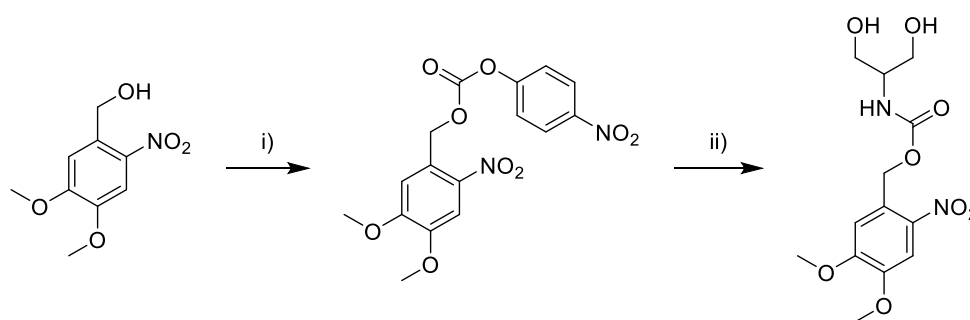
Scheme 7: Synthetic route of the light-responsive diol: i) 4-nitrophenyl chloroformate, DIPEA, DCM, rt, overnight, 91%; ii) serinol, TEA, MeCN, rt, overnight

Polycarbonates were synthesized by ring-opening-polymerization (ROP) of the cyclic carbonate or polycondensation with triphosgene and the diol. Furthermore, polyesters were synthesized using polycondensation of the diol with adipoyl

chloride.[131] One of these systems was formulated as nanoparticles and even evaluated for a controlled drug release *in vitro*.[132]

2.4   Redox-degradable polymers

Redox-responsive drug delivery systems are highly suitable for the therapy of cancer. To protect itself from oxidative cell damage, the cancer tissue overexpresses glutathione. This defense mechanism can be utilized by redox-responsive drug delivery systems. The most common redox-responsive moiety is the disulfide-bond. This bond is sensitive to reducing agents like glutathione and Cleland's reagent. Two glutathione molecules can convert a disulfide bond into thiols undergoing dimerization. The Cleland's reagent cleaves the disulfide bond by undergoing intramolecular cyclization (*Scheme 8*).
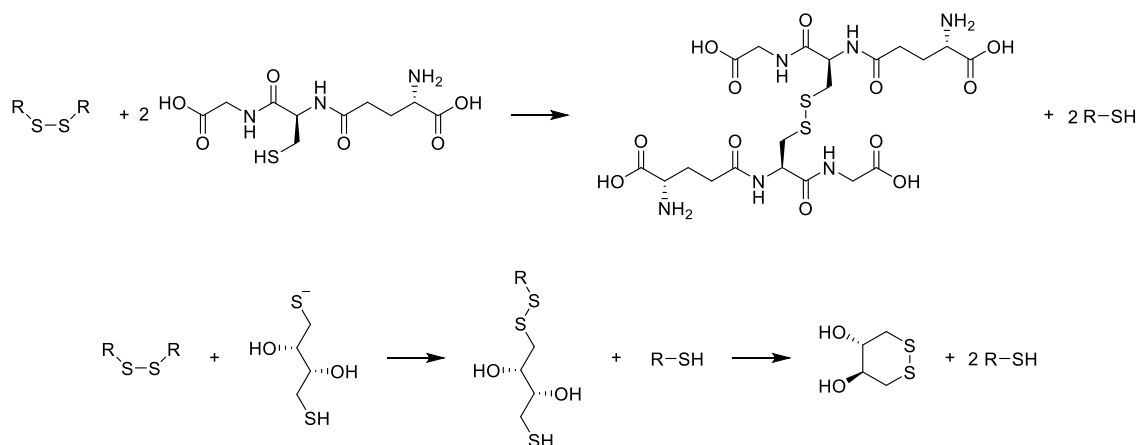
Scheme 8: Disulfide cleaving of glutathione (top) and Cleland's reagent (bottom).

Xia *et al.* developed a core-crosslinked micellar drug delivery system that consists of a polycarbonate backbone with redox-responsive side groups.[133] The redox-responsive groups (lipoic acid with azide functionality) were 'clicked' to the alkine-containing polycarbonate and micelles were formed, loaded with doxorubicin and core-crosslinked with Cleland's reagent in subsequent steps (*Scheme 9*).
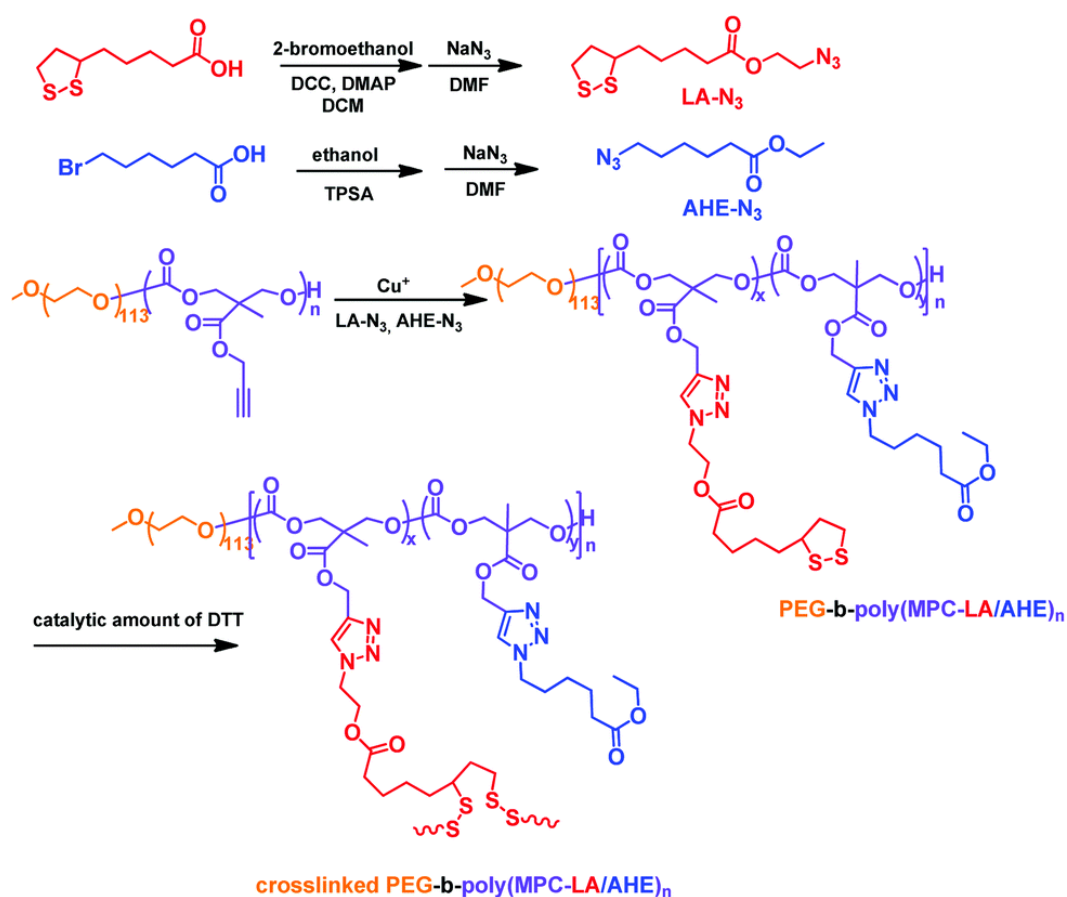
Scheme 9: Synthesis of core-crosslinked redox-responsive polycarbonate [Reprinted with permission from reference 133. Copyright © Royal Society of Chemistry 2021.].

In vitro drug release, *in vitro* cytotoxicity assays and *in vitro* cellular uptake evaluation were successfully performed with HeLa and HepG2 cells. The cellular internalization of DOX-loaded micelles was investigated by CLSM and flow cytometry. The CLSM images showed a clear blue fluorescence of the nuclei which were stained with Hoechst 3342 and a weaker red fluorescence which belongs to the released DOX. The highest cytotoxicity was observed in the concentration range of 4 µg mL^{-1} to 16 µg mL^{-1}. However, besides micelle disruption and DOX-release, no polymer degradation was observed.

Chen *et al.* built a redox-responsive monomer based of 3-methyl-3-oxetanmethanol.[134] First, the oxetane was opened employing hydrobromic acid and the bromo-functionality was substituted with a thiol, subsequently the thiol was protected using 2,2´-dithiodipyridine. The pyridyldisulfide-diol was transferred to a pyridyldisulfide-carbonate (PDSC) using ethyl chloroformate and the monomer was copolymerized with ε-caprolactone (*Scheme 10*). The thiol-

protecting-group was exchanged with thiolated PEG and micelles were formulated which were loaded with doxorubicin.
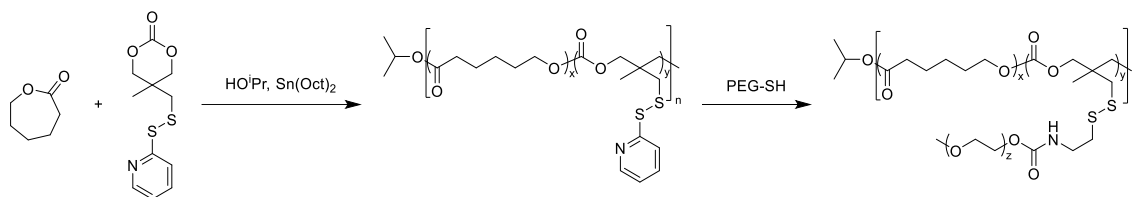
Scheme 10: Polymerization of redox-responsive amphiphilic poly(ε-caprolactone) [Reproduced with permission from reference 134 (W. Chen, Y. Zou, J. Jia, F. Meng, R. Cheng, C. Deng, J. Feijen and Z. Zhong, Macromolecules, 2013, 46, 699–707.). Copyright (2021) American Chemical Society.].

The PEG-block of the micelles can be cleaved by glutathione resulting in the disruption of the micelles and drug release. The drug release and antitumor activity of this system was successfully evaluated using HeLa cells. However, this system does not undergo self-accelerated degradation. The degradation mainly takes place because the copolymer is partly made of poly(ε-caprolactone).

A pH-responsive redox-degradable drug delivery system was developed by Li *et al.*[135] The monomer was synthesized from 2,2´-dithiodiethanol and epibromohydrin. The epoxy-group containing the monomer was copolymerized with ethanolamine. Afterwards, a fluorescent probe (coumarin) was coupled to some of the free hydroxy-groups of the polymer and doxorubicin loaded micelles were formulated (*Scheme 11*).
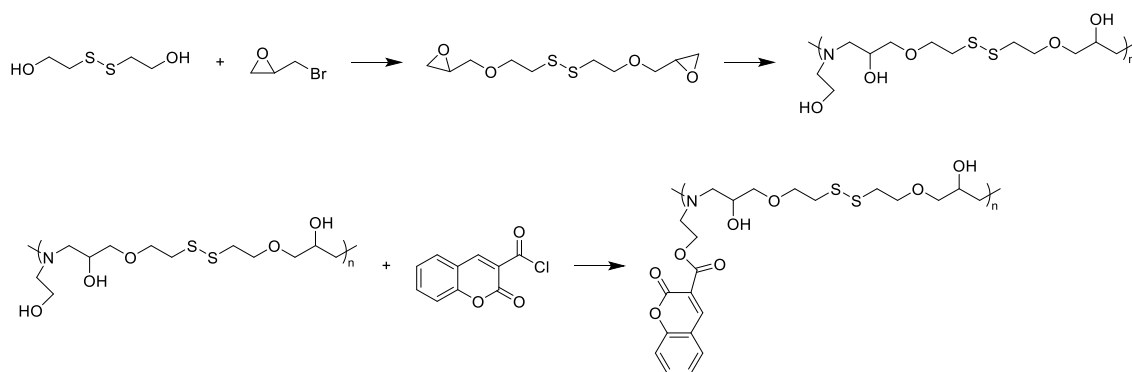
Scheme 11: Synthesis and postpolymerization modification of poly(β-hydroxyl amine) [Reproduced with permission from reference 135 (D. Li, Y. Bu, L. Zhang, X. Wang, Y. Yang, Y. Zhuang, F. Yang, H. Shen and D. Wu, Biomacromolecules, 2016, 17, 291–300.). Copyright (2021) American Chemical Society.].

Evaluation of the micelles *in vitro* showed a good cellular uptake in the fluorescent microscope in MCF-7 cells and a cell viability of the unloaded micelles determined

by CCK-8 assay. However, DOX-loaded micelles exhibit an efficient antitumor activity toward MCF-7 cells. Though, free DOX was more effective, but the half-maximal inhibitory concentration of the DOX-loaded micelles was about seven times higher than the free DOX. This polymer has a disulfide bond in each of the repeating units that can be cleaved after the endocytosis due to the higher concentration of glutathione. The disruption of the micelle is further enhanced by the lower pH-environment inside of the cells due to the protonation of the tertiary amine of the repeating unit.

Whang *et al.* reported the synthesis of a linear redox-sensitive polymer capable of self-immolative backbone cleavage.[136] Covalent conjugated to its primary and secondary amines are *p*-nitrobenzyl alcohol (*p*NBA) as a redox-trigger and *p*-hydroxybenzyl alcohol (*p*HBA) as self-immolative linker (*Scheme 12a*). Incorporation of *p*NBA highlights the polymer's functional variation from other redox-sensitive systems that primarily utilize disulfide reduction.
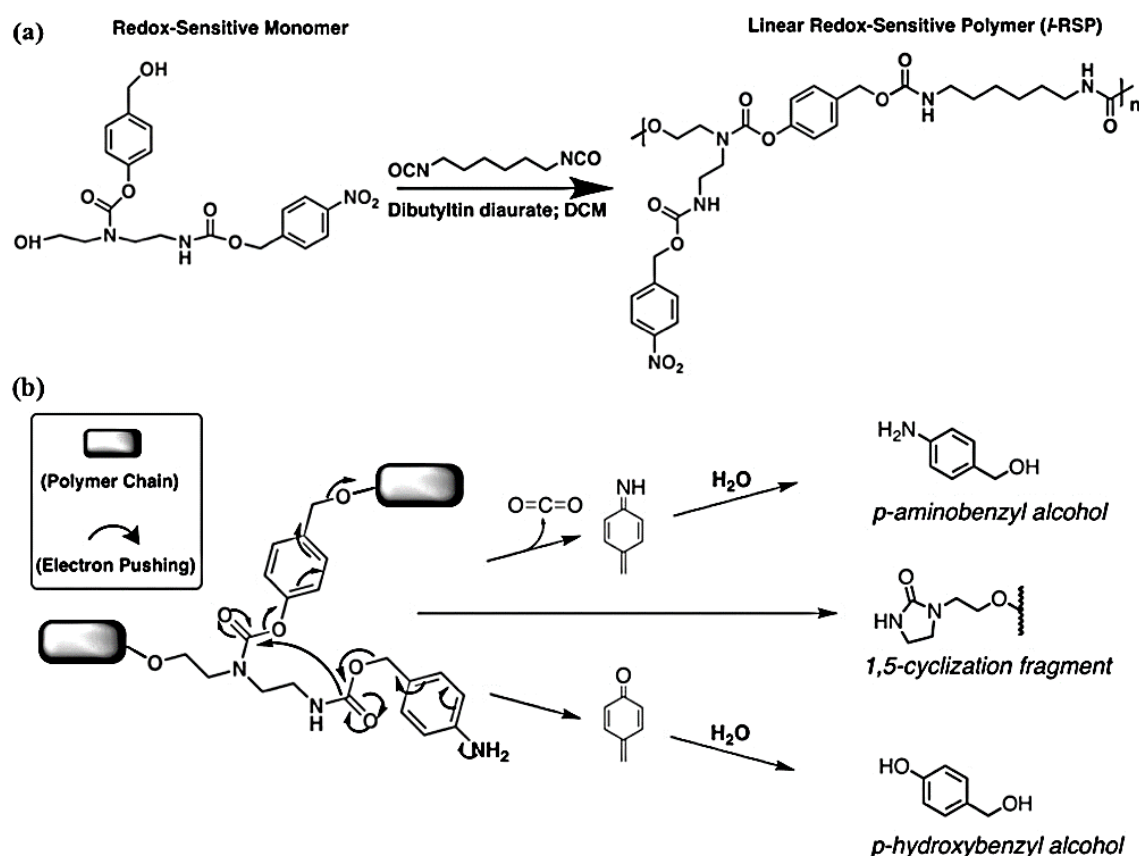
Scheme 12: a) Polymerization scheme to synthesize I-RSP. b) Focal point reduction-induced disassembly of the I-RSP. [Reprinted with permission from reference 136. Copyright © Wiley 2021).

The copolymerization with hexamethylene diisocyanate yields a linear redox-sensitive polymer capable of degrading *via* sequential 1,6-elimination decarboxylation and 1,5-cyclization reaction into biocompatible fragments safe for potential biomedical applications (*Scheme 12b*). Reduction of the pendant *p*NBA aryl nitro group into an amine initiates a cascade of self-immolative processes throughout the repeating units. The initial 1,6-elimination decarboxylation results in *p*-aminobenzyl alcohol (*p*ABA) and CO_2. The now unmasked primary amine undergoes an 1,5-intramolecular cyclization of the backbone. The electron pushing cascade continuous through *p*HBA resulting ultimately in systemic degradation of the polymer. The reduction was triggered by sodium dithionite ($Na_2S_2O_4$) and observed proton shifts were in accordance with the predicted degradation sequence. Polymeric nanoparticles were created by single oil-in-water emulsion using poly(vinyl alcohol) (PVA) as emulsion stabilizer. The Z-average diameter determined by DLS where 210 nm for blank particles and 232 nm for paclitaxel (PTX)-loaded particles. The addition of reducing agent ($Na_2S_2O_4$) led to a rapid increase in particle size up to 623 nm within 80 min due to the core`s solubility reversal. *In vitro* PTX release with and without $Na_2S_2O_4$ was monitored over 24 h. Reduced particles released around 84% of the encapsulated drug while the control system lost around 37% in the same time probably due to the low hydrophobicity of the polymer core. Whang *et al.* showed a creative approach to a biodegradable redox-triggered self-immolative polyurethane with good stimuli-responsiveness and high drug release but low loading capacity. Future improvements are minimizing the size distribution by PEGylation to create amphiphilic polymers which also should increase the loading capacity.

Santra *et al.* synthesized a biodegradable redox-responsive self-immolative polyurethane based amphiphile with a pH-responsive tertiary amine in the backbone.[137] This tertiary amine could be protonated at the tumor cells lower extracellular pH and help the nanocarrier for enhanced cellular internalization. For the synthesis of the monomer diethanolamine was treated with triethylene glycol monomethyl ether acrylate as the hydrophilic part of the amphiphile. This diol monomer was then condensed with hexamethylene diisocyanate and 2-hydroxyethyldisulfide which contains the reduction-responsive part to produce the polyurethane in *Scheme 13*. Another control polymer P2 was synthesized

following a similar procedure but without a disulfide linkage this polymer is not able to respond to a reductive environment. The self-assembly of nanocarriers was performed by nanoprecipitation. DLS-measurements revealed nanoparticles with hydrodynamic diameters of about 105 nm. TEM showed the presence of spherical micelles with diameters in the range of 80 - 100 nm. To test the encapsulation properties, the hydrophobic dye 1,1-dioctadecyl-3,3,3,3-tetramethylindocarbocyanine perchlorate (Dil) was used as a model guest molecule. By keeping the Dil concentrations constant, its absorbance intensity increased with the concentration of the polyurethane. An actual drug loading capacity was not reported.
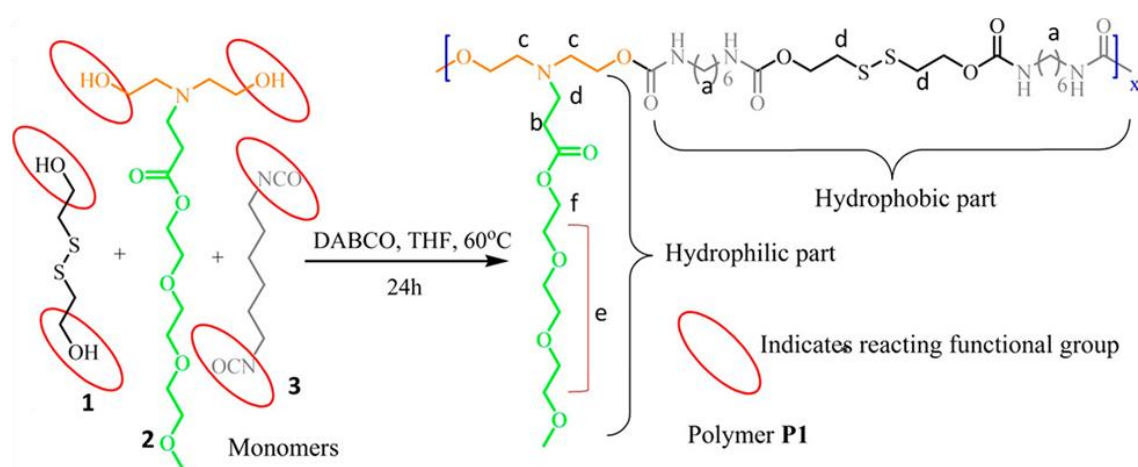
Scheme 13: Synthetic scheme of polymer P1 from three monomers [Reproduced with permission from reference 137 (S. Santra, M. A. Sk, A. Mondal and M. R. Molla, Langmuir, 2020, 36, 8282–8289.). Copyright (2021) American Chemical Society.].

Redox-responsive behavior and the release of Dil was carried out in a concentration of 10 mM GSH. *Figure 3* shows a release of 25% in the first 10 h and ultimately reaching 70% in 50 h. The control system without GSH released 9% in the first 10 h and a total of 40% in 50 h. In an additional test with a control polymer in the presence of GSH they observed only a small release about 7% of Dil in total. Confirming that the disulfide degeneration is responsible for the guest release.
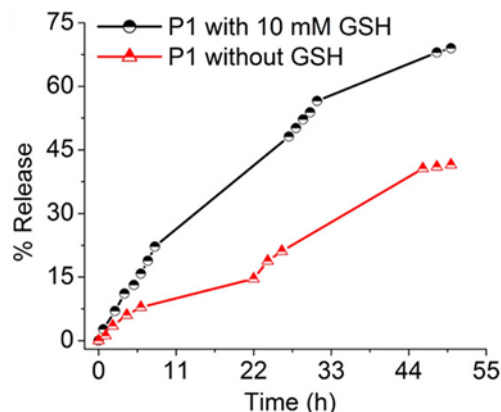
Figure 3: Study of redox-triggered guest release from a P1 micelle in the presence and absence of GSH. [Reproduced with permission from reference 137 (S. Santra, M. A. Sk, A. Mondal and M. R. Molla, Langmuir, 2020, 36, 8282–8289.). Copyright (2021) American Chemical Society.].

The pH-induced surface charge was investigated using zeta-potential measurements. At neutral pH values it is found to be -1.0 mV, a decrease in pH to 6.6 changes the surface charge to 38 mV due to the protonation of the tertiary amine. Because of the negative cell potential in tumor cells their uptake capacity for positively charged particles is increased. Furthermore, its initial natural surface charge limits the nonspecific interaction during its travel to a designated location.

Duan *et al.* formulated a glutathione-responsive amphiphilic drug self-delivery micelle with a one-pot synthetic approach.[138] The polymer is synthesized by the Michael addition at 80 °C with doxorubicin and a disulfide-based diacrylate in a first step, followed by the addition of amine end-capped mPEG (*Scheme 14*).
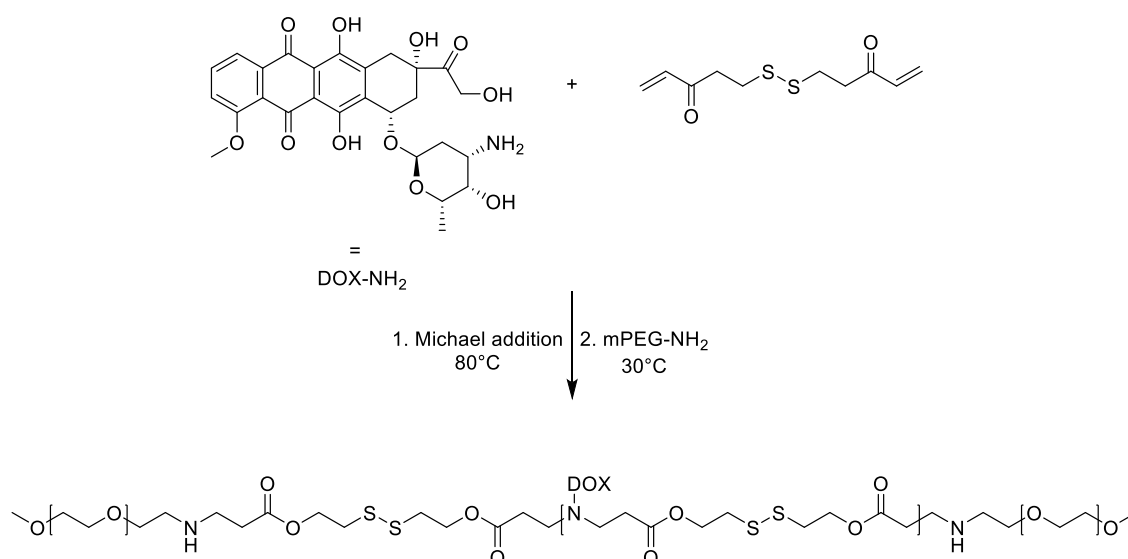
Scheme 14: Schematic depiction of the synthetic route of glutathione-responsive (DOX–DSDA–PEG) [Reproduced with permission from reference 138. Copyright © Royal Society of Chemistry 2021].

Upon treatment with a GSH solution (1 mg/mL) for 24 h the size of the micelle decreased from 175 nm to smaller than 100 nm (measured by DLS). The stability of the micelles was evaluated by centrifuging at 12000 rpm. The sample containing DOX-disulfide-based diacrylate (DSDA)-PEG that was incubated with GSH-solution showed a red sediment on the bottom of the centrifuge tube indicating the disruption of the micelles and the precipitation of DOX-containing smaller polymeric material. The drug loading and release was evaluated by UV/Vis-spectroscopy at 490 nm. The drug loading efficacy was 25.5%. The drug release was performed up to 72 h with a GSH-solution (1 mg/mL, pH 7.4). The micelles showed a drug release of 7.2% at 16 h, 21.3% at 24 h and 67.9% at 72 h. The drug release without applying GSH was at 22% after 72 h. Cell uptake and viability experiments confirmed the intake of the micelles by A549 cells. In conclusion, the system of Duan *et al.* is a facile approach for a self-accelerating polymeric drug delivery system.

2.5   pH-responsive polymers

Another frequently used stimulus is the pH-value due to its versatility. Most of the published work involves either the removal of an acid-labile group or the protonation of reactive groups with subsequent change in the polarity of the polymer.[139–144] Acid-labile polymers or DDS that are based on them can release

their cargo upon the change in the environmental pH-value. As already mentioned, the pH-responsive DDS benefit from the different environments in the human body. Healthy tissue exhibits a pH-value of approximately 7.4. The pH-responsive DDS will keep their cargo at this pH-value; however, it will release its cargo in cancerous tissue with the pH-value of lower than 6.5 or even 5 after lysosomal uptake. The lower pH-value of the cancer environment is due to the lactate formation by glycolysis.[145] This makes the pH-change an excellent trigger for DDS. In this work, the main focus lies on polymers, that degrade upon the application of a trigger. Typical examples of acid-labile moieties are depicted in *Scheme 15*.[146]
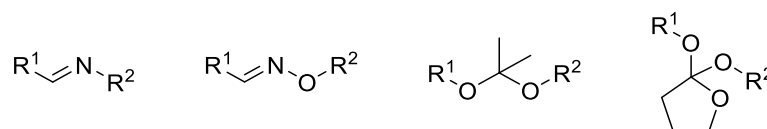
Scheme 15: Acid-labile group from left to right: imine, oxime, acetal and ortho ester.

By incorporating these functional groups into the polymer, pH-responsive self-accelerating DDS can be achieved. Wei *et al.* synthesized two novel poly(ortho ester amide) copolymers for highly efficient oral chemotherapy.[147] The monomers of the two copolymers are both synthesized from diglycerol. In the first step, the ortho ester functionality is formed on both glycerol parts. In the second step *N*-(2-hydroxyethyl)trifluoroacetamide is coupled to the ortho ester moieties, which is hydrolyzed to an amine in a third step. The resulting diamide is copolymerized in a polycondensation reaction with either disuccinimidylsuberate or disuccinimdyldodecanoate resulting in a poly(ortho ester amide) (POEA-4 and POEA-5 respectively). The molar mass was determined by SEC and the M_n had a size of 12400 g/mol with a dispersity of 1.59 for POEA-4 and 19300 g/mol with a dispersity of 1.93 for POEA-5. Both polymers had a high thermal stability of over 190 °C. Both polymers were loaded with 5-fluorouracil (5-FU) and release studies were performed at different pH values (7.4, 5.0 and 1.0). In the release test at pH = 7.4 there was a weight loss of roughly 10% and a cumulative release of 5-FU of 20% after 7 days. For the other pH-values, the weight loss and the cumulative release were near 100% after 7 days. The POEA were biologically verified by conducting *in vitro* tests against mouse embryonic fibroblast cell line NIH3T3. Both POEAs showed no obvious cytotoxicity against NIH3T3. The cell

viability was over 80% at the high concentration of 5 mg/mL for the duration of 24 h. POEA-5 was also tested *in vivo* in a subcutaneous liver cancer mouse model using the mouse hepatocellular cancer cell line H22. The mice were treated with daily oral gavage for 1 week with different drugs: saline (as control), POEA-5, 5-FU and POEA-5+5-FU. In the case of the treatment with saline and POEA-5, the body weight increased from 19 g to 21.5 g and 19.5 g to 23 g, respectively. This is due to the tumor growth. The body weight of 5-FU and POEA-5+5-FU treated mice almost remained unchanged, indicating the effective treatment of the cancer. Mice treated with POEA-5+5-FU had a smaller tumor weight (0.28 g in contrast to 0.51 g). The tumor growth inhibition was roughly 64% and nearly twice as high compared to the free 5-FU (34%). In summary, the presented DDS showed to be efficient in the used model and is a good example for a self-accelerating pH-responsive DDS.

Jin *et al.* synthesized a triblock copolymer consisting of a PEG-block, an oxime-linked polycaprolactone (OPCL) block and another PEG-block.[148] The OPCL-block was synthesized by the reaction of polycaprolactone with terephthalaldehydic acid. The aldehyde-terminated polycaprolactone (CHO-PCL-CHO). In a second-step, CHO-PCL-CHO was reacted with *O,O'*-1,3-propanediylbishydroxylamine (PBH) to create the oxime-tethered PCL (OPCL). The aminooxy groups of the OPCL reacted with aldehyde terminated PEG (PEG-CHO) to form the triblock polymer with a molecular weight of approximately 6000 g/mol and a dispersity of 1.3. The triblock polymer was used to fabricate DOX-loaded micelles (CMC = 0.066 mg/mL). The cytotoxicity was estimated in an *in vitro* test against NIH3T3 cells. The cell viability was over 80% when incubated with 1 mg/mL polymer concentration after 24 h. The DOX-loaded micelles have a hydrodynamic radius of approximately 260 nm with a PDI of 0.25. The micelles showed a leaking of the DOX of 20% at pH 7.4 after 60 h. At the same time micelles released the drug under acidic conditions (pH 5). 70% drug release was established after 60 h and 80% release after 100 h. A control micelle consisting of a triblock polymer without oxime links showed no significant drug release at both pH after 100 h. The cell internalization was established by flow cytometry and confocal laser scanning microscopy (CLSM). The flow cytometry indicated that the cellular uptake of DOX-loaded micelles is enhanced in comparison to free DOX. The CLSM indicated that the released DOX from DOX-

loaded micelles is taken up by the cells *via* the endocytosis process in comparison to the free DOX that is taken up by diffusion through the membrane. The cell viability of DOX-loaded micelles and free DOX was determined by MTT viability assay against HeLa cancer cells. The free DOX led to cell viability of 30% after 72 h incubation and the DOX-loaded micelles led to a cell viability of 10% after 72 h indicating the enhanced anticancer efficacy.

Guégain *et al.* developed a vinyl copolymer containing various amount of the pH-responsive 2-methylene-4-phenyl-1,3-dioxolane (MPDL).[149] The polymer was synthesized using a nitroxide-mediated radical ring-opening copolymerization of MPDL and methyl methacrylate or oligo(ethylene glycol) methyl ether methylacrylate (*Scheme 16*).


R = Me or OEG
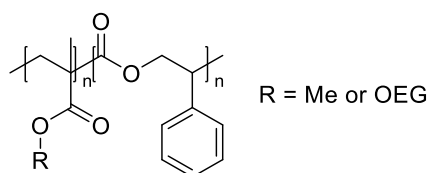
Scheme 16: Structure of P(MMA-co-MPDL) and P(OEGMA-co-MPDL).

The molar mass of the two degradable polymers ranged between 23000 - 35000 g/mol with the dispersity between 1.2 - 1.6. The fraction of MPDL ranged from 0.08 (feed of 0.2) to 0.27 (feed of 0.7) as determined by NMR. The polymers were tested for their long-term hydrolytic stability by incubating them in different media for up to 12 months. The MMA-based polymers had a lower degradation level (20%) after 12 months in PBS (0.1 M, pH 7.4, 37 °C) due to the higher hydrophobicity in comparison to the OEGMA-based polymers. The mass decrease in the OEGMA-based polymers depends on the molar fraction of MPDL and ranges from 20% for 0% MPDL, 40% for 9% MPDL, 60% for 15% and 70% for 27% MPDL after 12 months. However, no pH-dependence could be observed for the high MPDL ratio MMA-based polymers and high MPDL ratio OEGMA-based polymers. The mass decrease at pH 5.5 is insignificantly smaller than at pH 7.4. The ambient pH of the degradation medium lowers from 7.4 to around 7.0. In comparison, the degradation of PLGA and PLA lowers the ambient pH to 5.7 due to the liberated carboxylic acid chain ends. This can lead to the local acidification that results in local inflammatory response. Films were casted of the hydrophobic MMA-based polymer and hydrolytic degradation was evaluated. All

films showed no significant water uptake and only a mass loss of 10% after 12 months. The OEGMA-based polymers containing MPDL were evaluated *in vivo* in mice. Two samples with fractions of 15% MPDL and 27% MPDL were injected intravenously in a single injection in mice with concentrations from 0.8 - 2.4 g/kg. The body weight of the mice was nearly constant after 20 days similar to untreated mice. There was a trend observable that the copolymer concentration influences the body weight. The higher the concentration of the copolymer, the higher is the body weight loss, but no mortality was observed. This system proved to be an interesting attempt at for a material base that is used for long-terms (e.g., implants) and short-term applications as DDS with tunable degradation kinetics.

Fu *et al.* synthesized a degradable polyacetal from modular enyne monomers that were polymerized in a metathesis polymerization.[150] The monomer synthesis started from *tert*-butyl carbonate **1**, which was previously synthesized by Achmatowicz rearrangement of furfuryl alcohol (*Scheme 17*).
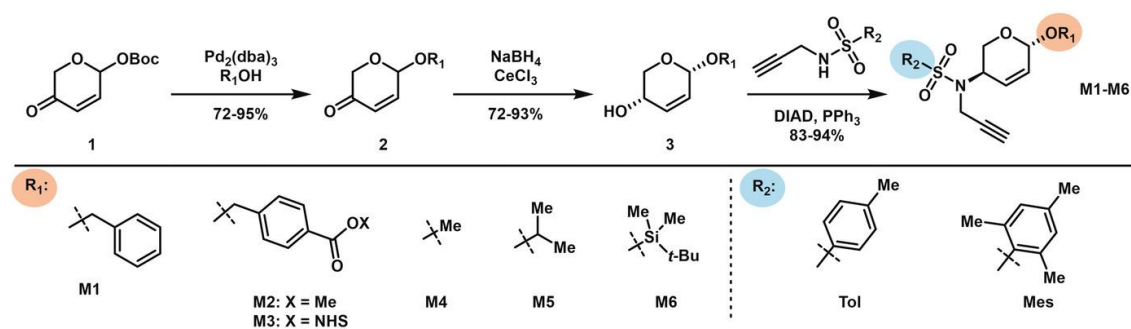
Scheme 17: Synthesis of enyne acetal monomers. [Reprinted with permission from reference 150. Copyright © Wiley 2021).

A Tsuji-Trost substitution was used to prepare **2** with a variety of groups. The ketone group was subsequently reduced by Luche reduction to yield the racemic *cis*-allylic alcohols **3**. The free alcohol group was converted in a Mitsunobu inversion using tolyl or mesityl propargyl sulfonamide to deliver the *trans*-enyne monomers. **M1$_{Tol}$** was polymerized in with a monomer:initiator ratio of 50:1 to give **P1$_{Tol}$** with a molar mass of 26000 g/mol and a dispersity of 1.18. Polymers were made from all variations of monomers with different monomer:initiator ratios. Polymers ranging from 10600 - 171100 g/mol were synthesized depending on the monomer:initiator ratio. The polymer **P1$_{Mes}$** was tested on its pH-responsive behavior under neutral, basic and acidic conditions in aqueous environment. The polymer was dissolved in THF/H$_2$O/triethylamine, THF/H$_2$O, THF/H$_2$O/acetic acid

and THF/H$_2$O/trifluoroacetic acid. The polymer showed no degradation when TEA is present and showed a mass loss of 60% after 48 days in THF/H$_2$O. The mass loss of the polymer in presence of acetic acid was 60% after 1 day and 80% reduction after 2 days. In presence of trifluoroacetic acid, the mass loss peaked after 10 h with a nearly complete degradation. This polymer seems to be a good base for a pH-responsive self-accelerating DDS, because the polymer is stable in basic conditions, but degrades under acidic conditions. However, further tests under physiological conditions are necessary to evaluate the suitability for a DDS.

2.6   Other triggers

The most commonly used triggers for smart-drug delivery systems are temperature, light, pH and redox reactions. However, there are more triggers that can be utilized in more specific cases including enzymes, fluorides, oxidation, ultrasound or hypoxia.

Olah *et al.* devised a self-immolative poly(benzyl ether) with an fluoride-labile end cap that leads to depolymerization upon the treatment with tetrabutyl ammonium fluoride (TBAF) The polymer is depicted in *Scheme 18*.[103]
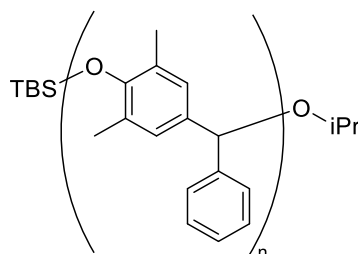

Scheme 18: Fluoride-labile self-immolative poly(benzyl ether) [Reproduced with permission from reference 103 (M. G. Olah, J. S. Robbins, M. S. Baker and S. T. Phillips, Macromolecules, 2013, 46, 5924–5928.). Copyright (2021) American Chemical Society.].

They synthesized their monomer 2,6-dimethyl-7-phenyl-1,4-benzoquinone methide out of benzoyl chloride and 1,6-dimethylphenol in four steps. The polymerization was end-capped with *tert*-butyldimethylsilyl chloride resulting in a fluoride-labile end-cap. By the addition of TBAF into a solution of the polymer, the depolymerization was completed in 30 min at 18 °C. Though the system reacts fast upon contact with the stimulus, drug delivery applications were not evaluated.

Iturmendi *et al.* developed a self-immolative polyphosphazene that degrades as a response to an oxidative trigger.[101] Each of the repeating units bears an arylboronic acid pinacol ester moiety that liberates a carboxylate group upon deprotection. The resulting poly(glycine)-phosphazene undergoes rapid self-catalyzed degradation to phosphates and ammonia (*Scheme 19*).
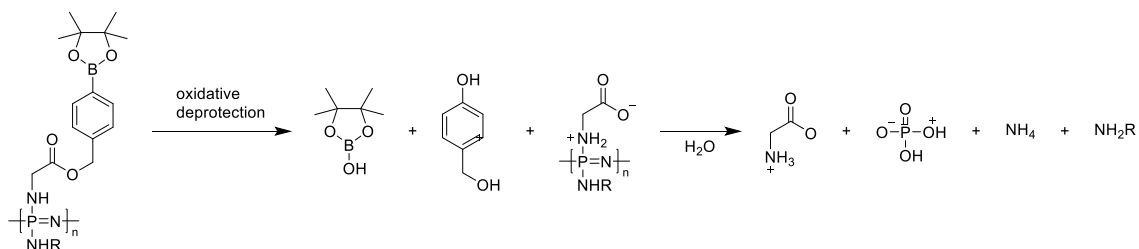
Scheme 19: Deprotection with subsequent aqueous degradation of the polyphosphazene. [Reproduced with permission from reference 101 (A. Iturmendi, U. Monkowius and I. Teasdale, ACS Macro Lett., 2017, 6, 150–154.). Copyright (2021) American Chemical Society.].

The polymer was fabricated using the monomer trichlorophosphoranimine ($Cl_3P=N-SiMe_3$) and in a postpolymerization reaction, Boc-gly-arylboronic acid pinacol ester was coupled to the polymer after initial deprotection of the Boc-group. The polymer is stable in aqueous medium but fully degrades to phosphates after addition of hydrogen peroxide within 30 days. Without the addition of hydrogen peroxide, the polymer was stable showing no significant signs of phosphates.

Kumar *et al.* developed a polymer that depolymerizes after treatment with reactive-oxygen-species (ROS) or ultrasound.[102] The poly(vinyl acetate-*alt*-sulfur dioxide) (PVAS) was synthesized out of vinyl acetate, sulfur dioxide and *tert*-butyl hydroperoxide as an initiator (*Scheme 20*).
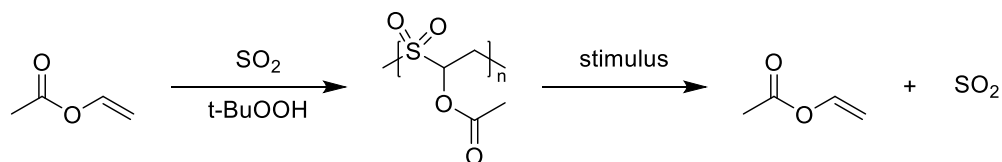
Scheme 20: Polymerization and depolymerization reaction of PVAS. [Reproduced with permission from reference 102 (K. Kumar and A. P. Goodwin, ACS Macro Lett., 2015, 4, 907–911.). Copyright (2021) American Chemical Society.].

The usability as a drug delivery system was evaluated by using different ROS. The system was not degrading upon application of weaker oxidizing agents like

hydrogen peroxide but depolymerized rapidly with stronger oxidizing agents like hypochlorite. Furthermore, the ultrasonic-accelerated degradation of PVAS dissolved in acetone was also tested applying 30 min of ultrasound. The generation of monomer was monitored even after a total of 4 h indicating a continuous depolymerization mechanism.

2.7   Nanoparticle synthesis

2.7.1   Desolvation technique

This technique is one of the most widely used techniques for the preparation of polymer nanoparticles and is useful for a variety of polymers. By changing the charge, the pH value or by the addition of a desolvation agent (e.g., ethanol or brine), polymeric particles can be obtained. The previously dissolved polymer is no longer soluble in the solvent and aggregates to NPs. Heat is not necessary for this process, therefore temperature-sensitive polymers can be used to form NPs.[151] One example of this method was published by Jun *et al.*, by fabricating bovine serum albumin (BSA) NPs.[152]

2.7.2   Dialysis technique

The dialysis technique is a very simple method to produce polymeric NPs with a narrow size distribution. In this method, a polymer sample is dissolved in an organic solvent and placed inside a dialysis tube with the desired molecular cutoff.[153] The dialysis tube is placed into a reservoir with a non-solvent for the polymer, but miscible with the solvent used to dissolve the polymer. The solvent inside the dialysis tube is slowly getting replaced by the solvent in the reservoir. The polymer aggregates due to the slow displacement of the solvent resulting in a homogeneous suspension of polymeric NPs. The process is not fully understood and has similarities to the nanoprecipitation method.[154]

2.7.3   Nanoprecipitation technique

In this method, a water-miscible polymer solution is slowly dropped into an aqueous phase with a stabilizing surfactant. As soon as the polymer solution drop hits the surface of the reservoir under heavy stirring, small droplets of

nanoparticles of defined narrow size stabilized by the surfactant are formed. These particles solidify after some time and can be either washed (centrifuged, decanted, redispersed with new water) or freeze dried to obtain the clean polymeric NP.[155,156]

2.7.4   Solvent evaporation technique

The solvent evaporation technique is similar to the nanoprecipitation technique. The polymer is dissolved in a water miscible organic solvent and added dropwise to water containing an emulsifier or surfactant under heavy stirring. The difference to the nanoprecipitation technique is that the organic solvent is removed from the aqueous phase. This can happen by either increasing the temperature, applying vacuum or let it stir without a lid for a longer duration resulting in a stable nanosuspension of polymeric NPs.[157,158]

2.7.5   Rapid expansion of supercritical fluid solution

An environmental-friendly method to avoid organic solvents to form polymeric NPs is the supercritical-fluid technique. The polymer is dissolved in a supercritical fluid and this solution is rapidly expanding over an orifice into the ambient air. During the expansion, homogeneous nucleation and narrow distributed NPs are obtained.[159,160]

2.8   Work plan

To achieve the goal of an effective base for a DDS and address the drug delivery in cancerous tissue the following triggers were chosen: UV light, acidic environment and redox environment. Upon application of the trigger, the polymers need to degrade. Therefore, a stimuli-responsive self-accelerating polymer is planned. Based on the previous work, a polymer is designed to bear protective groups that react to one of the stimuli. After the deprotection, a nucleophile is liberated that can subsequently backbite into a carbonate, urethane or ester group that is located in the backbone. After the transesterification or similar reactions, the backbone is cleaved, leading to the reduction of the molar mass of the polymer. Monomers will be synthesized similar

to the previously published work (*Scheme 7*).[128] The synthesis of the light-responsive *ortho*-nitrobenzyl alcohol (*o*NB) group bearing monomer is performed in seven steps with the use of highly reactive and toxic substance like sodium azide. It is necessary to find ways to synthesize a monomer that is at least as reactive as the already published ones, but with a facile synthesis involving less steps and work-up processes. The first trigger that should be addressed was light. A novel *o*NB-group was used to further improve the light-responsiveness compared to the previously used *o*NB-group that was based on 4,5-dimethoxy-2-nitro-benzylalkohol. The monomer was based on 6-nitropiperonal, which was modified to bear a secondary alcohol (1-(6-methylbenzo[d][1,3]dioxol-5-yl)ethan-1-ol). This protecting group was already used in recent literature.[161,162] Upon light irradiation, a ketone is generated instead of an aldehyde as in older works. The mechanism of the photoremoval of this group is shown in *Scheme 21*.
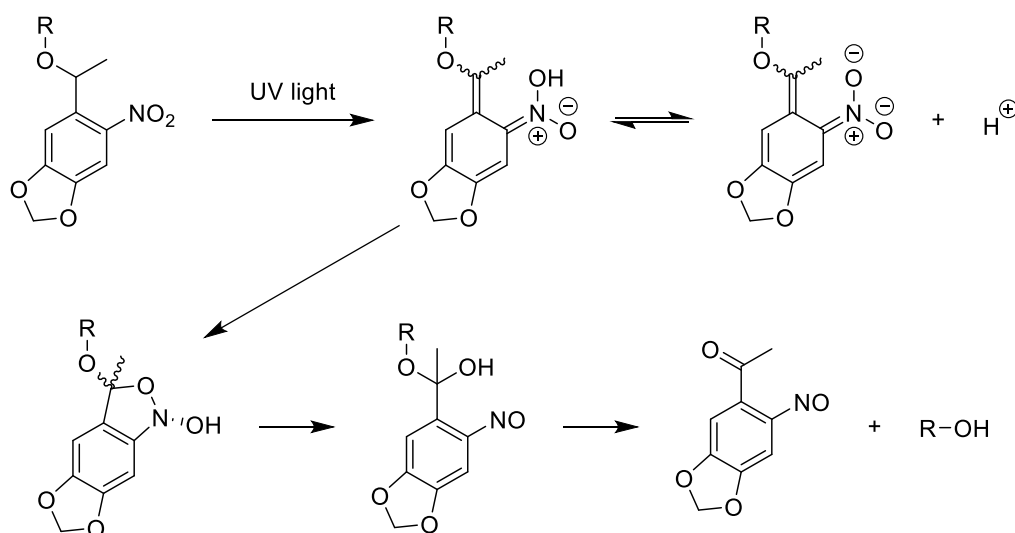
*Scheme 21: Photoremoval of an oNB-group.*

Aldehydes are highly toxic due to their reactivity.[163] Ketones are less reactive than aldehydes and some of the reaction pathways are hindered. In comparison to the previously published *o*NB-unit (*ortho*-nitroveratryl-group) the 6-nitropiperonal-based (6NP-based) *o*NB-group has a higher quantum yield ($\varphi_{o\text{NB}} = 0.0013$ vs. $\varphi_{6\text{NP}} = 0.0075$).[108]

The hydroxyl-group of the 6NP-group can be activated by *para*-nitrophenyl chloroformate. After the activation, the nucleophilic group (amine or alcohol) of the polymerizable unit can be protected as a carbamate or carbonate, respectively. However, the synthesis of the polymerizable unit was difficult.

Instead of synthesizing a molecule with a diol and an amine, serinol (2-amino-1,3-propandiol) can be used.

In the backbiting reaction of the serinol repeat unit, the amine functionality attacks the backbone and forms a five-membered cyclic carbonate or carbamate (*Scheme 22*).
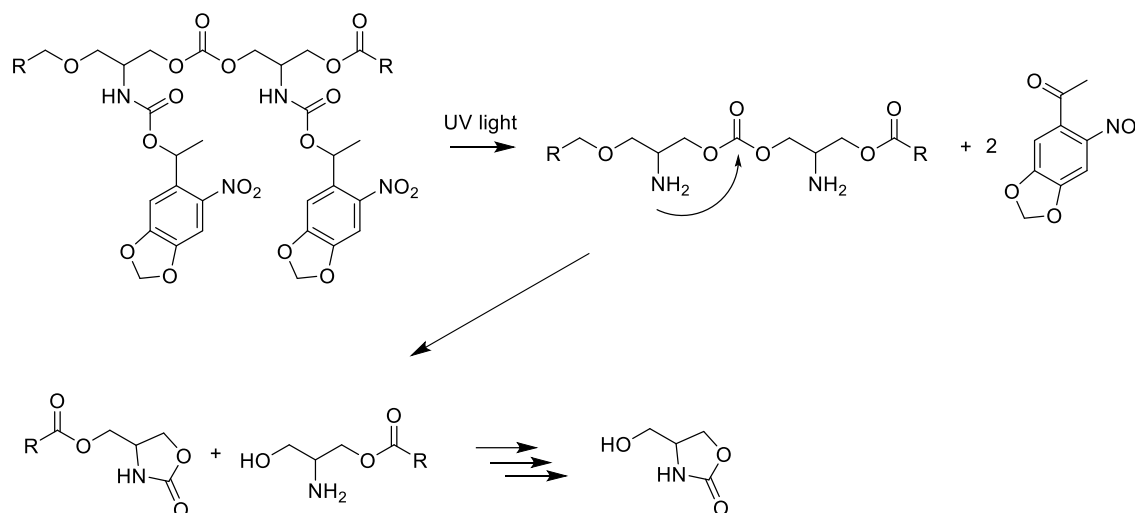
Scheme 22: Theoretical example of a polycarbonate with 6NP coupled to a serinol repeating unit and its degradation.

The neighboring repeating units in this homopolymer can backbite as well. After all the serinol repeating units underwent backbiting, the final product is the five-membered carbamate 4-(hydroxymethyl)oxazolidin-2-one as well as the leaving group 1-(6-nitrobenzo[d][1,3]dioxol-5-yl)ethan-1-one which left the repeating unit after the exposure to UV light. After the successful application of this polymer in a DDS, an accumulation in the filtering organs in the human body of the residues after the application of a trigger is unlikely due to the small size of the resulting molecules. The 6NP-group coupled to serinol seems to be a promising monomer.

One of the most frequently used redox-responsive groups is the disulfide bond. The disulfide bond can undergo cleavage by the reduction to two thiols. This is a suitable group especially for the reaction with glutathione which is overexpressed in cancerous tissue to protect the cancer cells against oxidation. There are only few protecting groups for thiols and 2,2′-dipyridyl disulfide (DPDS) is one of the most common groups.[164–166] The protection of thiols with this agent is facile and no heat or catalysts are necessary (*Scheme 23*).
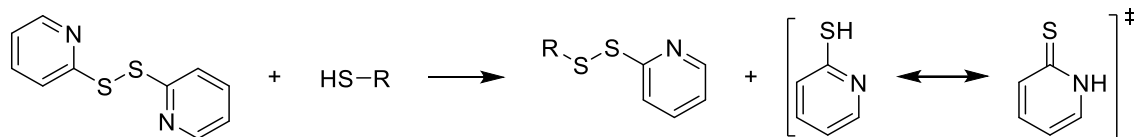
Scheme 23: Protection of a thiol with DPDS.

This protecting group can be coupled to a diol in two different ways. By using thioglycerol, DPDS can be directly used to synthesize the monomer with one primary hydroxyl group and one secondary hydroxyl group in a single step. By protecting the thiol of mercaptoethanol, activating the hydroxyl group and subsequently coupling it *via* a carbamate unit to serinol, a monomer is obtained with a 1,3-propanediol functionality (*Scheme 24*).
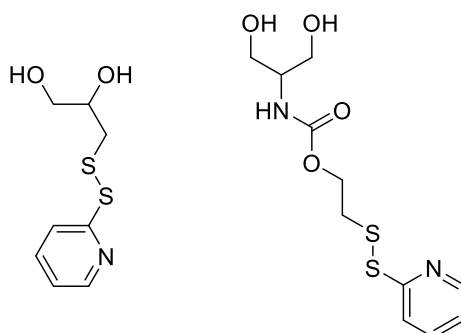
Scheme 24: Thioglycerol-based DPDS-protected monomer (left) and serinol-based DPDS-protected monomer (right).

In the case of the thioglycerol-based monomer, the thiol group is liberated upon treatment with glutathione or similar reducing agents (e.g., dithiothreitol). This thiol can backbite in a similar fashion like previously described in *Scheme 22*. Instead of an amine the liberated thiol acts as the nucleophile. The serinol-based polymer first undergoes a backbiting of the thiol to lead to either a five-membered cyclic thiocarbonate or a thiirane unit (*Scheme 25*).[167,168]
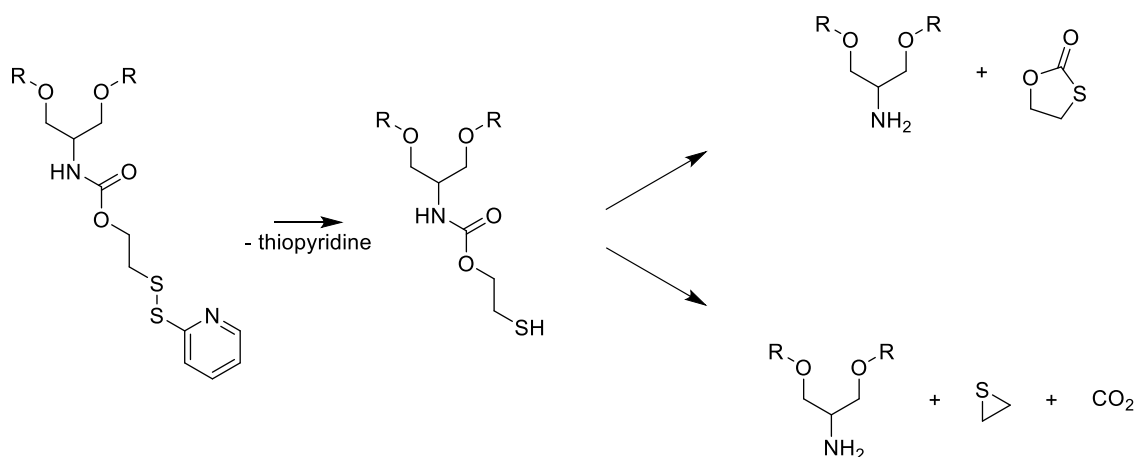
Scheme 25: Backbiting of the thiol to liberate the amine of the serinol unit.

After this first backbiting mechanism the nucleophilic amine of the serinol-group is liberated and can undergo the previously explained backbiting mechanism to cleave the polymer backbone (*Scheme 22*). Another type of redox-cleavable protecting groups was already introduced by Whang *et al.* (*Scheme 12*).[136] By coupling the 6-nitrobenzyl alcohol group to serinol *via* a carbamate group, another monomer can be obtained that is suitable for making a redox-responsive polymer (*Scheme 26*).
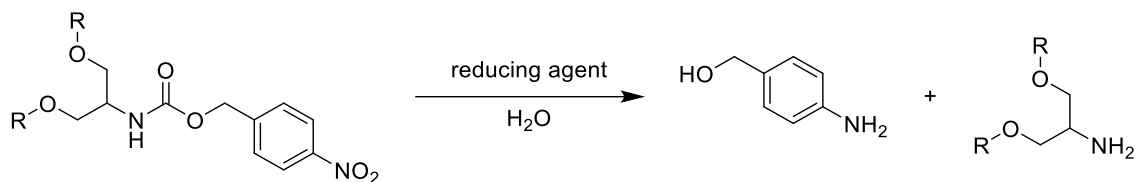

Scheme 26: The cleaving of the protecting group of the redox-responsive monomer 4-nitrobenzyl (1,3-dihydroxypropan-2-yl)carbamate.

After the reduction of the nitro group and after aqueous treatment, (4-aminophenyl)methanol and the amine functionality of the serinol unit is liberated, that can subsequently backbite like in previous examples.

The last trigger that should be addressed in this work is the change of the pH-value. DDS that are pH-responsive need to be stable under neutral conditions but degrade as soon as the pH-value drops under 6. The protective group of choice is the acetal group. The acetal protecting group is easy to synthesize and by choosing the right reactants, a one-step reaction can lead to the monomer. To obtain an acetal with a polymerizable diol, the building block of choice is pentaerythritol with its four hydroxyl groups. To form an acetal many different aldehydes can be used, but the aldehyde of choice was either benzaldehyde or

6-nitropiperonal which was used for the light-responsive monomer. The benzaldehyde-based acetal and the 6NP-based acetal is depicted in *Scheme 27*.
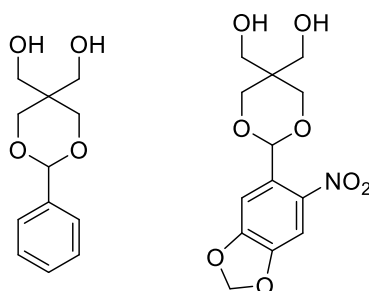
Scheme 27: Acid-responsive benzaldehyde-based acetal (left) and 6-nitropiperonal-based acetal (right).

Upon the treatment with acids in presence of water, one molecule of H_2O is added into the responsive molecule leading to the separation and the backwards reaction of the acetal. Two hydroxyl groups of the pentaerythritol are liberated if this cleavage reaction takes place in the polymer, one of these (or even both) liberated hydroxyl groups can act as a nucleophile and backbite into the polymer backbone leading to the cleavage of the polymer.

These monomers will be used for the fabrication of stimuli-responsive self-accelerating polymers, which then will partly be used for the fabrication of nanoparticles. The monomers and polymers and their degradation products will be analyzed by NMR, MS, UV/Vis spectroscopy and SEC. The nanoparticles made of these polymers and their degradation products will be analyzed by DLS, UV/Vis spectroscopy and SEC.

3   Experimental part

3.1   Chemicals and materials

Table 1: Used Chemicals and the manufacturer with purity.

Chemical	Manufacturer and purity
1,4-Benzenedimethanol	TCI, 99%
2,2'-Dipyridyl disulfide	Abcr, 98%
2-Mercaptoethanol	TCI, 98%
6-Nitropiperonal	TCI, >97%
Adipoyl chloride	Alfa Aesar, 98%
anhydrous 1,4-dioxane	VWR, 99.5%
anhydrous acetonitrile	Fisher Sci, >99%
Anhydrous dichloromethane	Grüssing, 99.5%
Benzaldehyde	Alfa Aesar, 99%
Chloroform-d_6	deutero, 99.8& + Ag
dibutyltin dilaurate	Sigma-Aldrich, 95%
Dimethyl sulfoxide-d_6	deutero, 99.8%
isophorone diisocyanate	Acros Organics, 98%
N,N-Diisopropylethylamine	Sigma-Aldrich, 99%
N,N-Dimethylformamide	Acros Organics, 99.8%
para-nitrophenyl chloroformate	Alfa Aesar, 97%
Pentaerythritol	Acros Organics, 98%
pyridine	Acros Organics, 99.5%
serinol	Abcr, 97%
tetrahydrofuran	Grüssing, 99.5%
thioglycerol	TCI, 95%
Toluene	Grüssing, 99.5%
triethylamine	Sigma-Aldirch, 99.5%
trimethylaluminium	Sigma-Aldrich, 2.0 M in heptane
triphosgene	Abcr, 98%

3.2 Methods of characterization

3.2.1 Nuclear magnetic resonance (NMR) spectroscopy

The NMR spectra were recorded on the spectrometer *Avance 500* from *Bruker* at 500 MHz (for ^{1}H) and 125 MHz (for ^{13}C). All measurements were performed at 25 °C and the chemical shifts (δ) and coupling constants (J) are given in ppm and Hz, respectively. Chloroform-*d* (CDCl$_3$, 99.8 D%) and dimethylsulfoxide-*d$_6$*, (DMSO-*d$_6$*, 99.5 D%) were used as solvents for the measurements. *TopSpin 4.0.6* (*Bruker*) was used for analysis of the data. The NMR spectra were calibrated on the following signals: CDCl$_3$ = 7.26 ppm (for ^{1}H NMR) and 77.16 ppm (for ^{13}C NMR) and DMSO-*d$_6$* = 2.50 ppm (for ^{1}H NMR) and 39.52 ppm (for ^{13}C NMR).

3.2.2 Size exclusion chromatography (SEC)

The molar masses (M$_n$) and dispersities (Đ) were analyzed by employing a size exclusion chromatography (SEC) system equipped with two consecutive columns (PSS-SDV columns filled with 5 µm gel particles with a defined porosity of 10^5 Å and 10^3 Å), a Knauer RI-detector and a Merck L4200 UV detector at 260 nm or 280 nm. The flow rate was 1 mL/min with polystyrene standard for calibration.

3.2.3 Electrospray ionization time-of-flightmass spectrometry (ESI-ToF-MS)

ESI-ToF-MS measurements were performed on the mass spectrometer *SYNAPT-G2 HDMS™* from *Waters*. Following parameters were set: capillary voltage: 2.5 kV; sampling cone voltage: 50 V; extraction cone voltage: 3 V.

3.2.4 Ultraviolet/visible (UV/Vis) spectroscopy

UV/Vis spectroscopy was performed on a *Specord-50plus* photometer from *Analytik Jena*. The spectra were recorded with the software Aspect UV and the data was processed and visualized with *Origin2020b*. Polymers or other chromophores were dissolved in concentrations of 1 mg/L to 30 mg/L depending on the absorbance of the substances. The solvent that was used to dissolve the chromophores was used as a reference measurement.

3.2.5   Melting point (T$_m$) of low molecular substances

The melting point (T$_m$) was measured with a *Melting Point B-545* from *Büchi*. heating gradient of 1 °C/min.

3.2.6   Thin layer chromatography (TLC)

TLC was performed on silica gel 60 F$_{254}$ aluminum plates from *Merck*. Absorbing compounds were analyzed under an UV-lamp from *Merck KGaA* with a wavelength of either 254 nm or 365 nm. Substances that do not absorb UV light were stained with a ninhydrin solution (20 g/L) or a basic potassium permanganate (KMnO$_4$) solution (1.5 g KMnO$_4$, 10 g K$_2$CO$_3$, 1.25 mL of 10% NaOH in 200 mL water) and subsequently processed with a heat gun.

3.2.7   Column Chromatography

The stationary phase was silica gel 60 (0.040 – 0.063 mm). All solvents used were prior cleaned by rotary evaporation and eluent ratios are given in synthesis procedures.

3.2.8   UV light irradiation

Samples were irradiated by the UV lamp *OmniCure® S1500*. The UV lamp was combined with a UV filter (320 – 480 nm), an optical fiber and an ocular. The intensity was adjusted to 298 mW/cm^2. A sample was put under the ocular and irradiated for the desired time using the built-in timer function of the lamp.

3.3   Synthesis of monomers and polymers

3.3.1   Synthesis of 1-(6-methylbenzo[d][1,3]dioxol-5-yl)ethan-1-ol **1**

This synthesis was adapted from literature.[169] In short, 6-nitropiperonal (5.00 g; 23.9 mmol; 1 eq.) was dissolved in anhydrous dichloromethane (DCM; 40 mL). To the reaction mixture a 2 M solution of trimethylaluminium in hexane (Me$_3$Al; 23 mL; 47.8 mmol; 2 eq.) which was previously diluted with hexane (15 mL) and DCM (15 mL) was added dropwise under ice-cooling and nitrogen (N$_2$)

atmosphere. After complete addition, the mixture was stirred at room temperature overnight. Afterwards, water was added slowly dropwise to the mixture under ice-cooling to deactivate unreacted Me_3Al. The brown precipitate was removed by vacuum filtration and the filtrate was separated into an aqueous phase and an organic phase. The organic phase was washed with brine and distilled water (3 times each 50 mL) and dried over magnesium sulfate ($MgSO_4$). The solvent was removed by rotary evaporation and the crude product was purified by column chromatography with acetone, yielding a brown solid (4.36 g; 86%; R_f = 0.9).
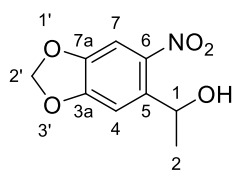
^{1}H NMR (CDCl$_3$): δ [ppm] = 1.51 (d, $^3J_{HH}$ = 6.3 Hz, 3H, $^2CH_3$), 5.43 (q, $^3J_{HH}$ = 6.3 Hz, 1H, ^1CH), 6.10 (dd, $^2J_{HH}$ = 1.3 Hz, $^2J_{HH}$ = 6.8 Hz, 2H, $^{2'}CH_2$), 7.25 (s, 1H, ^4CH), 7.42 (s, 1H, ^7CH)

3.3.2 Synthesis of 1-(6-nitrobenzo[d][1,3]dioxol-5-yl)ethyl (4-nitrophenyl) carbonate **2**

The synthesis was adapted from literature.[169] In short, a solution of **1** (6.75 g, 32 mmol; 1 eq.) and *para*-nitrophenyl chloroformate (*p*NPCF; 16.12 g; 80 mmol, 2.5 eq.) in anhydrous dioxane (160 mL) was cooled in an ice-water bath. After cooling, a mixture of triethylamine (TEA; 26.8 mL; 190 mmol; 6 eq.) in anhydrous dioxane (130 mL) was added dropwise to the solution under N_2-atmosphere and the reaction mixture was stirred overnight at room temperature. The reaction mixture was filtrated and the solvent of the filtrate was removed by rotary evaporation. The residue was dissolved in DCM (100 mL), added dropwise to *iso*-propanol (*i*PrOH; 400 mL) and after stirring overnight the product precipitated. This purification step can be repeated until sufficient purity is obtained. Isolation and drying *in vacuo* of the precipitate yielded a light-brown colored powder as pure product (8.3 g; 72%).
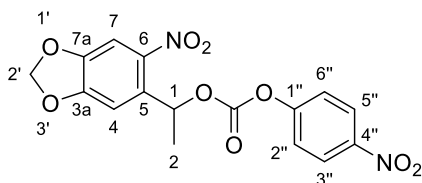
^{1}H NMR (CDCl$_3$): δ [ppm] = 1.76 (d, $^3J_{HH}$ = 6.4 Hz, 3H, ^{2}CH$_3$), 6.15 (s, 2H, $^{2'}$CH$_2$), 6.43 (q, $^3J_{HH}$ = 6.4 Hz, 1H, ^{1}CH), 7.13 (s, 1H, ^{4}CH), 7.35 (d, $^3J_{HH}$ = 9.3 Hz, 2H, $^{2''}$CH, $^{6''}$CH), 7.52 (s, 1H, ^{7}CH), 9.28 (d, $^3J_{HH}$ = 9.3 Hz, 2H, $^{3''}$CH, $^{5''}$CH)

3.3.3 Synthesis of 1-(6-nitrobenzo[d][1,3]dioxol-5-yl)ethyl (1,3-dihydroxypropan-2-yl)carbamate **3**

Serinol (0.85 g; 8 mmol; 1.5 eq.), **2** (2.00 g; 5.3 mmol, 1 eq.) and TEA (2.78 mL; 20 mmol; 3.75 eq.) were suspended in anhydrous acetonitrile (MeCN; 40 mL). The reaction mixture was stirred at room temperature for 48 h. The precipitated product was isolated by filtration and washed with DCM (45 mL). In case of low yield, the filtrate could be concentrated by rotary evaporation and the collected precipitate was recrystallized from acetone to obtain a light-yellow product (1.36 g; 78%).

T_m = 163 °C

$λ_{max}$ = 344 nm
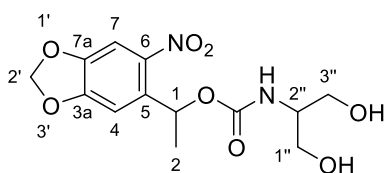
^{1}H NMR (DMSO-d6): δ [ppm] = 1.48 (d, $^3J_{HH}$ = 6.44 Hz, 3H, ^{2}CH$_3$), 3.28 (m, 1H, $^{2''}$CH), 3.35 (m, 4H, $^{1''}$CH$_2$, $^{3''}$CH$_2$), 4.55 (dt, 2H, $^3J_{HH}$ = 5.32 Hz, OH), 6.01 (q, $^3J_{HH}$ = 6.45 Hz, 1H, ^{1}CH), 6.24 (d, $^2J_{HH}$ = 13.0 Hz, 2H, $^{2'}$CH$_2$), 6.94 (bd, $^3J_{HH}$ = 6.65 Hz, 2H, NH), 7.16 (s, 1H, ^{4}CH), 7.59 (s, 1H, ^{7}CH)

^{13}C NMR (DMSO-d$_6$): δ [ppm] = 22.7 (^{2}C), 55.5 ($^{2''}$C), 61.0 ($^{1''}$C, $^{3''}$C), 67.7 (^{1}C), 104.1 ($^{2'}$C), 105.3 (^{4}C), 106.3 (^{7}C), 136.4 (^{5}C), 141.7 (^{6}C), 147.6 (^{7a}C), 152.9 (^{3a}C), 155.6 (OCONH)

HRMS (ESI): m/z calcd. for C$_{13}$H$_{16}$N$_2$O$_8$Na$^+$ 351.0804, obsd. 351.0807 [M+Na]$^+$

FT-IR (ATR): $\tilde{v}$ (cm^{-1}) = 3387 (m; C-OH), 3334 (m; N-H), 3059 (w; C-H$_{Ar}$), 2956 (w; C-H$_{Alk}$), 2920 (w; C-H$_{Alk}$), 2876 (w; C-H$_{Alk}$), 1689 (m; C=O), 1616 (w; C=C$_{Ar}$), 1500 (s; C-NO$_2$), 1450 (w; C-H$_{Alk}$), 1421 (w; C-H$_{Alk}$), 1394 (w; O-H), 1379 (w; O-H), 1332 (m; C-H$_{Alk}$), 1315 (s; C-NO$_2$), 1257 (s; C-O-C), 1068 (m; C-OH), 1032 (s; C-OH), 930 (m; C-H$_{Ar}$), 874 (m; C-H$_{Ar}$), 822 (w; C-H$_{Ar}$)

3.3.4 Synthesis of piperonal-based polyurethane **4** and **5**

In a Schlenk-tube **3** (328 mg; 1 mmol) and dibutyltin dilaurate (DBTDL; 0.5 wt%) were dissolved in dimethylformamide (DMF; 1 mL) under N$_2$-atmosphere. After the solution was heated to 70 °C under stirring, isophorone diisocyanate (IPDI; 0.22 mL; 1.05 mmol) was added dropwise. The solution was stirred at 70 °C for 3 d and stopped by the addition of methanol (MeOH; 0.2 mL). Precipitation from MeOH yielded a light-yellow powder **4** (280 mg; 50%).
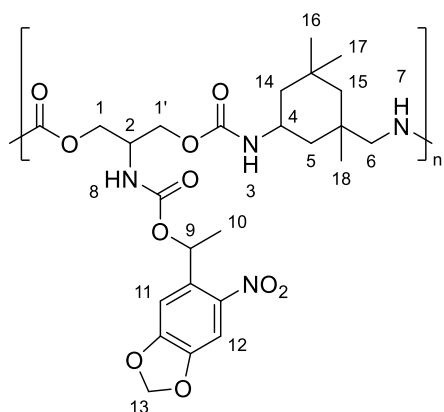
^{1}H NMR (DMSO-d6): δ [ppm] = 0.67-1.15 (m, 13H, ^{16}CH$_3$, ^{17}CH$_3$, ^{18}CH$_3$, ^{14}CH$_2$, ^{15}CH$_2$), 1.30-1.68 (m, 5H, ^{10}CH$_3$, ^{5}CH$_2$), 2.59-2.84 (m, 2H, ^{6}CH$_2$), 3.43-3.66 (m, 1H, ^{4}CH), 3.68-4.12 (m, 5H, ^{1}CH$_2$, $^{1'}$CH$_2$, ^{2}CH), 5.97-6.10 (m, 1H, ^{9}CH), 6.22 (m, 2H, ^{13}CH$_2$), 6.81-7.26 (m, 3H, ^{11}CH, ^{3}NH, ^{7}NH), 7.28-7.48 (m, 1H, ^{8}NH), 7.57 (m, 1H, ^{12}CH)

In a Schlenk-tube **3** (300 mg; 0.91 mmol) and DBTDL (0.5 wt%) were dissolved in DMF (1 mL) under N$_2$-atmosphere. Under stirring, hexamethylene diisocyanate (HDI; 0.15 mL; 0.95 mmol) was added dropwise. The solution was stirred at room temperature for 1 d and stopped by the addition of MeOH (0.2 mL). Precipitation from MeOH yielded a light-yellow powder **5** (250 mg; 54%).
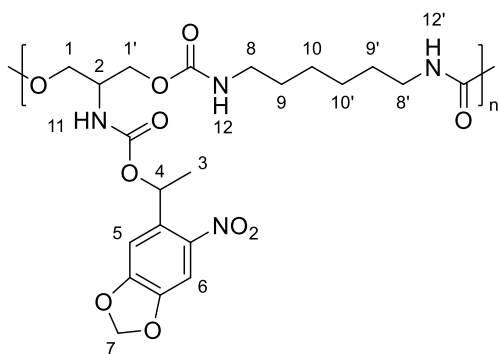
^{1}H NMR (DMSO-d6): δ [ppm] = 1.22 (s, 4H, $^{10}CH_2$, $^{10'}CH_2$), 1.35 (s, 4H, $^9CH_2$, $^{9'}CH_2$), 1.49 (d, $^3J_{HH}$ = 6.33 Hz, 3H, $^3CH_3$), 2.93 (m, 4H, $^8CH_2$, $^{8'}CH_2$), 3.86 (m, 5H, $^1CH_2$, $^{1'}CH_2$, ^2CH), 6.02 (q, $^3J_{HH}$ = 6.38 Hz, 1H, ^4CH), 6.22 (s, 2H, $^7CH_2$), 6.98-7.15 (m, 3H, ^{12}NH, $^{12'}NH$, ^5CH), 7.36 (d, $^3J_{HH}$ = 7.36 Hz, 1H, ^{11}NH), 7.57 (s, 1H, ^6CH)

3.3.5   Synthesis of piperonal-based polyester **6**

In a Schlenk-tube **3** (300 mg; 0.91 mmol) was dissolved in pyridine (1 mL) under N$_2$-atmosphere and added to DMF (3 mL). To that mixture adipoyl chloride (0.15 mL; 1 mmol) dissolved in DCM (2 mL) was added and stirred at room temperature overnight. The polymerization was stopped by addition of MeOH (0.2 mL) and precipitation from MeOH yielded a colorless powder (312 mg; 74%).
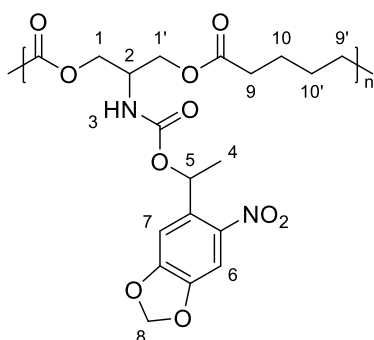
^{1}H NMR (DMSO-d6): δ [ppm] = 1.36-1.57 (m, 7H, $^{10}CH_2$, $^{10'}CH_2$, $^4CH_3$), 2.06-2.35 (m, 4H, $^9CH_2$, $^{9'}CH_2$), 3.8-4.09 (m, 5H, $^1CH_2$, $^{1'}CH_2$, ^2CH), 6.00 (m, 1H, ^5CH), 6.20 (m, 2H, $^8CH_2$), 7.09 (s, 1H, ^3NH), 7.47 (m, 1H, ^7CH), 7.55 (m, 1H, ^6CH)

3.3.6 Synthesis of piperonal-based polycarbonate **7**

In a Schlenk-flask, triphosgene (100 mg; 0.32 mmol) was dissolved in DCM (0.6 mL) under Argon-atmosphere. A solution of **3** (300 mg; 0.91 mmol) in pyridine (0.9 mL) was added dropwise over 90 min. After complete addition, the mixture was allowed to stir additional 2.5 h. The polymer was purified by precipitation into EtOH and dried *in vacuo* giving **7** (278 mg; 71%).
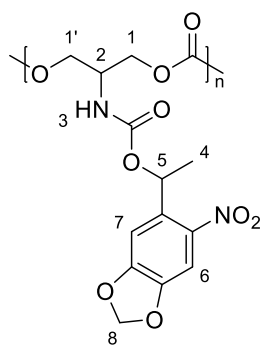
^{1}H NMR (DMSO-d6): δ [ppm] = 1.45-1.55 (m, 3H, ^{4}CH$_3$), 3.80-3.96 (m, 1H, ^{2}CH), 3.96-4.25 (m, 4H, ^{1}CH$_2$, $^{1'}$CH$_2$), 5.96-6.08 (m, 1H, ^{5}CH), 6.11-6.29 (m, 2H, ^{8}CH), 7.05-7.18 (m, 1H, ^{3}NH), 7.49-7.75 (m, 2H, ^{6}CH, ^{7}CH)

### 3.3.7 UV-light degradation of light-responsive polymers

Polymer stock solutions were prepared in DCM with a concentration of 25 mg/L for UV/Vis spectroscopy and a concentration of 800 mg/L for SEC analysis. For each analysis method, 3 mL of stock solution was added into a quartz cuvette and irradiated for different time intervals with UV light. The irradiated solution was directly placed into the UV/Vis spectrometer or the solution was removed and redissolved in the SEC solvent and measured subsequently.

3.3.8 Synthesis of 3-(pyridin-2-yldisulfaneyl)propane-1,2-diol **8**

This reaction was adapted from literature.[170] In short, 2,2'dipyridyldisulfide (2.914 g; 13.2 mmol; 1.4 eq.) was dissolved in anhydrous ethanol (40 mL) and α-thioglycerol (1 g; 9.25 mmol; 1 eq.) was added. The mixture was stirred at room temperature overnight and the solvent was removed by rotary evaporation. The crude mixture was purified by column chromatography on silica gel with ethyl

acetate (EtOAc) as eluent. The colorless product was obtained (R_f = 0.21; 1.24 g; 65%).

T_m = 65 °C
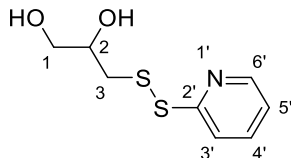
^{1}H NMR (DMSO-d6): δ [ppm] = 2.78 (dd, $^2J_{HH}$ = 13.9 Hz, $^3J_{HH}$ = 9.8 Hz, 1H, $^3CH_2$), 2.99 (dd, $^2J_{HH}$ = 13.9 Hz, $^3J_{HH}$ = 2.8 Hz, 1H, $^3CH_2$), 3.57 (dd, $^2J_{HH}$ = 11.3 Hz, $^3J_{HH}$ = 6.1 Hz, 1H, $^1CH_2$), 3.71 (dd, $^2J_{HH}$ = 11.3 Hz, $^3J_{HH}$ = 3.6 Hz, 1H, $^1CH_2$), 3.84 (m, 1H, ^2CH), 4.68 (t, $^3J_{HH}$ = 5.7 Hz, 1H, OH), 5.11 (d, $^3J_{HH}$ = 5.3 Hz, 1H, OH), 7.14 (ddd, $^3J_{HH}$ = 7.4 Hz, $^3J_{HH}$ = 5.0 Hz, $^4J_{HH}$ = 1.0 Hz, 1H, $^{5'}CH$) 7.38 (dt, $^3J_{HH}$ = 8.1 Hz, $^4J_{HH}$ = 1.0 Hz, 1H, $^{3'}CH$), 7.57 (ddd, $^3J_{HH}$ = 8.0 Hz, $^3J_{HH}$ = 7.4 Hz, $^4J_{HH}$ = 1.8 Hz, 1H, $^{4'}CH$), 8.49 (ddd, $^3J_{HH}$ = 5.0 Hz, $^4J_{HH}$ = 1.8 Hz, $^5J_{HH}$ = 0.9 Hz, 1H, $^{6'}CH$)

^{13}C NMR (DMSO-d$_6$): δ [ppm] = 43.7 (^3C), 65.6 (^1C), 69.0 (^2C), 121.8 ($^{5'}C$), 122.2 ($^{4'}C$), 137.2 ($^{3'}C$), 149.9 ($^{6'}C$), 159.0 ($^{2'}C$)

HRMS (ESI): m/z calcd. for $C_8H_{11}NO_2S_2Na^+$ 240.01234, obsd. 240.0119 [M+Na]$^+$

FT-IR (ATR): ṽ (cm^{-1}) = 3308 (m; O-H), 3043 (w; C-H$_{Ar}$), 2923 (m; C-H$_{Alk}$), 2870 (m; C-H$_{Alk}$), 1578 (m; C=C), 1562 (m; C=C), 1448 (s; C=C; C=N), 1419 (s; C=C; C=N), 1394 (m; O-H), 1304 (w; C-O), 1277 (w; C-O), 1244 (w, C-O), 1082 (s; C-H$_{Ar}$), 1040 (s; C-H$_{Ar}$), 997 (s; C-C$_{Ar}$), 766 (s; C-H$_{Ar}$)

3.3.9 Synthesis of thioglycerol-based redox-responsive polyurethane **9**

In a Schlenk-tube **8** (197.5 mg; 0.91 mmol) and DBTDL (1 wt%) were dissolved in DMF (1 mL) under N$_2$-atmosphere. After the solution was heated to 70 °C under stirring, IPDI (0.2 mL; 1 mmol) was added dropwise. The solution was stirred at 70 °C for 3 d and stopped by the addition of MeOH (0.2 mL). Precipitation from MeOH yielded a light-yellow powder **4** (145 mg; 35%).
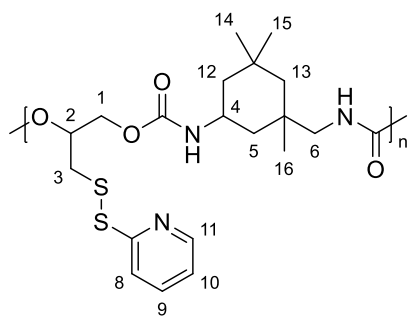
^{1}**H NMR (DMSO-d6):** δ [ppm] = 0.79-1.01 (m, 15H, $^5CH_2$, $^{12}CH_2$, $^{13}CH_2$, $^{14}CH_3$, $^{15}CH_3$, $^{16}CH_3$), 2.59-2.84 (m, 2H, $^6CH_2$), 2.94-3.20 (d, 2H, $^3CH_2$), 3.46-3.71 (m, 1H, ^4CH), 3.94-4.29 (m, 2H, $^1CH_2$). 4.89-5.09 (s, 1H, ^2CH), 6.95-7.29 (m, 3H, NH, NH, ^{10}CH), 7.68-7.84 (m, 2H, ^8CH, ^9CH), 8.45 (s, 1H, ^{11}CH)

3.3.10 Synthesis of thioglycerol-based redox-responsive polyester 10

In a Schlenk-tube **8** (197.5 mg; 0.91 mmol) was dissolved in pyridine (1 mL) under N_2-atmosphere and added to DMF (3 mL). To that mixture adipoyl chloride (0.15 mL; 1 mmol) dissolved in DCM (2 mL) was added and stirred at room temperature overnight. The polymerization was stopped by addition of MeOH (0.2 mL) and precipitation from MeOH. No polymer was obtained.

3.3.11 Synthesis of 4-nitrobenzyl (1,3-dihydroxypropan-2-yl)carbamate 11

In a round-bottom-flask serinol (0.91 g; 10 mmol; 1 eq.) was dissolved in MeCN (60 mL) while stirring. Afterwards, *p*NPCF (2.15 g; 10 mmol; 1 eq.) was added with the subsequent dropwise addition of diisopropyl ethylamine (DIPEA; 2 mL; 11.35 mmol; 1.13 eq.) under cooling. The reaction mixture was allowed to slowly heat up to room temperature und was stirred overnight. The solvent was removed by rotary evaporation and the residue was dissolved in EtOAc (100 mL) and washed three times with water (70 mL), followed by washing with sodium hydrogen carbonate solution (10%; 70 mL). The organic phase was dried with $MgSO_4$. After filtration the solvent was removed by rotary evaporation to give the product as a light-yellow solid (1.48 g; 55%).

T_m = 108 °C
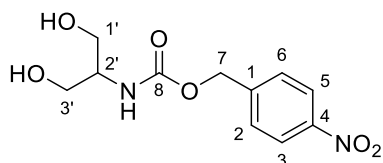
^{1}H NMR (DMSO-d6): δ [ppm] = 3.41 (m, 4H, $^{1'}CH_2$, $^{3'}CH_2$), 3.47 (m, 1H, $^{2'}CH$), 4.57 (t, $^3J_{HH}$ = 5.5 Hz, 2H, OH), 5.16 (s, 2H, $^7CH_2$), 7.00 (d, $^3J_{HH}$ = 7.8 Hz, 1H, NH), 7.62 (d, $^3J_{HH}$ = 8.8 Hz, 2H, ^2CH, ^6CH), 8.23 (d, $^3J_{HH}$ = 8.8 Hz, 2H, ^3CH, ^5CH)

^{13}C NMR (DMSO-d6): δ [ppm] = 55.1 ($^{2'}C$), 60.4 ($^{1'}C$, $^{3'}C$), 64.0 (^7C), 123.5 (^3C, ^5C), 128.1 (^2C, ^6C), 145.3 (^1C), 146.9 (^4C), 155.6 (^8C)

HRMS (ESI): m/z calcd. for $C_{11}H_{14}N_2O_6Na^+$ 293.0744, obsd. 293.0742 [M+Na]$^+$

FT-IR (ATR): ṽ (cm^{-1}) = 3338 (m; O-H), 3271 (m; N-H), 3117 (w; C-H$_{Ar}$), 3095 (w; C-H$_{Ar}$), 2964 (w; C-H$_{Alk}$), 2937 (w; C-H$_{Alk}$), 2887 (w; C-H$_{Alk}$), 2862 (w; C-H$_{Alk}$), 1686 (s; C=O), 1610 (m; C=C), 1518 (s; C-NO$_2$), 1468 (w; C-H$_{Alk}$), 1456 (w; C-H$_{Alk}$), 1389 (w; O-H), 1346 (s; C-NO$_2$), 1309 (s; C-O), 1236 (s; C-N$_{Alk}$), 1045 (s; C-O), 844 (m; C-H$_{Ar}$)

3.3.12 Synthesis of 2-(pyridin-2-yldisulfaneyl)ethan-1-ol **12**

2-Mercaptoethanol (2.24 g; 28.7 mmol; 1 eq.) was added to a solution of 2,2'-dipyridyl disulfide (9.49 g; 43.1 mmol; 1.5 eq.) in MeOH (30 mL). The mixture was stirred at room temperature overnight, then the reaction solvent was removed by rotary evaporation and redissolved in DCM (100 mL). The solution was washed with an aqueous solution of sodium hydroxide (NaOH; 10% w/v; 70 mL) and brine (70 mL). The product was purified on a silica gel column with EtOAc:DCM (20:80) and isolated as a yellow oil (4.13 g; 77%; R$_f$ = 0.47).
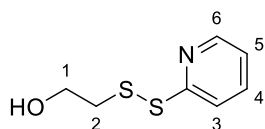
^{1}H NMR (CDCl₃): δ [ppm] = 2.93 (t, $^3J_{HH}$ = 5.2 Hz, 2H, $^2CH_2$), 3.78 (t, $^3J_{HH}$ = 5.2 Hz, 2H, $^1CH_2$), 4.25 (bs, 1H, OH), 7.12 (ddd, $^3J_{HH}$ = 7.4 Hz, $^3J_{HH}$ = 5.0 Hz, $^4J_{HH}$ = 1.0 Hz, 1H, ^5CH), 7.40 (dt, $^3J_{HH}$ = 8.1 Hz, $^4J_{HH}$ = 1.0 Hz, 1H, ^3CH), 7.56 (ddd, $^3J_{HH}$ = 8.0 Hz, $^3J_{HH}$ = 7.4 Hz, $^4J_{HH}$ = 1.8 Hz, 1H, ^4CH), 8.48 (ddd, $^3J_{HH}$ = 5.0 Hz, $^4J_{HH}$ = 1.8 Hz, $^5J_{HH}$ = 0.9 Hz, 1H, ^6CH)

3.3.13 Synthesis of 4-nitrophenyl (2-(pyridin-2-yldisulfaneyl)ethyl) carbonate **13**

A solution of **12** (1.00 g; 7.35 mmol; 1 eq.) in MeCN (40 mL) and TEA (0.8 mL; 8.09 mmol; 1.1 eq.) was cooled to 0 °C. Afterwards, pNPCF (1.24 g; 8.89 mmol; 1.21 eq.) was added and the reaction mixture was stirred overnight. After concentration by rotary evaporation, the residue was purified in a silica gel column with EtOAc:DCM (1:1). The product was afforded as a yellowish oil (1.45 g; 77%; R_f = 0.45).
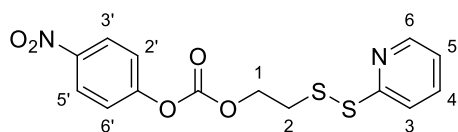
^{1}H NMR (CDCl$_3$): δ [ppm] = 3.15 (t, $^3J_{HH}$ = 6.4 Hz, 2H, ^{2}CH$_2$), 4.54 (t, $^3J_{HH}$ = 6.4 Hz, 2H, ^{1}CH$_2$), 7.12 (ddd, $^3J_{HH}$ = 7.0 Hz, $^3J_{HH}$ = 4.9 Hz, $^4J_{HH}$ = 1.5 Hz, 1H, ^{5}CH), 7.36 (d, $^3J_{HH}$ = 9.3 Hz, 2H, $^{2'}$CH, , $^{6'}$CH), 7.66 (dd, $^3J_{HH}$ = 7.0 Hz, $^4J_{HH}$ = 1.8 Hz, 1H, ^{4}CH), 7.69 (dt, $^3J_{HH}$ = 8.1 Hz, $^4J_{HH}$ = 1.2 Hz, 1H, ^{3}CH), 8.25 (d, $^3J_{HH}$ = 9.3 Hz, 2H, $^{3'}$CH, $^{5'}$CH), 8.47 (ddd, $^3J_{HH}$ = 4.9 Hz, $^4J_{HH}$ = 1.7 Hz, $^5J_{HH}$ = 1.0 Hz, 1H, ^{6}CH)

3.3.14 Synthesis of 2-(pyridin-2-yldisulfaneyl)ethyl (1,3-dihydroxypropan-2-yl)carbamate **14**

Serinol (2.94 g; 27.8 mmol; 1.5 eq.), **13** (6.52 g; 18.5 mmol; 1. eq.) and TEA (9.66 mL; 69.4 mmol; 3.75 eq.) were suspended in dry MeCN (140 mL). The reaction mixture was stirred overnight. After concentration under vacuum, the residue was purified using column chromatography with silica gel and a mixture of EtOAc:DCM (2:1) to remove side products and flush with acetone to elute the desired product (4.34 g; 77%; R_f = 0.6).

T_m = 81 °C
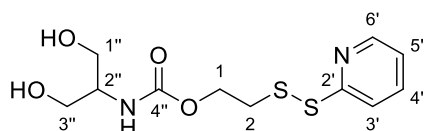
^{1}H NMR (DMSO-d6): δ [ppm] = 3.07 (t, $^3J_{HH}$ = 6.2 Hz, 2H, ^{2}CH$_2$), 3.40 (m, 5H, $^{1''}$CH$_2$, $^{3''}$CH$_2$, $^{2''}$CH), 4.15 (t, $^3J_{HH}$ = 6.2 Hz, 2H, ^{1}CH$_2$), 4.57 (t, $^3J_{HH}$ = 5.5 Hz, 2H,

OH), 6.82 (bd, $^3J_{HH}$ = 7.6 Hz, 1H, NH), 7.24 (ddd, $^3J_{HH}$ = 7.3 Hz, $^3J_{HH}$ = 4.8 Hz, $^4J_{HH}$ = 1.0 Hz, 1H, $^{5'}$CH), 7.79 (d, $^3J_{HH}$ = 8.1 Hz, 1H, $^{3'}$CH), 7.83 (dt, $^3J_{HH}$ = 7.7 Hz, $^4J_{HH}$ = 1.8 Hz, 1H, $^{4'}$CH), 8.45 (ddd, $^3J_{HH}$ = 4.8 Hz, $^4J_{HH}$ = 1.7 Hz, $^5J_{HH}$ = 0.8 Hz, 1H, $^{6'}$CH)

^{13}C NMR (DMSO-d$_6$): δ [ppm] = 37.5 (^{2}C), 55.0 ($^{2''}$C), 60.5 ($^{1''}$C, $^{3''}$C), 61.4 (^{1}C), 119.3 (^{3}C), 121.2 (^{5}C), 137.9 (^{4}C), 149.6 (^{6}C), 155.6 ($^{4''}$C), 159.1 (^{2}C)

HRMS (ESI): m/z calcd. for $C_{11}H_{16}N_2O_4S_2Na^+$ 327.0444, obsd. 327.0441 [M+Na]$^+$

FT-IR (ATR): ṽ (cm^{-1}) = 3294 (s; O-H), 3055 (w; C-H$_{Ar}$), 2931 (m; C-H$_{Alk}$), 2876 (m; C-H$_{Alk}$), 1687 (s; C=O), 1578 (m; C=C), 1555 (m; C=C), 1461 (m; C-H$_{Alk}$), 1448 (s; C=C; C=N), 1419 (s; C=C; C=N), 1404 (m; O-H), 1384 (m; O-H), 1317 (m; C-O), 1247 (s; C-N$_{Alk}$), 1080 (s; C-H$_{Ar}$), 1026 (s; C-O), 985 (s; C-C$_{Ar}$), 766 (s; C-H$_{Ar}$)

3.3.15 Synthesis of serinol-based redox-responsive polyurethanes **15**, **16** and **14**

In a Schlenk-tube **8** (246 mg; 0.91 mmol) and DBTDL (1 wt%) were dissolved in DMF (1 mL) under N$_2$-atmosphere. After the solution was heated to 70 °C under stirring, IPDI (0.2 mL; 1 mmol) was added dropwise. The solution was stirred at 70 °C for 1°d to be found solidified.

In a Schlenk-tube **11** (135 mg; 0.5 mmol), 1,4-benzenedimethanol (BDM; 70 mg; 0.5 mmol) and DBTDL (1 wt%) were dissolved in DMF (4 mL) under N$_2$-atmosphere. After the solution was heated to 70 °C under stirring, IPDI (0.2 mL; 1 mmol) was added dropwise. The solution was stirred at 70 °C for 3 d and stopped by the addition of MeOH (0.2 mL). Precipitation from MeOH yielded a light-yellow powder **15** (92 mg; 22%).

Experimental part
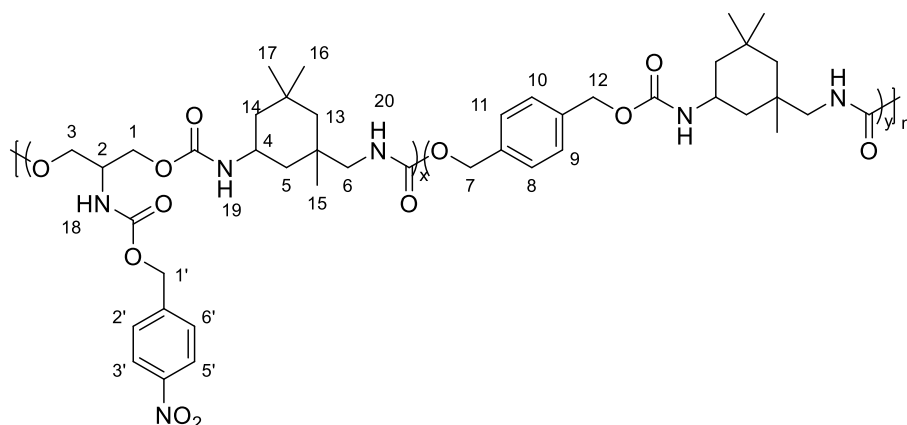
¹H NMR (DMSO-d6): δ [ppm] = 0.80-1.02 (m, 30H, $^5CH_2$, $^{13}CH_2$, $^{14}CH_2$, $^{15}CH_3$, $^{16}CH_3$, $^{17}CH_3$), 2.64-2.81 (m, 4H, $^6CH_2$), 3.54-3.65 (m, 2H, ^4CH), 3.84-4.07 (m, 5H, $^1CH_2$, $^3CH_2$, ^2CH), 4.93-5.05 (m, 4H, $^7CH_2$, $^{12}CH_2$), 5.11-5.23 (s, 2H, $^{1'}CH_2$), 6.94-7.25 (m, 5H, ^{18}NH, ^{19}NH, ^{20}NH), 7.30-7.35 (s, 4H, ^8CH, ^9CH, ^{10}CH, ^{11}CH), 7.56-7.64 (d, 2H, $^{2'}CH$, $^{6'}CH$), 8.19-8.26 (d, 2H, $^{3'}CH$, $^{5'}CH$)

In a Schlenk-tube **14** (152.2 mg; 0.5 mmol), BDM (70 mg; 0.5 mmol) and DBTDL (1 wt%) were dissolved in DMF (4 mL) under N₂-atmosphere. After the solution was heated to 70 °C under stirring, IPDI (0.1 mL; 0.5 mmol) was added dropwise. The solution was stirred at 70 °C for 2°d and stopped by the addition of MeOH (0.2 mL). Precipitation from MeOH yielded a light-yellow powder **16** (72 mg; 16%).
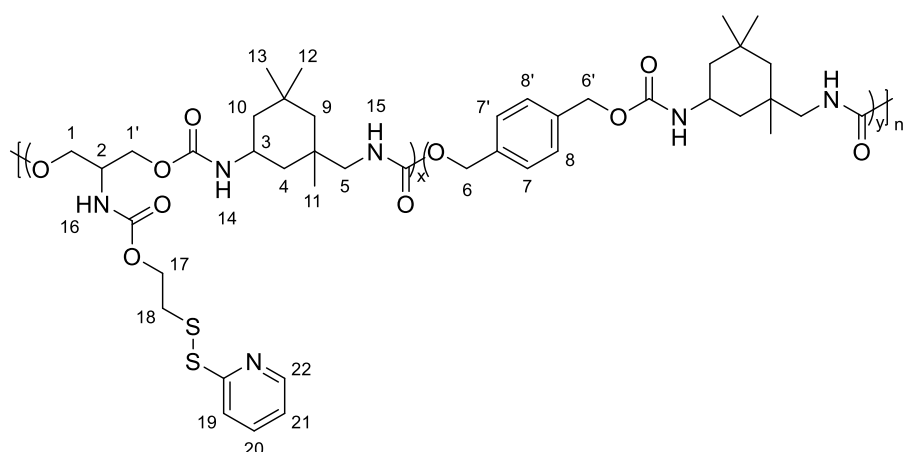
¹H NMR (DMSO-d6): δ [ppm] = 0.81-1.02 (m, 30H, $^4CH_2$, $^9CH_2$, $^{10}CH_2$, $^{11}CH_3$, $^{12}CH_3$, $^{13}CH_3$), 2.66-2.79 (m, 4H, $^5CH_2$), 3.01-3.11 (t, 2H, $^{18}CH_2$), 3.54-3.66 (m, 2H, ^3CH), 3.80-4.07 (m, 5H, $^1CH_2$, $^{1'}CH_2$, ^2CH), 4.12-4.22 (t, 2H, $^{17}CH_2$), 4.91-5.06 (m, 4H, $^6CH_2$, $^{6'}CH_2$), 5.11-5.23 (s, 2H, $^{1'}CH_2$), 6.99-7.18 (m, 5H, ^{14}NH, ^{15}NH),

7.20-7.26 (m, 2H, ^{16}NH, ^{21}CH), 7.30-7.36 (s, 4H, ^{7}CH, $^{7'}$CH, ^{8}CH, $^{8'}$CH), 7.74-7.79 (m, 1H, ^{19}CH), 7.79-7.84 (m, 1H, ^{20}CH), 8.42-8.48 (m, 1H, ^{22}CH)

3.3.16 Synthesis of (2-phenyl-1,3-dioxane-5,5-diyl)dimethanol 17

Pentaerythritol (5.00 g; 36.7 mmol) was dissolved in water (36 mL) at 60 °C. The solution was cooled to room temperature and conc. hydrochloric acid (HCl; 0.2 mL) was added followed by slow addition of benzaldehyde (0.2 mL; 2 mmol). After precipitation, another load of benzaldehyde (4.5 mL; 44.5 mmol) was added dropwise and the reaction was stirred for 3 h. The precipitate was filtered off and washed several times with ice-cold sodium carbonate solution (5%) and ice-cold diethyl ether. Two recrystallizations from toluene gave the product as a white solid (5.19 g; 63%).

T_m = 135 °C
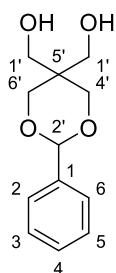
^{1}H NMR (DMSO-d6): δ [ppm] = 3.25 (d, $^{3}J_{HH}$ = 4.0 Hz 2H, $^{1'}$CH$_2$), 3.67 (d, $^{3}J_{HH}$ = 4.6 Hz, 2H, $^{1'}$CH$_2$), 3.79 (d, $^{2}J_{HH}$ = 11.6 Hz, 2H, $^{4'}$CH$_2$, $^{6'}$CH$_2$), 3.91 (d, $^{2}J_{HH}$ = 11.6 Hz, 2H, $^{4'}$CH$_2$, $^{6'}$CH$_2$), 4.52 (t, $^{3}J_{HH}$ = 4.8 Hz, 1H, OH), 4.60 (t, $^{3}J_{HH}$ = 4.8 Hz, 1H, OH), 5.40 (s, 1H, $^{2'}$CH), 7.35 (m, 3H, ^{3}CH, ^{4}CH, ^{5}CH), 7.41 (m, 2H, ^{2}CH, ^{6}CH)

^{13}C NMR (DMSO-d6): δ [ppm] = 39.1 ($^{5'}$C). 59.5 ($^{1'}$C), 61.0 ($^{1'}$C), 69.1 ($^{4'}$C, $^{6'}$C), 100.7 ($^{2'}$C), 126.2 (^{2}C, ^{6}C), 128.0 (^{3}C, ^{5}C), 128.6 (^{4}C), 138.8 ($^{2'}$C)

HRMS (ESI): m/z calcd. for $C_{12}H_{16}O_4Na^+$ 247.0941, obsd. 247.0937 [M+Na]$^+$

FT-IR (ATR): ṽ (cm^{-1}) = 3273 (m; O-H), 3234 (m; O-H), 3055 (w; C-H$_{Ar}$), 2968 (w; C-H$_{Alk}$), 2881 (w; C-H$_{Alk}$), 2856 (w; C-H$_{Alk}$), 2829 (w; C-H$_{Alk}$), 1597 (w; C=C$_{Ar}$), 1553 (w; C=C$_{Ar}$), 1497 (w; C=C$_{Ar}$), 1473 (w; C-H$_{Alk}$), 1454 (m; C-H$_{Alk}$), 1385 (s; O-H), 1242 (w; C-H$_{Alk}$), 1151 (m; C-O-C), 1101 (m; C-O-C), 1038 (s; C-O), 746 (s; C-H$_{Ar}$), 696 (s; C-H$_{Ar}$)

3.3.17 Synthesis of (2-(6-nitrobenzo[d][1,3]dioxol-5-yl)-1,3-dioxane-5,5-diyl)dimethanol **18**

Pentaerythritol (2.5 g; 18.4 mmol) was dissolved in water (36 mL) at 60 °C. The solution was cooled down to 30 °C and conc. HCl (0.2 mL) was added, followed by the addition of 6-nitropiperonal (0.82 mmol, 160 mg). After precipitation, more 6-nitropiperonal (1.38 g; 18.5 mmol) was added and stirred for 3 d at 60 °C. Afterwards, the filtered product was recrystallized two times from toluene:tetrahydrofuran (9:1) and gave the dark yellow product (3.80 g; 66%)

T_m = 178-181 °C
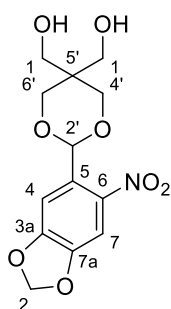
¹H NMR (DMSO-d6): δ [ppm] = 3.23 (s, 2H, $^1CH_2$), 3.60 (s, 2H, $^1CH_2$), 3.79 (d, $^2J_{HH}$ = 11.6 Hz, 2H, $^{4'}CH_2$, $^6CH_2$), 3.88 (d, $^2J_{HH}$ = 11.5 Hz, 2H, $^{4'}CH_2$, $^6CH_2$), 4.53 (s, 1H, OH), 4.59 (s, 1H, OH), 5.83 (s, 1H, $^{2'}CH$), 6.23 (s, 2H, ^2CH), 7.18 (s, 1H, ^4CH), 7.56 (s, 1H, ^7CH)

¹³C NMR (DMSO-d₆): δ [ppm] = 39.5 ($^{5'}C$), 59.9 (^1C), 61.2 (^1C), 69.3 ($^{4'}C$, ^6C), 96.6 ($^{2'}C$), 103.9 (^2C), 105.5 (^7C), 106.4 (^4C), 128.9 (^5C), 142.6 (^6C), 148.1 (^{7a}C), 151.4 (^{3a}C)

HRMS (ESI): m/z calcd. for $C_{13}H_{15}NO_8Na^+$ 336.0690, obsd. 336.0688 [M+Na]⁺

FT-IR (ATR): $\tilde{v}$ (cm⁻¹) = 3319 (m; O-H), 3263 (m; O-H), 3099 (w; C-H$_{Ar}$), 3078 (w; C-H$_{Ar}$), 2941 (w; C-H$_{Alk}$), 2877 (w; C-H$_{Alk}$), 1612 (w; C-H$_{Ar}$), 1519 (s; C-NO₂), 1435 (s; C-H$_{Alk}$), 1329 (s; C-NO₂), 1269 (s; C-O-C), 1242 (w; C-H$_{Alk}$), 1226 (w; C-H$_{Alk}$), 1176 (w; C-H$_{Alk}$), 1140 (s; C-O$_{Alk}$), 1095 (m; C-O-C), 1039 (s; C-O),

3.3.18 Synthesis of acetal-based acid-responsive polyurethanes **19** and **20**

In a Schlenk-tube **17** (112 mg; 0.5 mmol), BDM (70 mg; 0.5 mmol) and DBTDL (1 wt%) were dissolved in DMF (4 mL) under N_2-atmosphere. After the solution was heated to 40 °C under stirring, IPDI (0.2 mL; 1 mmol) was added dropwise. The solution was continuously stirred at 40 °C for 3 d and stopped by the addition of MeOH (0.2 mL). Precipitation from MeOH yielded a colorless powder **19** (252 mg; 62%).
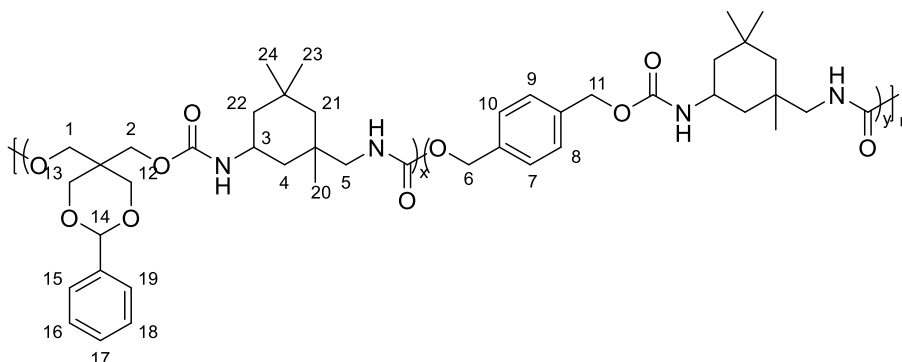
^{1}H NMR (DMSO-d6): δ [ppm] = 0.74-1.05 (m, 30H, $^4CH_2$, $^{20}CH_3$, $^{21}CH_2$, $^{22}CH_2$, $^{23}CH_3$, $^{24}CH_3$), 2.62-2.85 (m, 4H, $^5CH_2$), 3.54-3.67 (m, 2H, ^3CH), 3.71-3-91 (m, 4H, $^1CH_2$, $^2CH_2$), 3.92-4.38 (m, 4H, $^{12}CH_2$, $^{13}CH_2$), 4.86-5.09 (m, 4H, $^6CH_2$, $^{11}CH_2$), 4.87-5.08 (s, 1H, ^{14}CH), 6.97-7.26 (m, 4H, NH), 7.29-7.44 (m, 9H, ^7CH, ^8CH, ^9CH, ^{10}CH, ^{15}CH, ^{16}CH, ^{17}CH, ^{18}CH, ^{19}CH)

In a Schlenk-tube **18** (156 mg; 0.5 mmol), BDM (70 mg; 0.5 mmol) and DBTDL (1 wt%) were dissolved in DMF (4 mL) under N_2-atmosphere. After the solution was heated to 40 °C under stirring, IPDI (0.2 mL; 1 mmol) was added dropwise. The solution was stirred at 40 °C for 1 d and stopped by the addition of MeOH (0.2 mL). Precipitation from MeOH yielded a colorless powder **20** (372 mg; 83%).
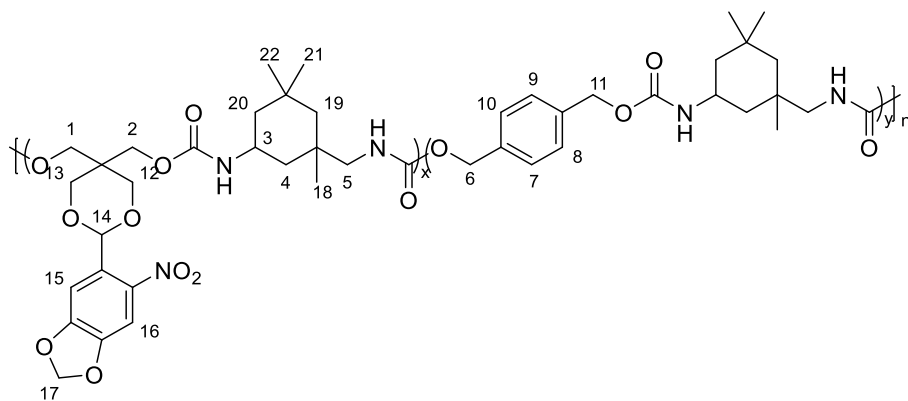
¹H NMR (DMSO-d6): δ [ppm] = 0.82-1.03 (m, 30H, $^4CH_2$, $^{18}CH_3$, $^{19}CH_2$, $^{20}CH_2$, $^{21}CH_3$, $^{22}CH_3$), 2.66-2.82 (m, 4H, $^5CH_2$), 3.56-3.63 (m, 2H, ^3CH), 3.71-4.33 (m, 8H, $^1CH_2$, $^2CH_2$, $^{12}CH_2$, $^{13}CH_2$), 4.90-5.12 (m, 4H, $^6CH_2$, $^{11}CH_2$), 5.85-5.97 (s, 1H, ^{14}CH), 6.15-6.28 (s, 2H, $^{17}CH_2$), 6.85-7.25 (m, 5H, NH, ^{15}CH), 7.26-7.37 (m, 4H, ^7CH, ^8CH, ^9CH, ^{10}CH), 7.51-7.61 (s, 1H, ^{16}CH)

4 Results and discussion

This chapter is divided into three parts devoted to the different triggers. Each of these parts is again divided into the following parts: monomer synthesis, polymer synthesis and degradation studies.

4.1 Light-responsive self-accelerating polymers

The light-responsive polymers are based on 6-nitropiperonal (6NP) and serinol. First, the 6NP needs to be converted to a secondary alcohol. After this, the alcohol should be activated by *para*-nitrophenyl chloroformate (*p*NPCF) to be coupled to the amine functionality of the serinol in the subsequent step. This monomer will be polymerized yielding either a polycarbonate, a polyester or a polyurethane.

4.1.1 Monomer synthesis

The first step of the monomer synthesis is the reductive methylation of 6NP with trimethylaluminum (Me₃Al). Me₃Al exists as a dimer and is a highly reactive organoaluminium compound that reacts violently with water or the moisture from the air and can lead to ignition of this compound. Therefore, it is necessary to work under dry conditions and be extremely cautious while handling this substance. The final aqueous workup is especially dangerous as already a few drops can lead to a heavy exothermic reaction potentially causing an overflow of the reaction mixture and thus endangerment of the operator as well as the equipment in the fume hood. The synthesis of 1-(6-methylbenzo[d][1,3]dioxol-5-yl)ethan-1-ol (**1**) is summarized in *Scheme 28*.
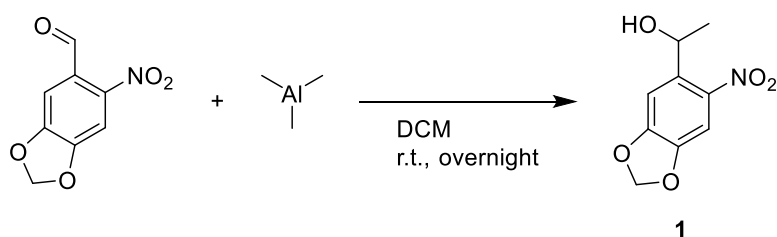
*Scheme 28: Synthesis of **1**: flame dried equipment, in DCM and hexane, stirred under ice-cooling, dropwise addition of Me₃Al under N₂-atmosphere; stirred overnight and dropwise addition of water to deactivate unreacted Me₃Al; filtrated and washed with brine and distilled water followed by column chromatography.*

The yield of 86% is that high due to the high reactivity of Me_3Al. A small percentage of the yield was lost in the sludge that was created by the addition of water. This sludge was hard to filtrate due to the high viscosity and insolubility and therefore some product could remain in the sludge. The next step in the monomer synthesis was the activation of the secondary alcohol of **1** leading to 6-nitrobenzo[d][1,3]dioxol-5-yl)ethyl (4-nitrophenyl) carbonate **2** (*Scheme 29*).
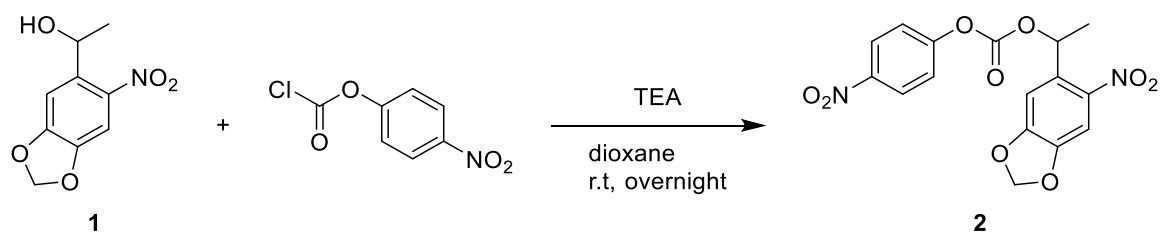
*Scheme 29: Synthesis of **2**: pNFCP and **1** were dissolved in dioxane under ice-cooling following the slow addition of TEA under N_2-atmosphere.*

This reaction was performed with triethylamine (TEA) to neutralize the hydrochloric acid in this condensation reaction. The product was dissolved in DCM and precipitated in *iso*-propanol (*i*PrOH) several times until sufficient purity with a yield of 72% was achieved.

The last step of the synthesis of the monomer 1-(6-nitrobenzo[d][1,3]dioxol-5-yl)ethyl (1,3-dihydroxypropan-2-yl)carbamate **3** is the coupling of **2** to serinol with acetonitrile (MeCN) as solvent. Again, TEA was used which started the reaction (*Scheme 30*).
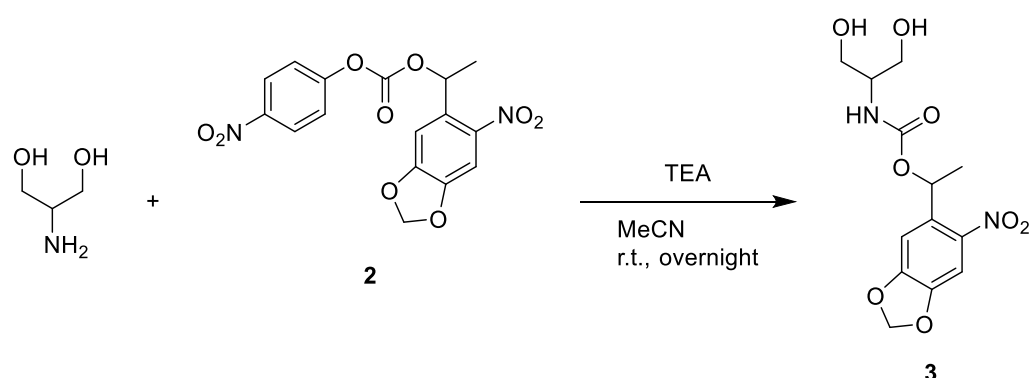
*Scheme 30: Synthesis of **3**: serinol and **2** were suspended in MeCN with a dropwise addition of TEA under stirring; the product was filtered off and recrystallized from acetone.*

This synthesis was facile because the product is insoluble in MeCN and precipitates. After filtration the product was collected and the residual solvent was removed by

rotary evaporation. The residue was recrystallized from acetone and combined with the first fraction with a total yield of 78%. Monomer **3** was obtained after three facile steps with a total yield of 48%.

The monomer structure was determined by NMR spectroscopy and ESI-ToF-MS. In accordance with the structural similarity to 6NP, monomer **3** was analyzed by UV/Vis spectroscopy to see which wavelength was needed for the excitation of the 6NP-group to trigger the deprotection of the amine functionality of serinol. The absorbance of the monomer is depicted in *Figure 4.*
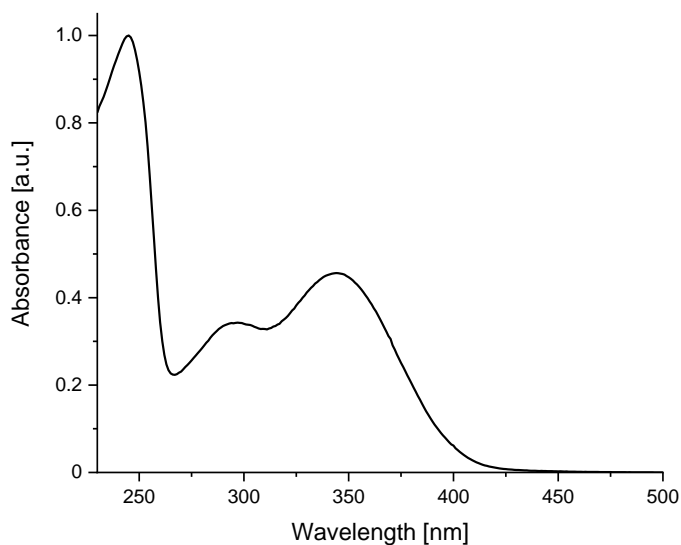
*Figure 4: UV/Vis spectrum of monomer **3**.*

The three absorbance maxima are located at 245 nm, 296 nm and 345 nm (measured in DCM). The three absorbance maxima of the starting molecule (6-nitropiperonal) are located at 260 nm, 309 nm and 350 nm. The absorbance maxima of monomer **3** are at a lower wavelength than the absorbance maxima of 6-nitropiperonal but are still at a higher wavelength in comparison to piperonal ($\lambda_{max,1}$ = 233 nm, $\lambda_{max,2}$ = 273 nm and $\lambda_{max,3}$ = 312 nm, *Figure 5*).
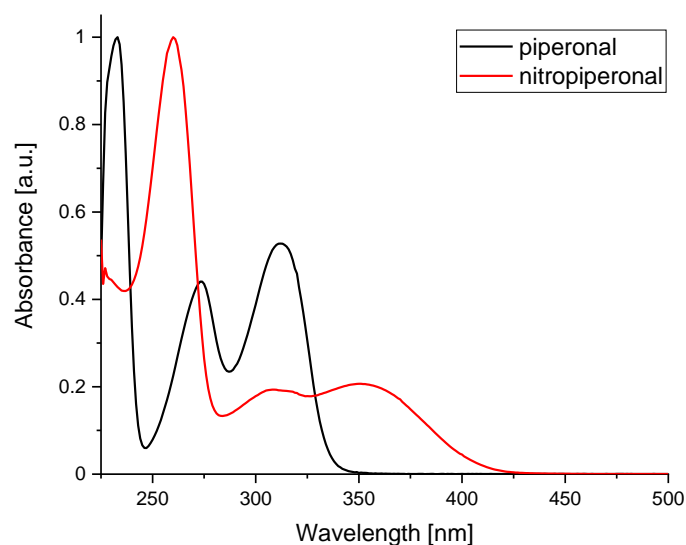
Figure 5: UV/Vis spectrum of piperonal and 6-nitropiperonal.

4.1.2   Polymer synthesis

Monomer **3** was used in two different polymerization techniques and four different polymers were synthesized in total. The first polymerization technique that was applied was the polycondensation with adipoyl chloride to obtain polyester **6** (*Scheme 31*).
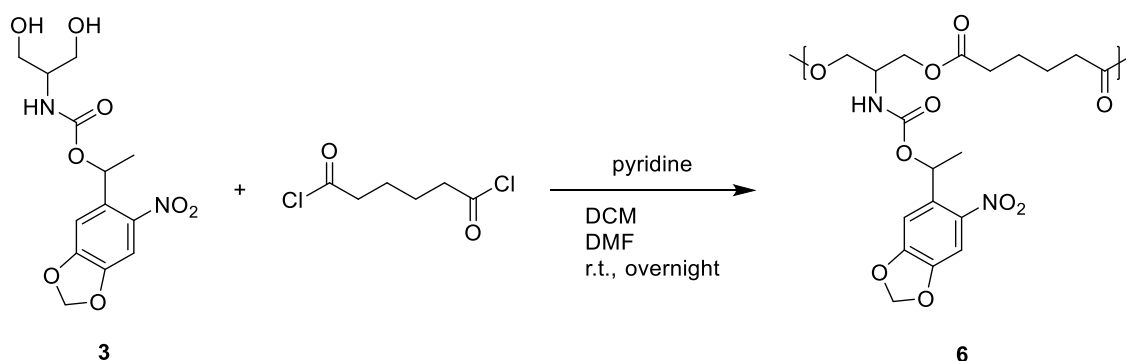
*Scheme 31: Synthesis of polymer **6**: monomer **3** was dissolved in pyridine and added to DMF in a Schlenk-flask followed by the dropwise addition of adipoyl chloride in DCM. The mixture was stirred overnight at room temperature and the polymer was precipitated from MeOH.*

The yield of this polymerization reaction was around 74% and typical M_n obtained with this technique were about 6400 – 8300 g/mol with a dispersity of 1.8 – 2.1 (measured by SEC in THF, *Figure 6*).
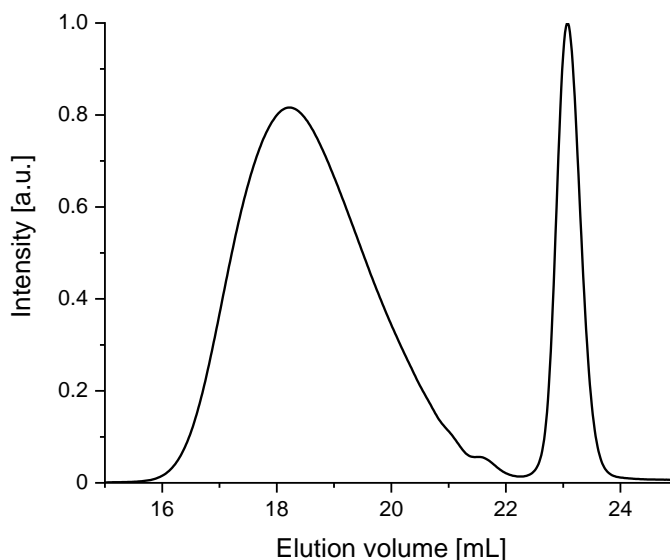
*Figure 6: SEC elugram of polymer **6**.*

The elugram shows a monomodal, but broad signal spanning from 16 – 22 mL. The polymer had a light-yellow color and was analyzed by NMR spectroscopy, SEC and UV/Vis spectroscopy. A typical absorbance pattern of these light-responsive polyesters (LrPEs) is depicted in *Figure 7*.
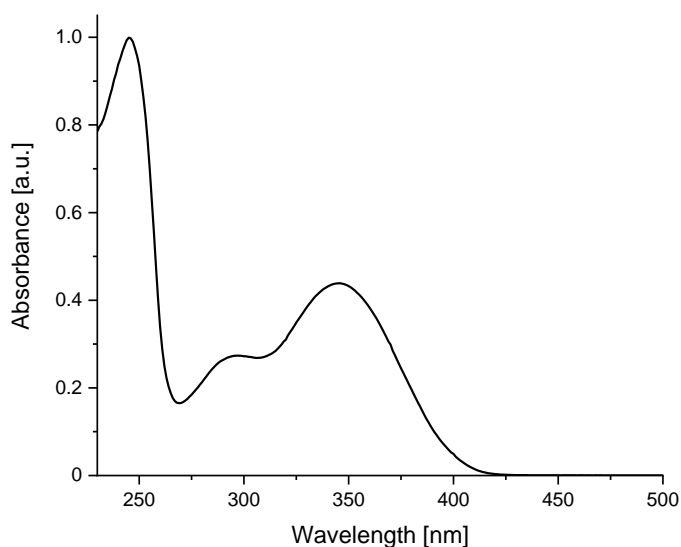
*Figure 7: UV/Vis spectrum of polymer **6**.*

The absorbance maxima are located at $\lambda_{max,1} = 245$ nm, $\lambda_{max,2} = 297$ nm and $\lambda_{max,3} = 346$ nm (measured in DCM). These maxima are nearly on the same wavelengths as in the monomer **3** ($\lambda_{max,1} = 245$ nm, $\lambda_{max,2} = 296$ nm and $\lambda_{max,3} = 345$ nm). This polymer was further used for the degradation studies.

After the successful polycondensation with adipoyl chloride, another polycondensation with triphosgene was tested. Triphosgene is a highly reactive

and commonly used substance to obtain polycarbonates by the reaction with diols. Triphosgene was used with monomer **3** to obtain a light-responsive polycarbonate (LrPC) **7** (*Scheme 32*).
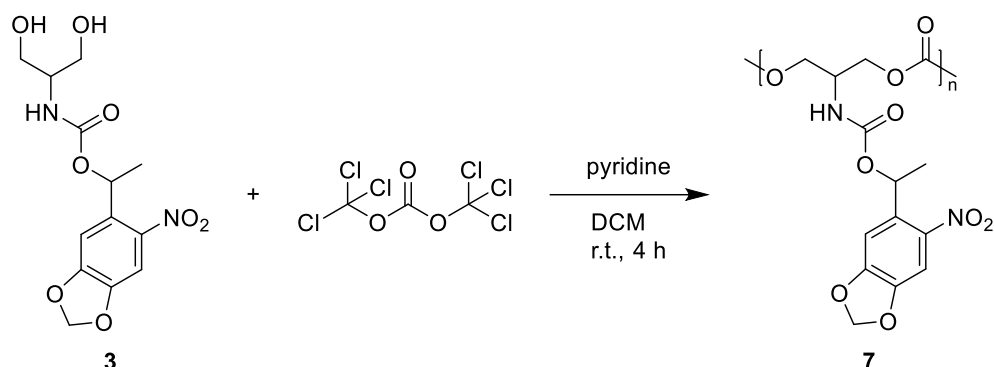
*Scheme 32: Synthesis of polymer **7**: to a solution of triphosgene in DCM, a solution of **3** in pyridine was added dropwise over 90 min and stirred for 2.5 h. The polymer was precipitated from EtOH.*

The yield of these polymerization reactions was around 70%, but the molar mass was only ranging from 1700 g/mol to 3200 g/mol with a dispersity of 1.24 – 1.5 (measured *via* SEC in THF, *Figure 8*).
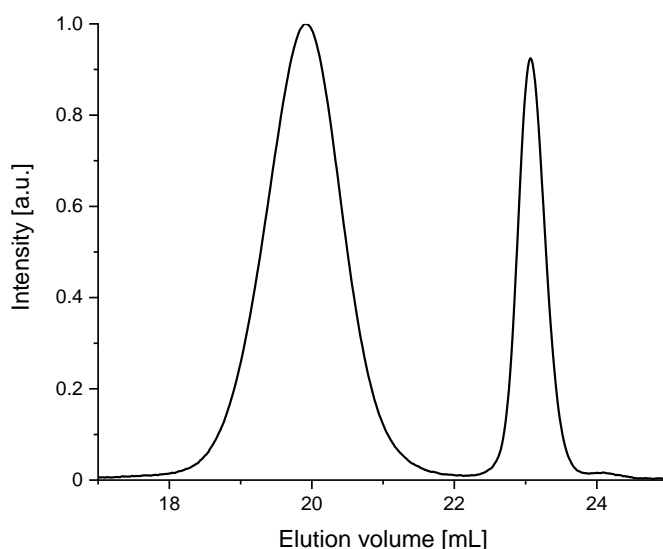
*Figure 8: SEC elugram of polymer **7**.*

These polymers were analyzed by NMR spectroscopy, SEC and UV/Vis spectroscopy. The absorbance maxima were on the same wavelengths as for monomer **3** and LrPE **6.** The absorbance spectrum is depicted in *Figure 9*.
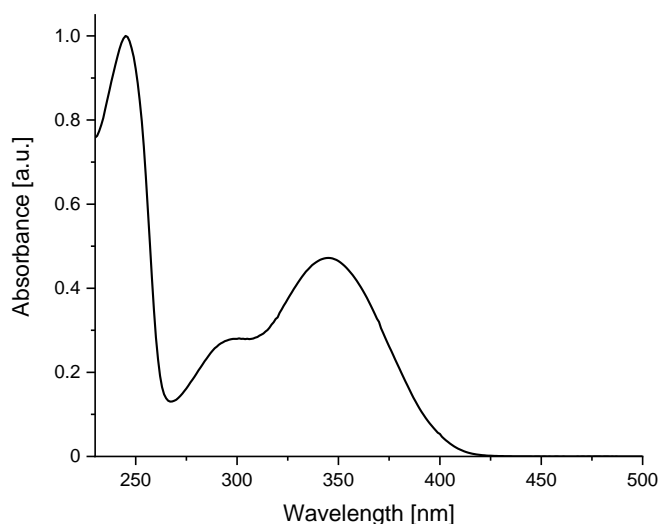
Figure 9: UV/Vis spectrum of polymer 7.

The maxima are located at $\lambda_{max,1}$ = 245 nm, $\lambda_{max,2}$ = 298 nm and $\lambda_{max,3}$ = 345 nm. Though the LrPCs showed a smaller molar mass in comparison to the LrPEs (1700 – 3200 g/mol vs. 6400 – 8300 g/mol) some degradation studies were still performed.

The second polymerization technique was the polyaddition with **3** and diisocyanates. Two diisocyanates were tested, hexamethylene diisocyanate (HDI) and isophorone diisocyanate (IPDI). The reaction with **3** and HDI is depicted in *Scheme 33*.
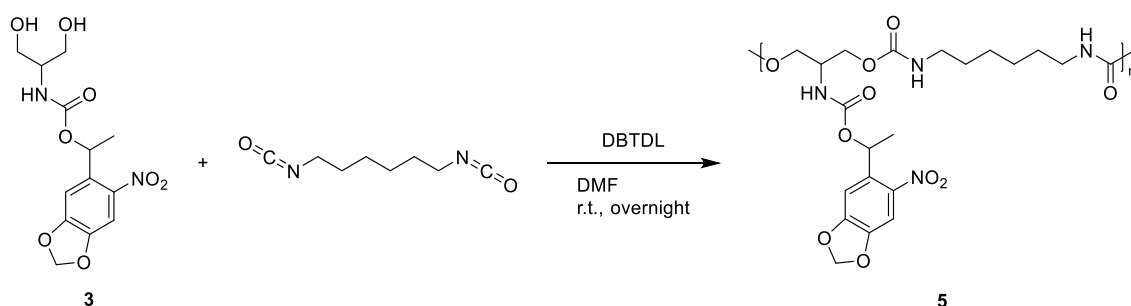
Scheme33: Synthesis of polymer 5: DBTDL and monomer 3 were dissolved in DMF under N₂-atmosphere and HDI was added dropwise under stirring. The reaction mixture was stirred at room temperature overnight and precipitated from MeOH.

The yield of this polymerization is 54% and the molar mass is in the range of 5100 g/mol with a dispersity of 1.3 (measured in THF, *Figure 10*).
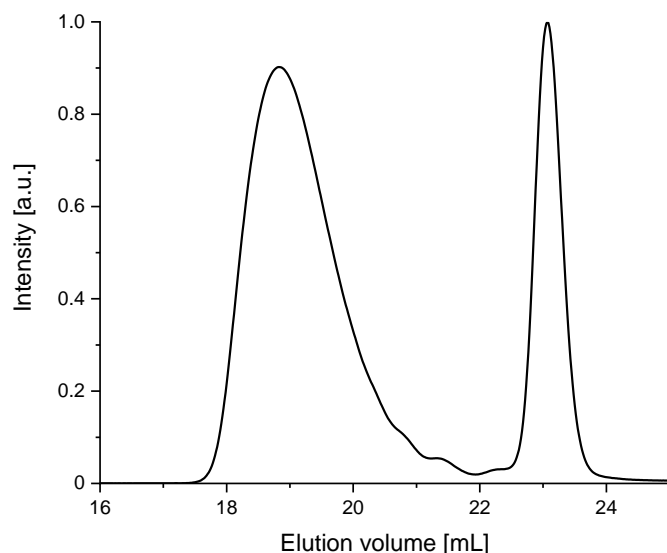
*Figure 10: SEC elugram of polymer **5**.*

This light-responsive polyurethane with HDI in the backbone (LrPU$_{HDI}$) was analyzed by NMR spectroscopy, SEC and UV/Vis spectroscopy. The absorbance pattern of LrPU$_{HDI}$ is shown in *Figure 11*.
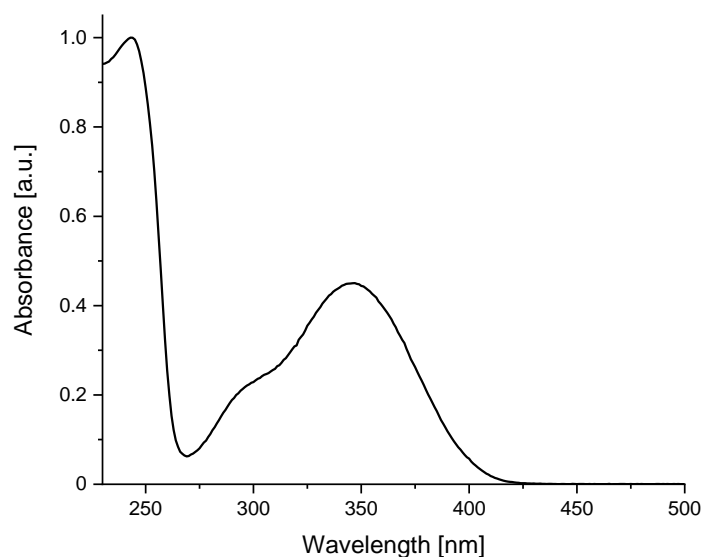
*Figure 11: UV/Vis spectrum of polymer **5**.*

One absorbance maximum is located at $\lambda_{max,3} = 243$ nm and the other at $\lambda_{max,3} = 347$ nm. The other maximum that was located at 297 nm in the other polymers could not be seen clearly. There was a shoulder to the left of the absorbance maximum at 347 nm indicating that the other maximum might be around 300 nm.

The last light-responsive polyurethane with IPDI (LrPU$_{IPDI}$) in the backbone was synthesized in the same fashion as the LrPU$_{HDI}$, but at 70 °C instead of room

temperature and the reaction time was longer (3 d instead of 1 d). The synthesis of polymer **4** is depicted in *Scheme 34*.
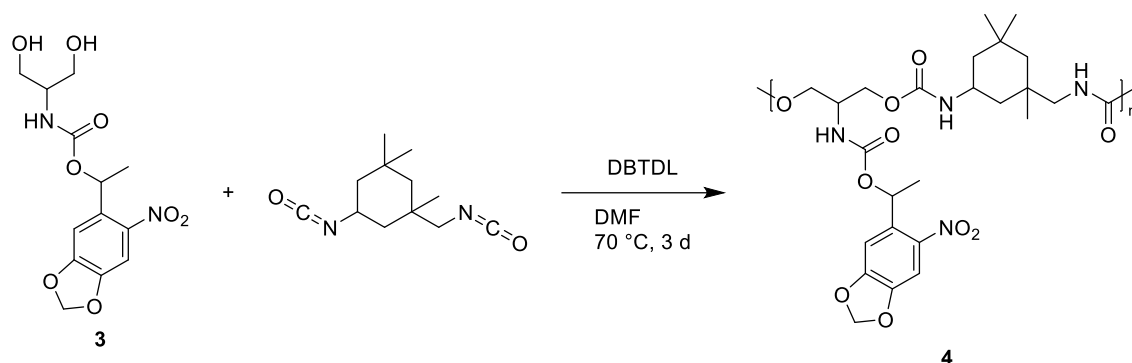
*Scheme 34: Synthesis of polymer **4**: DBTDL and monomer **3** were dissolved in DMF under N_2-atmosphere and IPDI was added dropwise under stirring. The reaction mixture was stirred at 70 °C for 3 d and precipitated from MeOH.*

The polymer was analyzed by NMR spectroscopy, SEC and UV/Vis spectroscopy. The molar mass of the polymer was around 4400 – 6600 g/mol with a dispersity ranging between 1.39 – 1.90 (measured *via* SEC in THF, *Figure 12*).
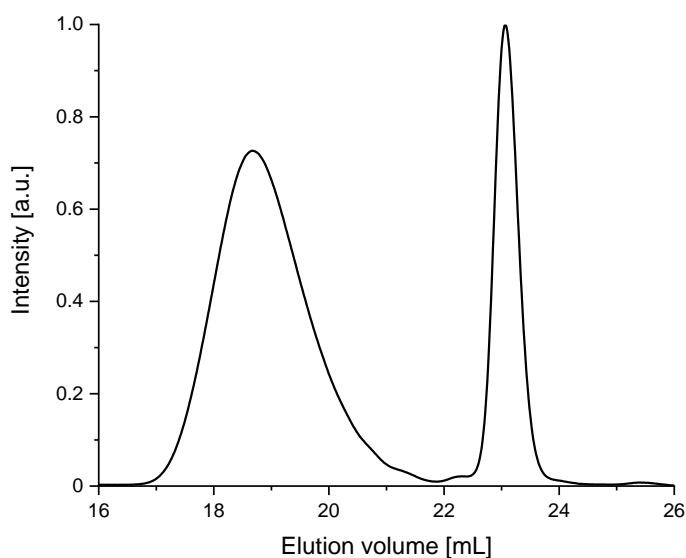
*Figure 12: SEC elugram of polymer **4**.*

The absorbance curve looks very similar to the previous ones, but all maxima can clearly be found (*Figure 13*).
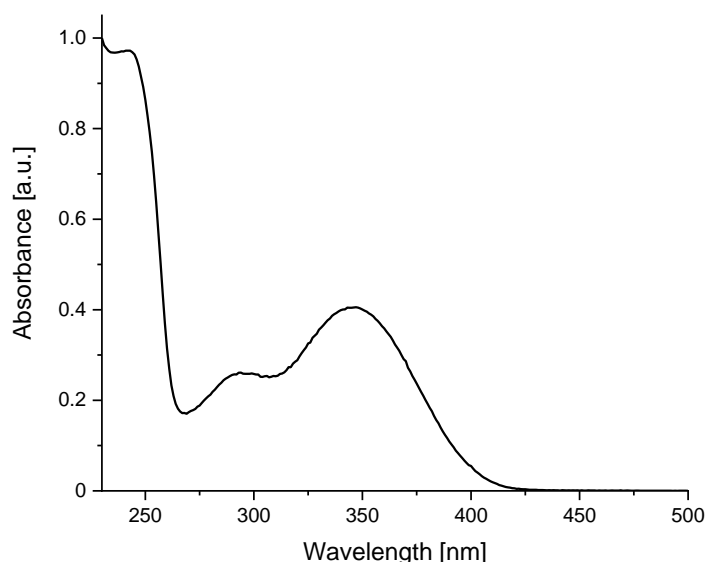
*Figure 13: UV/Vis spectrum of polymer **4**.*

The absorbance maxima of the light-yellow powdered polymer **4** were at $\lambda_{max,1}$ = 243 nm, $\lambda_{max,2}$ = 294 nm and $\lambda_{max,3}$ = 347 nm (measured in DCM). All of these four presented polymers were used for the UV-degradation studies in the next chapter.

4.1.3 Degradation studies

An easily applicable trigger is light. The previously shown polymers were dissolved in DCM in a concentration of 25 mg/L to be analyzed by UV/Vis spectroscopy. For the degradation analysis with SEC, the polymers were dissolved in DCM with a concentration of 800 mg/L. The polymer solutions were irradiated in a quartz cuvette with a wavelength of 320 – 480 nm and an intensity of 297 mW/cm^2 for a specific amount of time between 0 – 240 s. After the irradiation, the cuvette was either placed in the UV/Vis spectrometer or the solution was removed by rotary evaporation and the residue was redissolved in the SEC solvent to be measured. Different analysis techniques were applied to the polymer solutions and the different light-responsive polymers were compared.

In the UV/Vis spectroscopy, the absorbance of an analyte is measured at certain wavelengths. By measuring the solvent in which the analyte will be dissolved, the background is measured and can be subtracted from future measurements. This way, only the absorbance of the analyte can be obtained. A quartz cuvette is normally used to lower the absorbance cutoff for the measuring cell. Different

solvents also have different UV/Vis absorbance cutoffs. The solvent that was used during these degradation tests was DCM with a cutoff of 220 nm.[171] The first sample was irradiated for 15 s as previous light-responsive polymers and after the second irradiation step no change in the UV/Vis spectrum was observed. Therefore, the polymer solution was irradiated for a total of 10 s in 1 s steps. After each irradiation, the absorbance of the polymer solution was measured. The first light-responsive polymer that was analyzed was polyester **6**. The UV/Vis spectrum of the irradiation series and the cleavage reaction is shown in *Figure 14*.
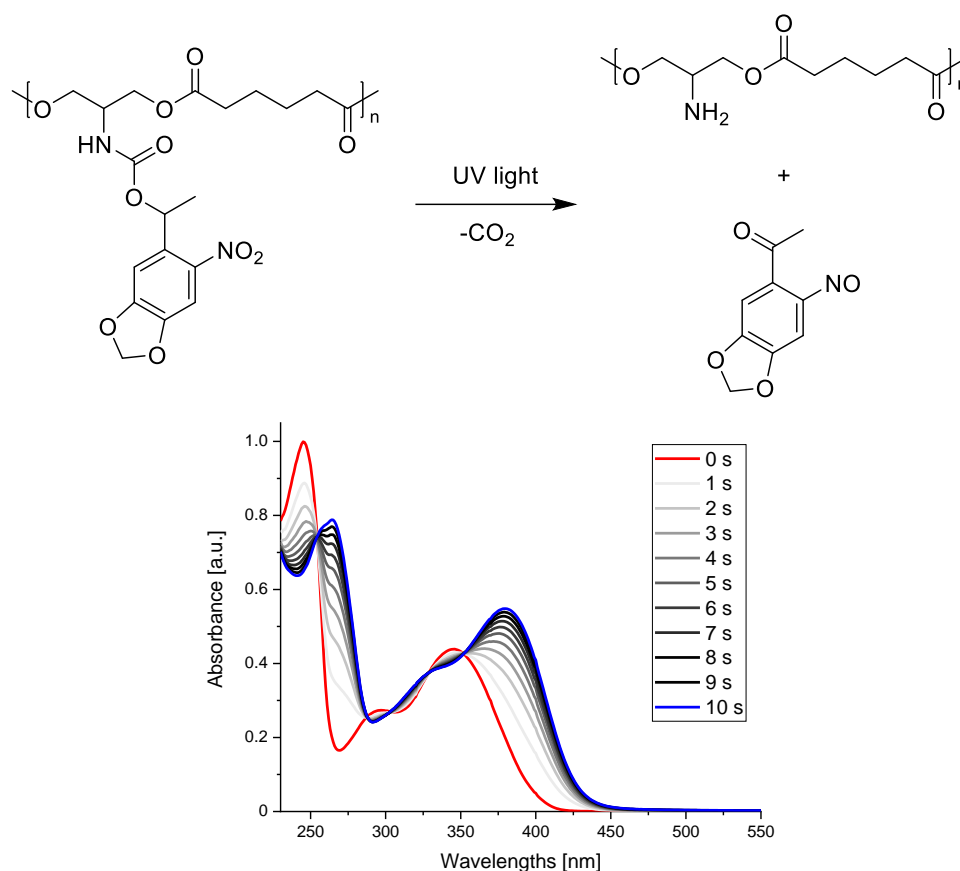
*Figure 14: UV/Vis spectrum of an irradiation series of the light-responsive polyester **6**.*

The absorbance curve of the non-irradiated polymer sample is depicted in red with its previously described absorbance maxima ($\lambda_{max,1}$ = 245 nm, $\lambda_{max,2}$ = 297 nm and $\lambda_{max,3}$ = 346 nm). These maxima were heavily reduced in absorbance the longer the sample was irradiated. All of the maxima shifted to higher wavelengths. The first absorbance maximum $\lambda_{max,1}$ shifted from 245 nm to approximately 265 nm and the third absorbance maximum $\lambda_{max,3}$ shifted from 346 nm to 381 nm. The shift of $\lambda_{max,2}$ could not be displayed, as no clear maximum could be observed. The overall process is surprisingly fast, compared

to the longer irradiation times needed in previous works.[128] The UV cleavage of the previously published light-responsive polymers took up to 240 s to reach a point where the change in absorbance is minimal. In polymer **6** however, the UV cleavage seems to be much faster. The absorbance of the measurement after 9 s of irradiation and after 10 s of irradiation has only an insignificant change indicating a high conversion of the UV cleavage. The UV light induced polymer degradation was analyzed by SEC. Therefore, a stock solution of the polymer in DCM was irradiated for different amounts of time (0 s, 30 s, 90 s, 150 s and 240 s) and the solvent was subsequently removed by rotary evaporation after each step. Afterwards, the residues were dissolved in the THF with BHT as standard and measured (*Figure 15*).
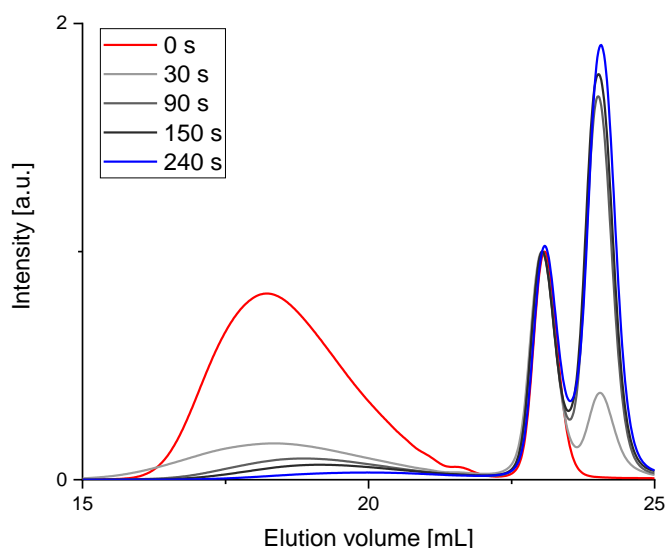
Figure 15: SEC elugram of the irradiation induced degradation series of polymer
***9**.*

The initial signal loses intensity after 30 s of irradiation. However, a new signal emerges at 24 mL. After 90 s, the polymer signal decreases in the intensity and shifts to a higher elution volume. The intensity of the signal that came after BHT increases drastically. The signals after 150 s of irradiation follow the same trend. After 240 s of irradiation there is almost no polymer signal present and the signal in the small molecular regime is at its maximum. This indicates a successful polymer degradation induced by UV light.

The same UV/Vis cleavage analysis was carried out on the light-responsive polycarbonate **7**. The cleavage reaction and the UV/Vis spectrum of the irradiation series is depicted in *Figure 16*.
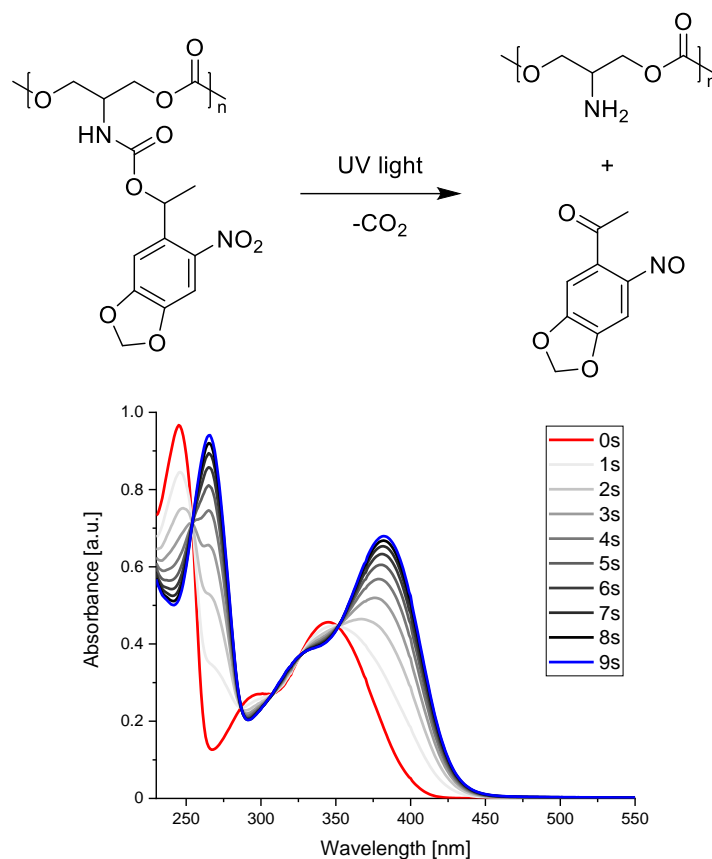
Figure 16: UV/Vis spectrum of an irradiation series of the light-responsive polycarbonate 7.

Similar to the UV cleavage of the polyester **6**, the polycarbonate **7** showed a similar behavior in the absorbance of the irradiation series. All of the absorbance maxima shift towards longer wavelengths. The first absorbance maximum before the irradiation $\lambda_{max,1}$ shifted from 245 nm to approximately 265 nm and $\lambda_{max,3}$ shifted from 346 nm to 382 nm. The second absorbance maximum $\lambda_{max,2}$ shifted also to higher wavelengths, but no clear maximum could be observed. This shift and the new maxima are nearly on the same wavelengths as in the irradiation series of polyester **6** indicating that all of the observed absorbance maxima are originating from the light-responsive leaving-group based on 6-nitropiperonal (6NP). The UV light induced polymer degradation was not tested, as polymer **7** consists of oligomers and cannot be compared to the other polymers.

Polymers **4** and **5** showed the same behavior upon irradiation as the previous polymers. The UV cleavage of the light-responsive polyurethane **5** bearing HDI in the backbone is depicted in *Figure 17*.
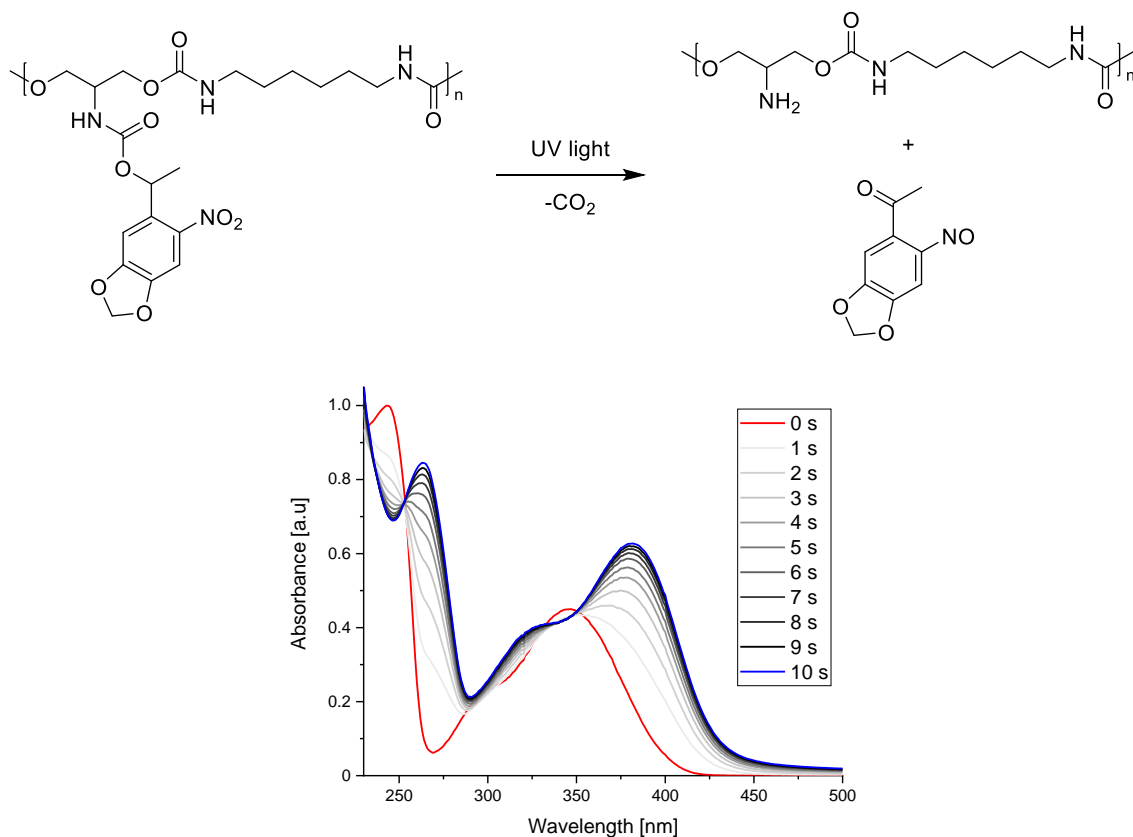
*Figure 17: UV/Vis spectrum of an irradiation series of the light-responsive polyurethane **5**.*

A similar shift of the absorbance maxima as well as a higher absorbance of the signals above 300 nm can be observed compared to the previous examples. The signals shifted about from 243 nm to 263 nm ($\lambda_{max,1}$) and from 347 nm to 382 nm ($\lambda_{max,3}$). The second absorbance maximum shifted from roughly 300 nm to roughly 325 nm. The signals after irradiation are on the same wavelengths as previous examples. Similar to polyester **6** (*Figure 15*), the UV light induced polymer degradation was analyzed by SEC (*Figure 18*).
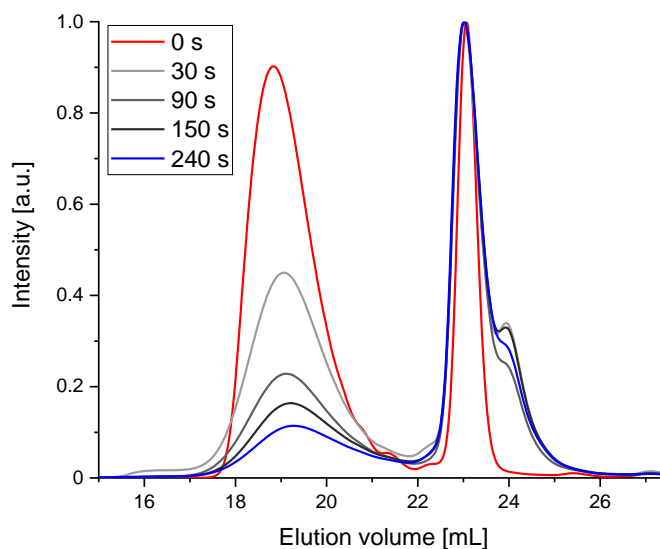
Figure 18: SEC elugram of the irradiation induced degradation series of polymer **4**.

A similar trend can be observed as for polymer **9**. The intensity of the polymer signal decreases with higher irradiation times. And again, a small molecular weight signal emerges after the BHT signal indicating the degradation. However, the intensity of the signal after the BHT is not proportional to the irradiation time as in the degradation series of polymer **9**. The shift of the signal to a higher elution volume is also lower compared to polymer **9**. This shift can be explained by the size of the degradation products. The degradation products of polymer **4** are slightly larger than the degradation products of polymer **9**.

The last light-responsive polyurethane is polymer **5** with IPDI incorporated in the backbone. This polymer was also analyzed like the previous polymers (*Figure 19*).
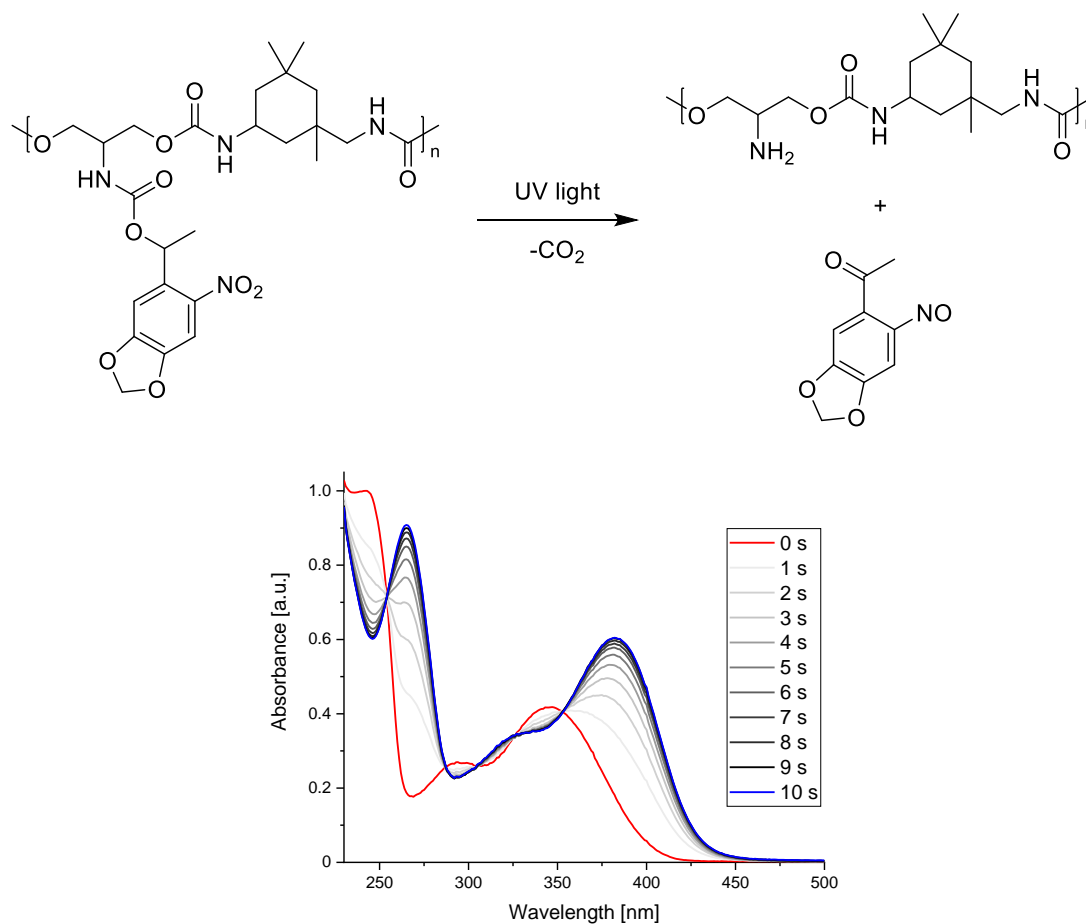
Figure 19: UV/Vis spectrum of an irradiation series of the light-responsive polyurethane 4.

The UV cleavage in polymer **5** shows the same behavior and the same shift compared to the UV cleavage of polymer **4**. Only two of the absorbance maxima can clearly be found. The first absorbance maximum shifted from 243 nm to 265 nm ($\lambda_{max,1}$) and the third maximum shifted from 347 nm to 382 nm ($\lambda_{max,3}$). The UV light induced polymer degradation by SEC is depicted in *Figure 20*.
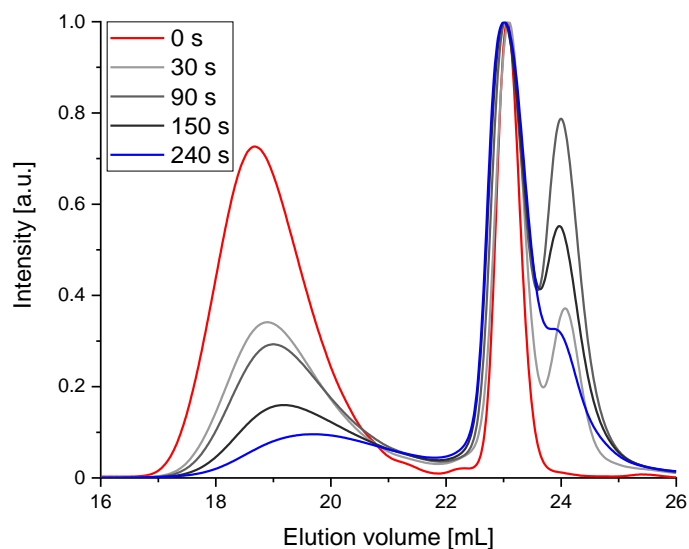
Figure 20: SEC elugram of the irradiation induced degradation series of polymer 5.

The light-responsive leaving group based on 6NP seems to behave similar independently from the comonomer. By taking the wavelengths of the global maximum at around 380 nm and measure the absorbance depending on irradiation time first order kinetics fitting can be obtained (*Figure 21*).
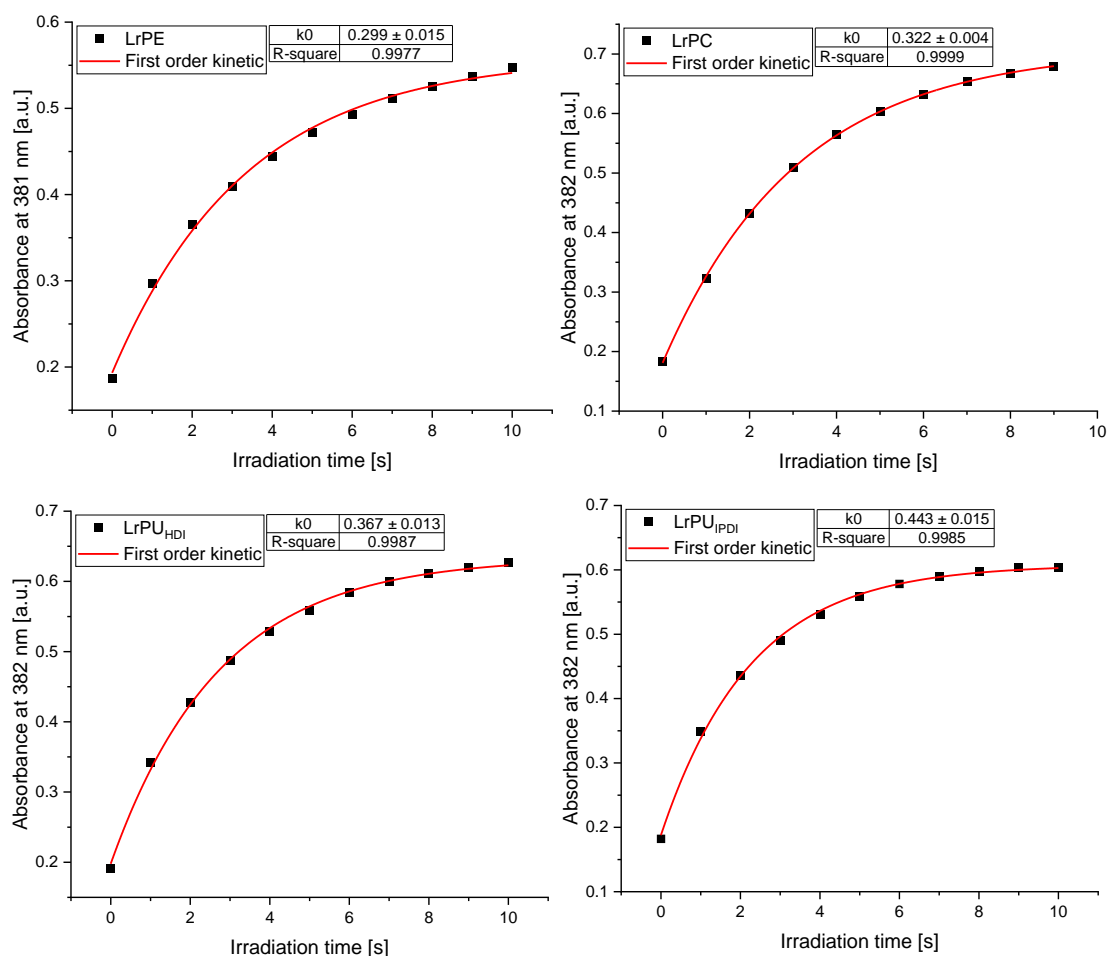
*Figure 21: UV/Vis spectra of the irradiation time vs. the absorbance at the wavelength of the individual maximum at around 380 nm of polymers **6** (top left), **7** (top right), **4** (bottom left) and **5** (bottom right).*

All of the UV cleavages have a relatively high reaction constant. Surprisingly, the reaction constant differs between different polymers and are ranging from 0.299 – 0.443 s^{-1} The reaction constants are summarized in *Table 2*.

Table 2: Summarized reaction constants for the specific light-responsive polymer.

Polymer	LrPE	LrPC	LrPU$_{HDI}$	LrPU$_{IPDI}$
Reaction constant [s^{-1}]	0.299 ± 0.015	0.322 ± 0.004	0.367 ± 0.013	0.443 ± 0.015

A clear tendency can be seen. First the constants between LrPE and LrPC will be discussed as the reaction constant is very similar ($k_{UV,6} = 0.299$ s^{-1} vs. $k_{UV,7} = 0.322$ s^{-1}). From the achieved data it is hard to find the reason and explain the data based on the structural differences without further variants of polyesters

and polycarbonates. The difference in the backbone of these two polymers is the 'linking unit'. An ester-group is less polar than a carbonate group. That may be the reason for the enhanced cleavage reaction of the leaving group. Going from the LrPC to the LrPU$_{HDI}$, the polarity becomes lower, but the carbamate group is more basic. The hydrogen atom from the carbamate could participate or catalyze the reaction. However, no investigations were conducted regarding this phenomenon. By comparing the reaction constant of LrPU$_{HDI}$ and LrPU$_{IPDI}$ a relatively big difference of 0.076 s^{-1} is observable ($k_{UV,5}$ = 0.443 s^{-1} and $k_{UV,4}$ = 0.367 s^{-1} for LrPU$_{IPDI}$ and LrPU$_{HDI}$, respectively). This difference may be due to the higher stiffness in the backbone of LrPU$_{IPDI}$ compared to the LrPU$_{HDI}$. To what extent this affects the UV cleavage cannot be explained and needs further experiments. All of these polymers exhibit a first order kinetic of the UV cleavage and only small differences are visible. The UV cleavage can also be analyzed by plotting the absorbance of specific irradiation times against each other to obtain absorbance differences (AD) diagrams.[171] The difference in absorbance at the growing maximum at approximately 260 nm was used as the x-axis. For this, the x-values are calculated for the example wavelength of 260 nm in the form of AD = A(λ_{260},t) − A(λ_{260},t$_0$). The y-axis consists of the AD at the specific irradiation time of the disappearance of the signals at roughly 245 nm and 345 nm and the appearance of the maxima at roughly 380 nm in the form of AD = A(λ_x,t) − A(λ_x,t$_0$). The AD diagrams of the four light-responsive polymers are depicted in *Figure 22*.
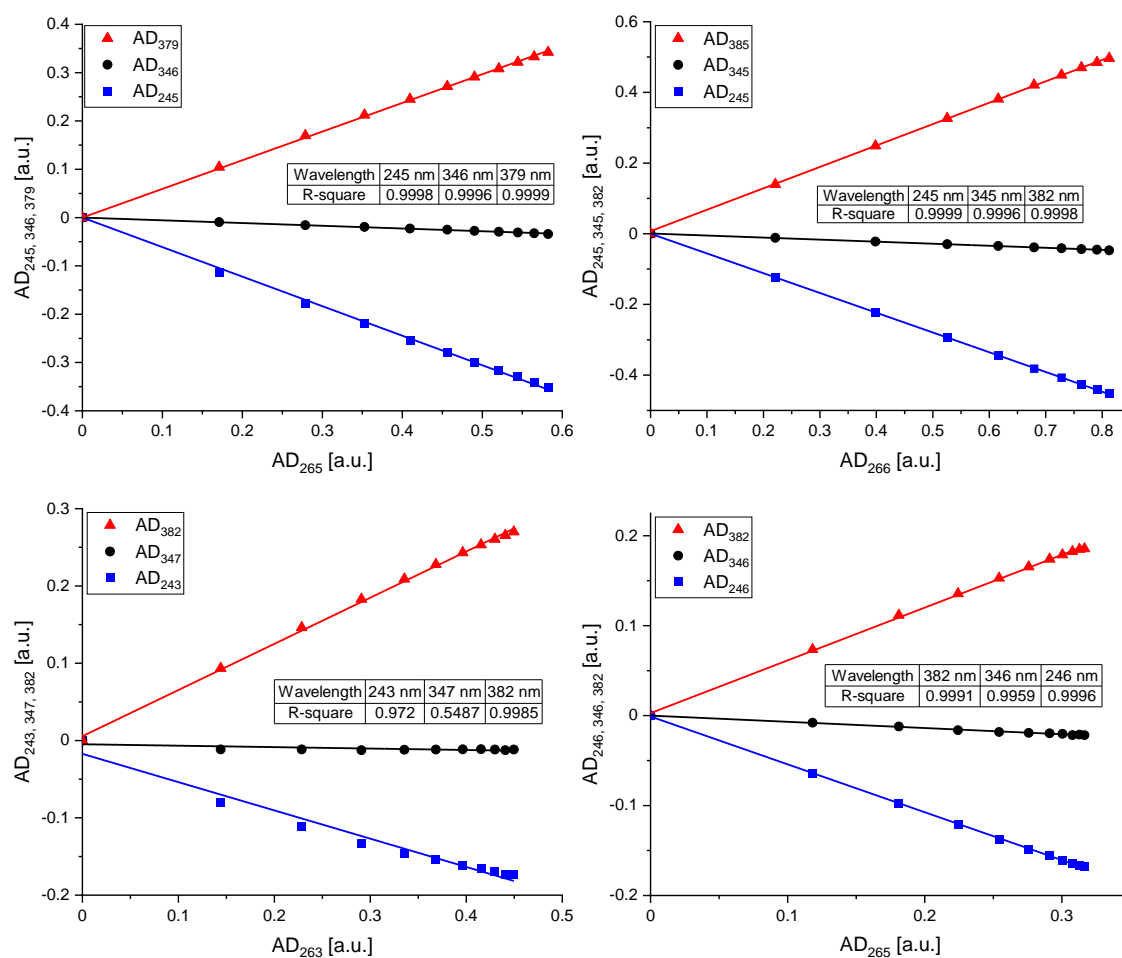
*Figure 22: AD-diagrams of polymers **6** (top left), **7** (top right), **4** (bottom left) and **5** (bottom right).*

The data points are fitted by linear regression and the coefficient of determination was calculated. The slopes belonging to similar absorbance maxima (e.g., 380 nm) have similar slopes independent of the polymer. The coefficient of determination is above 0.99 in every case except for polymer **4** (LrPU$_{HDI}$). The worst value was found for the AD$_{347}$. The main reason for this is that the initial maximum of the chosen wavelength does not undergo a reduction of absorbance after UV light irradiation, because an isosbestic point appears on this wavelength after irradiation. Therefore, the difference in absorbance has a constant value, but the first point of every calculated AD value is at 0. Even when the AD$_{347}$ values are as small as -0.011, the coefficient of determination becomes big due to the first AD value of 0. The data points of the AD$_{382}$ values for LrPU$_{HDI}$ with the irradiation time from 0 – 7 s show a clear linear progression, but the following data points deviate from this linear progression indicating a non-uniform conversion after 8 s of UV irradiation. The AD$_{243}$ values show a bad accordance of the linear fit. The values of 0 – 4 s are located under the linear regression and

the values of 7 – 10 s are located above the linear regression. This behavior could also be fitted by an exponential decay function. The UV cleavage of LrPU_HDI is in total still a more or less uniformly proceeding reaction. The other polymers show a strictly uniform photoreaction process. However, this photocleavage is not directly related to the degradation of the whole polymer. The amine that is liberated through the photocleavage of the 6NP-based leaving group is responsible for the degradation in the polymer backbone as previously described in *Scheme 22*. The polymer degradation was analyzed by SEC after irradiating the polymers dissolved in DCM (800 mg/L) for a specific time (0 – 240 s). All polymers except polymer **7** (LrPC) were used for this experiment as the LrPC was too small. The polymer samples were irradiated for 0 s, 30 s, 90 s, 150 s and 240 s, followed by the removal of the solvent and redissolving in the SEC solvent (THF with BHT for calibration) and subsequent analysis of the two polymers. The molar mass and dispersity after a specific time of irradiation are summarized in *Table 3*.

*Table 3: Summarized molar masses and dispersities for the degradation of polymer **6**, **5** and **4** after UV irradiation.*

Irradiation time [s]	LrPE		LrPU_IPDI		LrPU_HDI	
	M_n [g/mol]	Đ	M_n [g/mol]	Đ	M_n [g/mol]	Đ
0	6460	1.81	5780	1.40	5120	1.30
30	6350	2.30	4570	1.42	4660	1.32
90	4600	1.85	4310	1.43	4320	1.40
150	3990	1.75	3790	1.46	4160	1.38
240	3240	1.63	3160	1.42	4100	1.36

Surprisingly, the dispersity of polymer **5** is in the same range before and after irradiation (1.40 – 1.46). In contrast, the dispersity of polymer **6** is strongly fluctuating between 1.63 – 1.85 with one extreme value of 2.3. The molar masses of the polymers were initially at roughly 5800 g/mol and 6500 g/mol, but both ended up at roughly 3200 g/mol after 240 s of irradiation with a relatively low dispersity of 1.42 vs. 1.63, respectively. Both polymers seem to have the same degradation speed. Polymer **4** behaves differently. The difference in M_n of 0 s

Results and discussion

and 240 s is only 1000 g/mol. The dispersity was in the range of 1.30 – 1.40 and the biggest part of the degradation was already achieved after 90 s of irradiation. By plotting the M_n against the irradiation time, the reaction constant of the degradation process was calculated with a fit of an exponential decay (*Figure 23*).
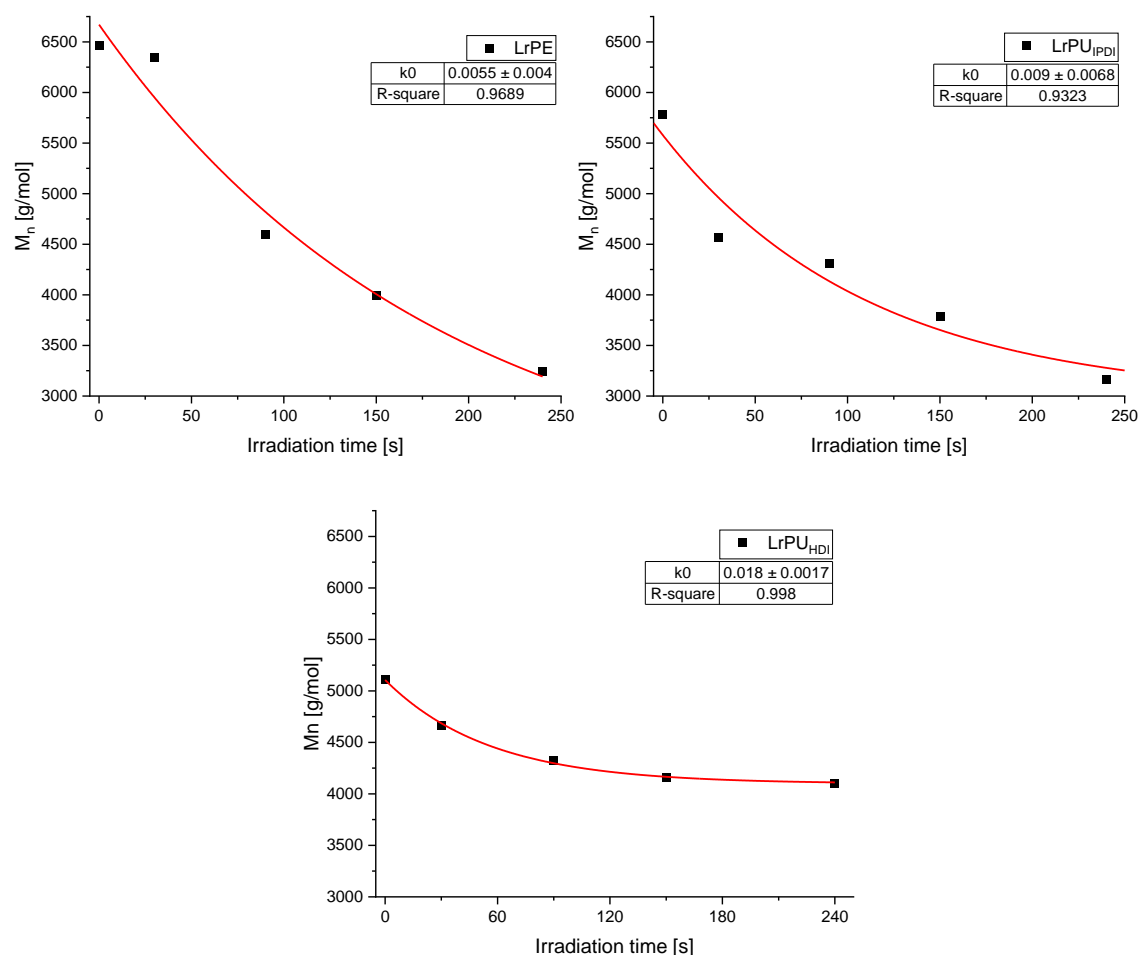
*Figure 23: Polymer degradation analyzed by SEC: polymer **6** (top left), polymer **5** (top right) and polymer **4** (bottom) measured in THF with a PS standard.*

The reaction constant for the polymer degradation for polymer **6** is $k_{deg,6}$ = 0.0055 s^{-1}. The reaction constant for polymer **5** is $k_{deg,5}$ = 0.009 s^{-1} and therefore 63% higher than $k_{deg,6}$. The coefficient of determination is 0.969 for polymer **6** and 0.932 for polymer **5** and therefore the fit is still in good accordance with the data points. Polymer **4** had a reaction constant of $k_{deg,4}$ = 0.018 s^{-1}. This reaction constant is the highest, but the decrease in molar mass is lower compared to the other polymers. Compared to the reaction constants of the UV cleavage (*Table 2*), the UV cleavage reaction is 55 times faster than the degradation reaction in the case of the LrPE ($k_{UV,6}$ = 0.299 s^{-1} vs. $k_{deg,6}$ = 0.0055 s^{-1}), 49 times faster than the degradation reaction of LrPU$_{IPDI}$

($k_{UV,5}$ = 0.443 s^{-1} vs. $k_{deg,6}$ = 0.009 s^{-1}) and 20 times faster than the degradation reaction of LrPU$_{HDI}$ ($k_{UV,4}$ = 0.367 s^{-1} vs. $k_{deg,6}$ = 0.018 s^{-1}). All degradation reactions have reaction constants in the same order of magnitude. The lower $k_{deg,6}$ can be explained by the nucleophilic attack of the liberated amine. This amine can only lead to polymer degradation by an intermolecular attack or by an intramolecular approach that leads to bigger cyclic molecules. A nucleophilic attack to the nearest carbonyl does not lead to a cleavage of the polymer backbone. However, the second carbonyl could lead to a cleavage by undergoing a cyclization to a 10-membered cyclic molecule (*Scheme 35*).
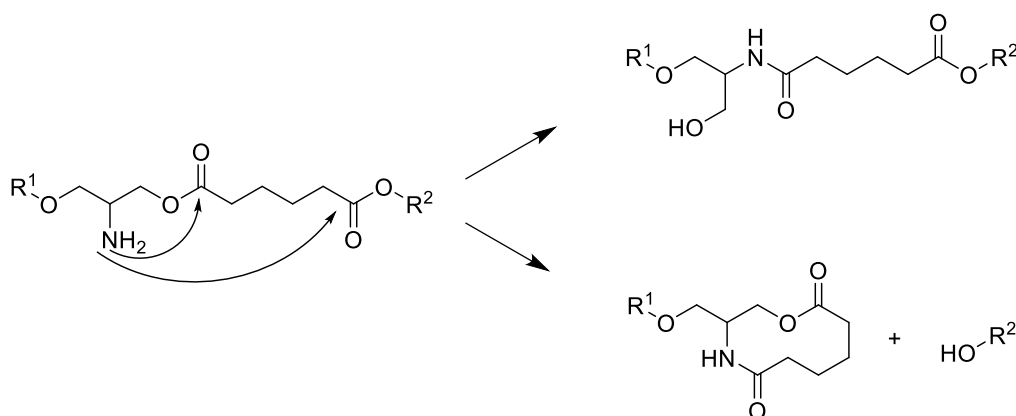
*Scheme 35: Degradation reaction for polymer **6**.*

In contrast, the intramolecular attack of the liberated amine in the LrPU$_{IPDI}$ can always lead to the cleavage of the backbone as proposed in *Scheme 22*. However, the nucleophilic attack proceeds without the need of UV light. All the samples were dried immediately after the irradiation. Another experiment was conducted by irradiating a LrPU$_{IPDI}$ sample for 240 s and let it stir overnight followed by the SEC analysis. The molar mass of the polymer was reduced to 2900 g/mol with a dispersity of 1.38. There is no significant difference between the sample that was stirred overnight after the irradiation for 240 s or the one that was measured immediately after the irradiation for 240 s (*Table 3*). This result could mean, that the degradation reaction is finished before the SEC measurement was conducted. After the irradiation, the polymer solution is transferred into a vial and the solvent is slowly removed by rotary evaporation. Afterwards, the dry polymer sample is redissolved in the SEC solvent and measured. This time interval may be sufficient for the degradation to get to a point where no further degradation can be observed. The UV/Vis spectra of irradiated

polymers have nearly no change after 10 s of irradiation. However, there is no proof, that this irradiation time already leads to the leaving of the protection group. A change in the molecule might be visible by UV/Vis spectroscopy, but the liberation of the amine group cannot be qualitatively analyzed by this method. The protecting group might need longer UV irradiation to actually leave the polymer side-chain. An argument for this can be seen in *Table 3*. If only 10 s irradiation were necessary to remove the protecting group, the degradation reaction should proceed to yield the same molar mass. This is not observed. It seems that the irradiation time is in proportion to the degradation and the loss in molar mass. This may conclude that for the removal of the protecting group a longer irradiation is needed.

4.1.4   Nanoparticle analysis

In the previous work in the working group of Prof. Dr. Kuckling, Dr. Jingjiang Sun prepared various polymers bearing a light-responsive side group. This side group was derived from 4,5-dimethoxy-2-nitrobenzyl alcohol coupled to serinol and was already introduced in the introduction part (*Scheme 7*). Among others, a light-responsive polyester very similar to polymer **6** was prepared and Dr. Anderski and Timo Schoppa of the working group of Prof. Dr. Klaus Langer (WWU Münster) used this polymer to formulate nanoparticles which were analyzed by photon correlation spectroscopy (PCS) and atomic force microscopy (AFM).[129] Due to our cooperation with the WWU Münster, NPs of polymer **6** were prepared and analyzed by PCS and scanning electron microscopy (SEM). The NPs were loaded with the photosensitizer 5,10,15,20-tetrakis(*m*-hydroxyphenyl)chlorine (*m*THPC) and the release was analyzed. Cell viability tests and quantification of intracellular *m*THPC uptake were performed as well by the Langer group.[172]

By the addition of 2 mg of *m*THPC during the NP preparation, *m*THPC containing NPs were obtained and referred to as *m*THPC-LrPE-NP. Without the incorporation of *m*THPC, NPs called LrPE-NP were obtained. By using different amounts of LrPE and poly(lactic-co-glycolic acid) (PLGA) during the NP preparation, LrPE^x-PLGA^{100-x}-NP were prepared. Incorporation of *m*THPC during the NP preparation, *m*THPC-LrPE^x-PLGA^{100-x}-NP were obtained. The size, polydispersity index (PDI) and the zeta potential were analyzed by PCS and the

drug loading content of formulated NPs containing *m*THPC was analyzed by high-performance liquid chromatography system equipped with diode array detector (HPLC-DAD system). The NP analysis results are summarized in Table 4.

*Table 4: NP analysis and drug loading content of NP made of polymer **6**.*

Nanoparticle system	Hydrodynamic diameter [nm]	PDI	Zeta potential [mV]	Drug loading [µg *m*THPC/mg NP]
LrPE-NP	238.2 ± 7.5	0.09 ± 0.06	-4.9 ± 3.4	
*m*THPC-LrPE-NP	229.4 ± 9.6	0.07 ± 0.03	-24.3 ± 2.8	95.4 ± 11.7
LrPE^{25}-PLGA^{75}-NP	230.4 ± 3.6	0.09 ± 0.02	-21.6 ± 1.6	
*m*THPC-LrPE^{25}-PLGA^{75}-NP	224.0 ± 18.3	0.14 ± 0.01	-25.7 ± 2.9	72.5 ± 11.8
LrPE^{50}-PLGA^{50}-NP	229.6 ± 2.5	0.10 ± 0.01	-14.8 ± 0.9	
*m*THPC-LrPE^{50}-PLGA^{50}-NP	226.5 ± 14.1	0.09 ± 0.05	-26.4 ± 7.4	75.4 ± 5.7

The NPs with *m*THPC incorporated tended to be 3-9 nm smaller than without *m*THPC. NP in the size range of 200 nm can utilize the EPR effect.[109] The PDI was in all cases below 0.14, which indicates a monodisperse size distribution and the zeta potential was in a range of -4.9 to -26.4 mV. Additionally, the NPs were stabilized with a steric stabilizer (PVA), therefore a low zeta potential did not show any negative effects on colloidal stability. The zeta potential changed upon UV light irradiation from a negative value to a positive value (*Figure 24*).
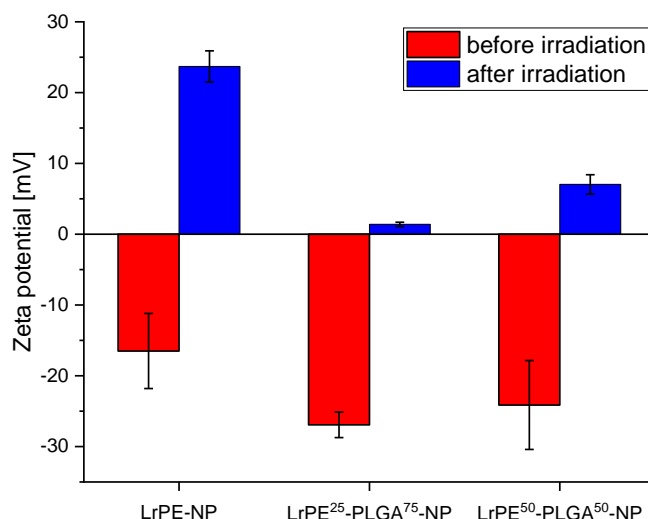
Figure 24: Change of the zeta potential of LrPE-NP, LrPE^{25}-PLGA^{75}-NP and LrPE^{50}-PLGA^{50}-NP before and after irradiation with UV light for 5 min.

The zeta potential changed from -16.5 mV to +23.7 mV after UV light irradiation for 5 min in the case of LrPE-NP, from -26.9 mV to +1.4 mV and from -24,1 mV to +7.0 mV in the case of LrPE^{25}-PLGA^{75}-NP and LrPE^{50}-PLGA^{50}-NP, respectively. This increase in zeta potential can be explained by the liberation of the amine in the serinol-block of the polymer due to the UV cleavage (*Scheme 22*). This liberated amine can subsequently lead to the degradation of the polymer and also to the decomposition of the NPs. To further investigate the decomposition, NPs were irradiated and analyzed by PCS. Under defined parameters the detected count rate correlates with the concentration of the NPs in the solution. Therefore, a decrease of scattering light correlates with the decomposition of NPs. NP suspensions were irradiated for 5 min with UV light with a wavelength of 365 nm and the count rate was measured at different time intervals over 24 h (*Figure 25*).
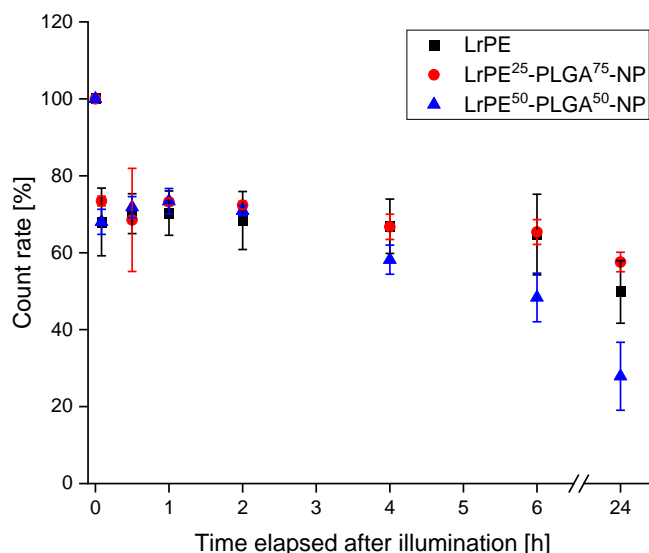
Figure 25: PCS analysis of the count rate after UV light irradiation of LrPE-NP.

After irradiation, a rapid decrease of the count rate by roughly 30% was detected for all NPs. The count rate stayed at about 70% for the next 2 h and dropped to 50% for LrPE-NP, to 58% for LrPE^{25}-PLGA^{75}-NP and to 28% for LrPE^{50}-PLGA^{50}-NP after 24 h incubation. However, the NPs did not decompose completely. An explanation for this might be the low water-solubility of the polymer and its degradation products. The polymeric parts and degradation products might not dissolve and leave the NP. In this case the NP is kept together and leaving of small water-soluble molecules can lead to pores in the NP without tearing the NP apart. By complete decomposition or even with pores on intactly staying NP suspensions, a drug release can still occur. Therefore, release studies of loaded NPs were performed by incubating lyophilized *m*THPC containing NPs in Dulbecco's Modified Eagle Medium (DMEM) containing 10% fetal bovine serum (FBS) at 37 °C after irradiation for 5 min at 365 nm. The samples were centrifuged (20000 g, 15 min) after certain time intervals (15 min, 30 min, 1 h, 2 h, 4 h, 6 h and 24 h). The supernatant was diluted with acetone and the dissolved *m*THPC was separated from precipitated proteins by another centrifugation step. The amount of dissolved *m*THPC was analyzed by a HPLC equipped with a fluorescence detector with an excitation wavelength of 421 nm and an emission wavelength of 652 nm and a calibration curve for *m*THPC. The results of this experiment are depicted in *Figure 26*.
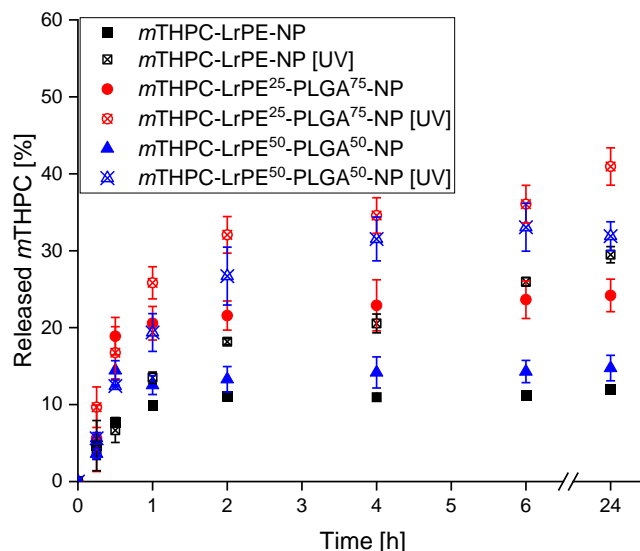
Figure 26: Drug release kinetic of mTHPC-LrPE-NP, mTHPC-LrPE^{25}-PLGA^{75}-NP or mTHPC-LrPE^{50}-PLGA^{50}-NP suspensions before and after UV light irradiation for 5 min and 365 nm.

Non-illuminated *m*THPC-LrPE-NPs exhibited a release of *m*THPC of around 12%. Within the first two hours the release reached 11% and increased very slowly afterwards. The release of *m*THPC of the NPs that were irradiated for 5 min steadily increased until it reached its maximum at 29%. After 2 h, 18% of *m*THPC was released and after 6 h even 26% of *m*THPC was released. The irradiation of *m*THPC-LrPE-NPs led to a higher release of *m*THPC from the particle matrix compared to the *m*THPC-LrPE-NPs that were not irradiated. However, a release of roughly 30% is not satisfactory. The *m*THPC-release of *m*THPC-LrPE^{25}-PLGA^{75}-NP after 24 h after irradiation was 41% and the maximum *m*THPC-LrPE^{50}-PLGA^{50}-NP after 24 h was 32% and therefore higher than the *m*THPC-release of *m*THPC-LrPE-NPs. However, the release of *m*THPC-LrPE^{25}-PLGA^{75}-NPs without irradiation showed a release of 24% and is two times higher than the release of non-irradiated *m*THPC-LrPE-NPs. *m*THPC-LrPE^{50}-PLGA^{50}-NPs released only 15% without illumination. One reason for an elevated release might be the inhomogeneity of the particle matrix due to the incorporated PLGA leading to porous structures. The more PLGA was incorporated, the higher was the release with and without illumination. The anticancer efficacy was tested by incubating *m*THPC-LrPE^{50}-PLGA^{50}-NPs at different concentrations with cells of the cell line HT-29 and irradiation with 365 nm and/or 652 nm. The results of the WST-1 assay are depicted in *Figure 27*.
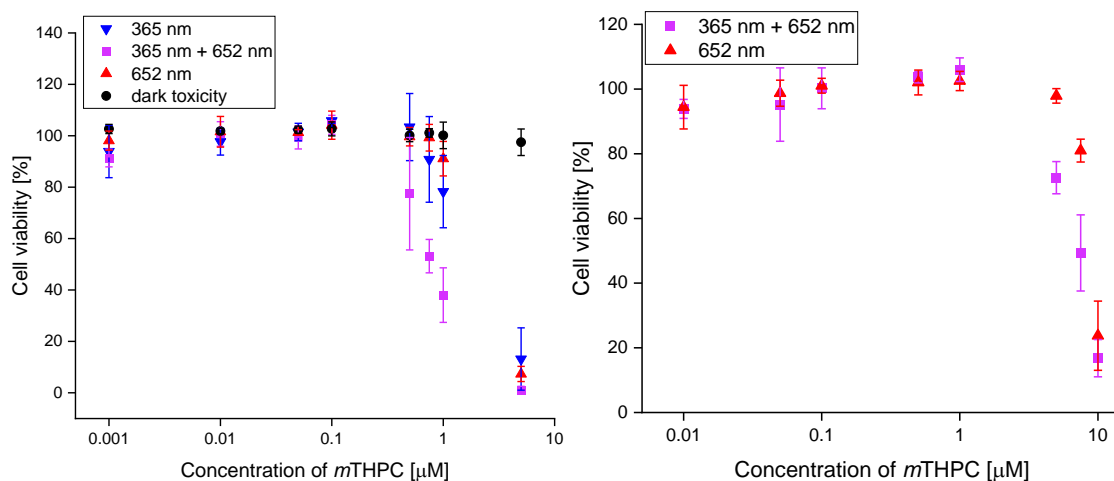
Figure 27: Cytotoxic potential of mTHPC-LrPE^{50}-PLGA^{50}-NPs in HT-29 cells after irradiation with two different light sources (365 nm and 652 nm) or each light-sources separately (left). Cytotoxic potential of mTHPC-LrPE^{50}-PLGA^{50}-NPs in HT-29 cells pre-irradiated at 365 nm or non-pre-irradiated (right). After cell incubation for 24 h an irradiation at 365 nm was performed.

Incubating NPs without irradiating them led to nearly no cell toxicity. By irradiation of either 365 nm or 652 nm, the NPs showed a toxic effect. The cell viability drops after 0.5 µM mTHPC from 100% to 13% after the irradiation with 365 nm and to 7% after irradiation with 652 nm at a concentration of 5 µM. The EC$_{50}$ value of the single illumination at different wavelengths are EC$_{50,365nm}$ = 1.259 ± 0.171 µM mTHPC and EC$_{50,652nm}$ = 1.291 ± 0.351 µM mTHPC. However, combining both wavelengths led to a higher toxicity of EC$_{50,combined}$ = 0.801 ± 0.035 µM mTHPC. The pre-irradiated (365 nm) NPs showed a similar toxicity of EC$_{50,pre-irrad.}$ = 6.196 ± 0.371 µM mTHPC to the non-pre-irradiated EC$_{50,non-irrad.}$ = 7.934 ± 0.295 µM mTHPC. However, the particles that were pre-irradiated showed a significantly (p ≤ 0.001) higher release of mTHPC at certain concentrations. The light-responsive properties of the polymeric NPs showed a positive effect in anticancer efficiency. This toxicity was still significantly lower compared to the samples that were incubated and irradiated afterwards. The intracellular concentration of mTHPC was tested to further understand the cytotoxic potential of the polymer NPs. NPs with a corresponding concentration of 1 µM mTHPC were added to HT-29 cells and the incubation medium was removed and the cells were washed after specific time points. The cells were washed and the cell number and volume were determined after detachment with a trypsin/EDTA solution. The cells were incubated in DMSO and centrifuged

(30000 g, 15 min) to extract the *m*THPC and the amount of *m*THPC was determined by HPLC-FLD (*Figure 28*).
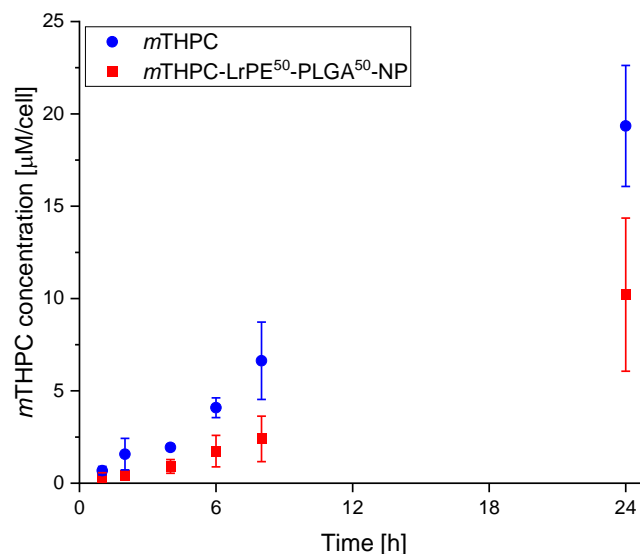
Figure 28: Intracellular concentration of mTHPC in HT-29 cells of mTHPC-LrPE^{50}-PLGA^{50}-NP and pure mTHPC. Analysis was performed with HPLC-FLD after lysis of the cells.

The measured concentrations follow a linear course. The longer the incubation time was, the higher was the concentration of internalized *m*THPC per cell. The highest concentration was reached after 24 h with 10.2 µM/cell for *m*THPC-LrPE^{50}-PLGA^{50} and the intracellular concentration after the addition of pure *m*THPC reached the maximum after 24 h with 19.4 µM/cell. The uptake of *m*THPC is enhanced due to its lipophilic character. However, the uptake of polymeric NPs depends on active processes like endocytosis.[173] To measure the cellular interaction, Live-Cell imaging of cells incubated with pure *m*THPC or *m*THPC-LrPE^{50}-PLGA^{50}-NPs was performed. The cells were scanned every hour for 1 d and the kinetics of cellular interaction are depicted in *Figure 29*.
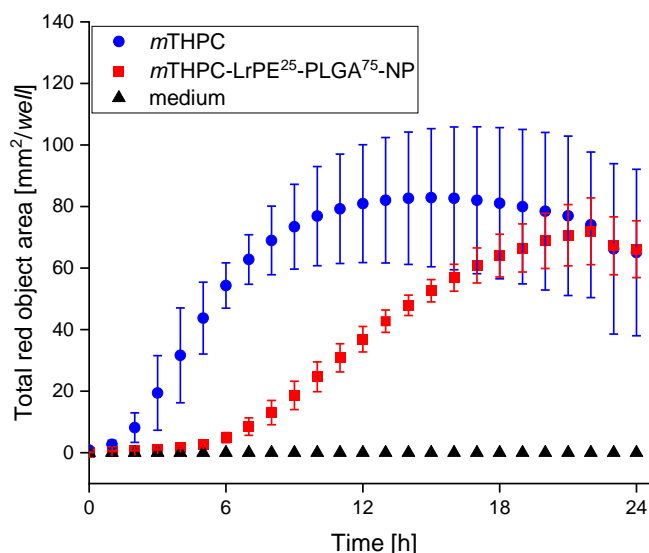
Figure 29:Cellular interaction of mTHPC-LrPE^{50}-PLGA^{50}-NPs and pure mTHPC in HT-29 cells.

The free *m*THPC showed the highest total object red area. The polymeric NPs with *m*THPC incorporated show a slower increase in total red object area compared to free *m*THPC. However, the value after 24 h is in the same range as free *m*THPC. Quantitative HPLC analysis of the incorporated *m*THPC showed a concentration of 7.5 ± 0.5 µM *m*THPC/cell for the incorporated *m*THPC and a concentration of 14.0 ± 3.6 µM *m*THPC/cell for the free *m*THPC. This result supports the previous analysis techniques that were applied for the *m*THPC-LrPE^{50}-PLGA^{50}-NP. In conclusion, the NP formulation show an effective uptake of *m*THPC and the light-responsive self-immolative 6NP-based polyester seems to be a suitable candidate as a basis for a light-responsive drug delivery system.

4.2   Redox-responsive self-accelerating polymers

4.2.1   Monomer synthesis

Three different redox-responsive monomers were planned. Monomer **8** was synthesized in a single step by protecting the thiol of thioglycerol with 2,2'dipyridyldisulfide (DPDS). 2-Mercaptopyridine is the side-product of this reaction (*Scheme 36*).
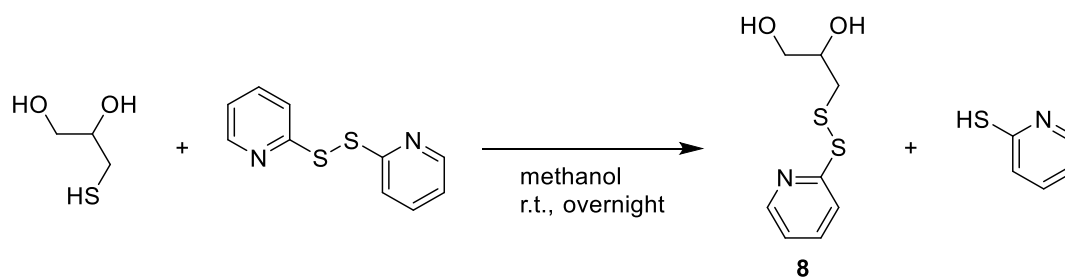
*Scheme 36: Synthesis of monomer **8**. DPDS was dissolved in MeOH and thioglycerol was added dropwise. The mixture was stirred overnight and **8** was purified by column chromatography.*

Monomer **8** was analyzed by ESI-ToF-MS, NMR and UV/Vis spectroscopy. Thioglycerol is not UV active and therefore no spectrum could be obtained. The absorbance maximum of DPDS is located at 282 nm (measured in DMAc). Monomer **8** has an absorbance maximum located at 291 nm and the side product 2-mercaptopyridin has absorbance maxima located at 295 nm and 375 nm (*Figure 30*).
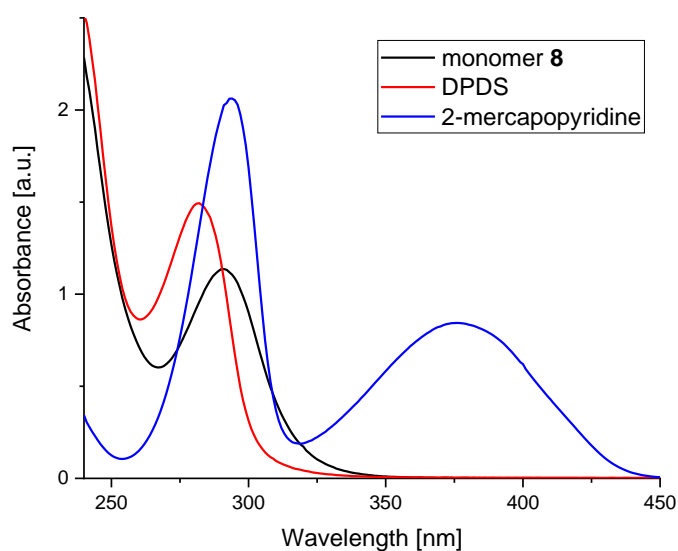
*Figure 30: UV/Vis spectra of monomer **8** (black), DPDS (red) and 2-mercaptopyridine (blue).*

After the deprotection, the thiol of the thioglycerol unit is liberated under release of 2-mercaptopyridin that has a strong yellow color (*Scheme 37*).
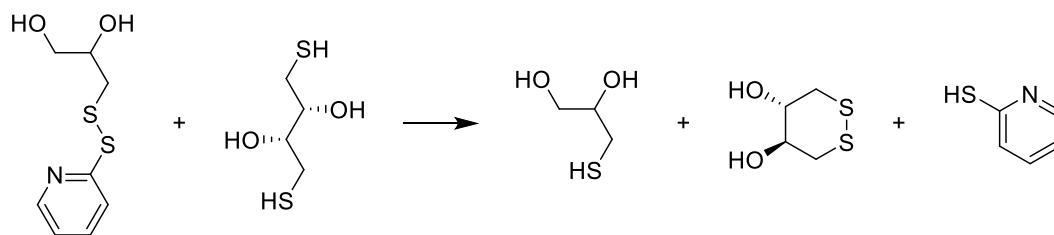
*Scheme 37: The deprotection mechanism with monomer **8** and DTT.*

The new absorbance maximum that arose after this reaction (375 nm) can be used for quantitative analysis of the deprotection mechanism of a polymer that is made from monomer **8**, because the leaving group and deprotection mechanism are the same for the monomer and polymer.

The second monomer is **11**. The monomer is synthesized in a single step out of serinol and *para*-nitrobenzyl chloroformate (*p*NBCF) and diisopropyl ethylamine (DIPEA) as a proton catcher (*Scheme 38*).
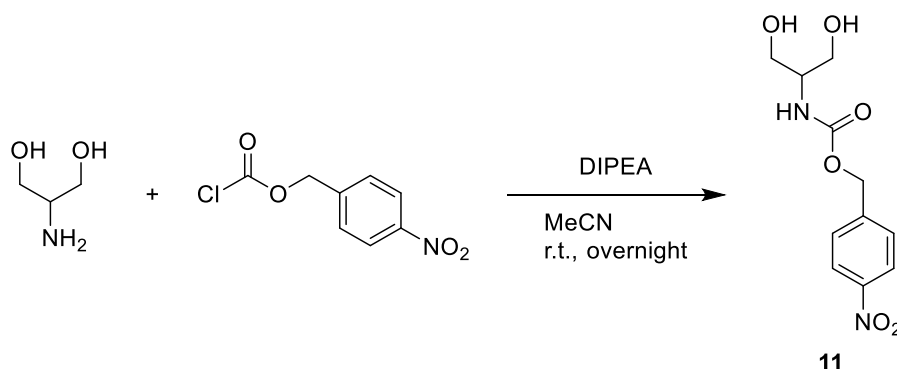
*Scheme 38: Synthesis of monomer **11**: serinol and pNBCF were dissolved in MeCN followed by the addition of DIPEA under ice-cooling. Afterwards, the mixture was stirred overnight and purified by extraction.*

The yield of 55% is quite low for and monomer product could be lost due to excessive extraction and the relatively high polarity of the monomer. Reactions with the structurally similar *p*NPCF lead to a higher yield of 72%. Monomer **11** was analyzed by NMR spectroscopy and ESI-ToF-MS.

The third monomer was synthesized in three steps from DPDS, mercaptoethanol and serinol. First, the thiol group of mercaptoethanol is protected by DPDS resulting in **12** (*Scheme 39*).
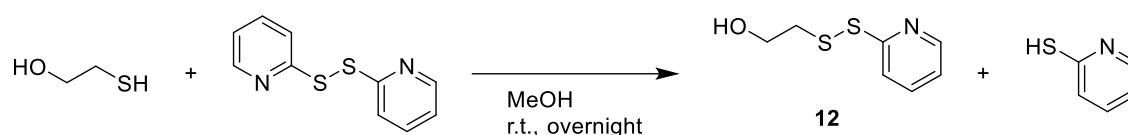
*Scheme 39: Synthesis of **12**: DPDS was dissolved in MeOH and mercaptoethanol was added dropwise. The mixture was stirred overnight and the product was purified by column chromatography.*

The yield of 77% is sufficiently high and the product was analyzed by NMR spectroscopy. After the isolation of the product, the hydroxyl group of the product was activated by *p*NPCF in MeCN with TEA as a base to couple it to serinol in a subsequent step (*Scheme 40*).
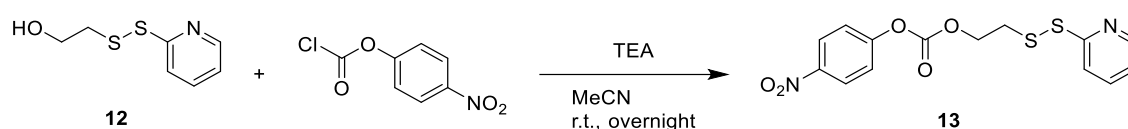
*Scheme 40: Synthesis of **13**: pNPCF and **12** were dissolved in MeCN followed by a dropwise addition of TEA. The reaction mixture was stirred overnight and the product was purified by column chromatography.*

The synthesis of **13** had a yield of 77% and the product was analyzed by NMR spectroscopy. To finally obtain the monomer, **13** was coupled to serinol in the same fashion as in the previously described light-responsive monomer synthesis to obtain monomer **14** (*Scheme 41*).
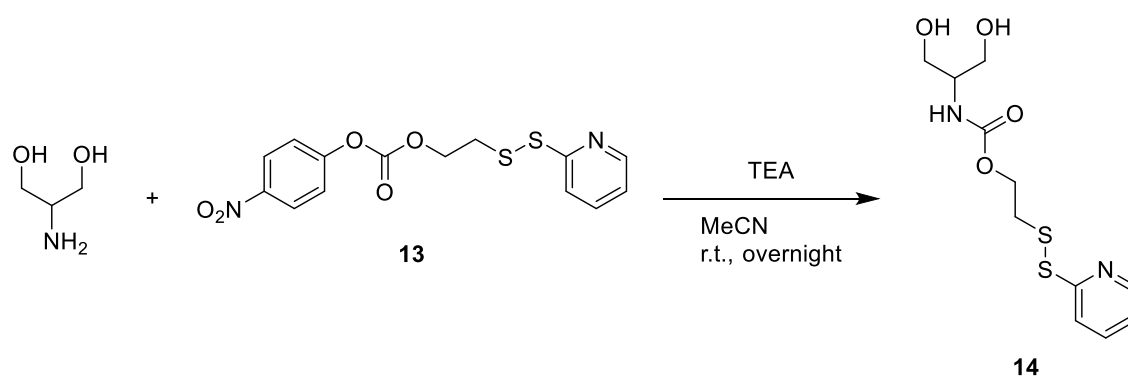
*Scheme 41: Synthesis of **14**: serinol and **13** were dissolved in MeCN followed by the dropwise addition of TEA. The mixture was stirred overnight and the monomer was purified by column chromatography.*

The total yield of the monomer synthesis over three steps is 46%. This monomer should react in a similar way as already described in *Scheme 25*. And similar to the thioglycerol-based redox-responsive monomer, the leaving group 2-mercaptopyridine can be detected by UV/Vis spectroscopy. The purification was

facile, because **14** can hardly be dissolved in the first solvent mixture in the column chromatography. After the removal of the side-products through the column, the monomer was flushed through with acetone.

4.2.2 Polymer synthesis

In the first polymerization, monomer **8** was polymerized with adipoyl chloride in a polycondensation reaction (*Scheme 42*).

*Scheme 42: Synthesis of polymer **10**: monomer **8** was dissolved in pyridine and added to DMF in a Schlenk-flask followed by the dropwise addition of adipoyl chloride in DCM. The mixture was stirred overnight at room temperature and the polymer was precipitated from MeOH. No product was obtained.*

This polymerization was carried out exactly like the polymerization with monomer **3** to obtain the light-responsive polyester **6** (*Scheme 31*). However, no polymer was obtained after the precipitation step. The polymerization was repeated to exclude mistakes during the experimental procedure, but still no polymer was obtained. The secondary hydroxyl group of the monomer seems to be less reactive and this 1,2-propanediol group seems to be less suitable for a polyester synthesis. Another attempt to synthesize the redox-responsive polyester **10** was performed with an addition of a catalytic amount of 4-dimethylaminopyridine (DMAP). DMAP is known for the catalysis of esterifications.[174,175] The polymerization with DMPA as an additive was unsuccessful and no polyester was obtained. Therefore, another polymerization technique was used. Monomer **8** was polymerized in a polyaddition reaction with IPDI (*Scheme 43*).

*Scheme 43: Synthesis of polymer **9**: DBTDL and monomer **8** were dissolved in DMF under N₂-atmosphere and IPDI was added dropwise under stirring. The reaction mixture was stirred at 70 °C for 3 d and precipitated from MeOH.*

The obtained redox-responsive polyurethane **9** was analyzed by SEC, NMR spectroscopy and UV/Vis spectroscopy. The molar mass of polymer **9** is ranging between 7400 – 12000 g/mol with a dispersity of 1.66 – 1.92 (measured in THF, *Figure 31 left*). The polymer sample with the molar mass of 12000 g/mol (in THF) was also analyzed by SEC with dimethylacetamide (DMAc) as solvent resulting in a molar mass of 27000 g/mol with a dispersity of 1.65 (measured in DMAc with a polystyrene standard, *Figure 31 right*). The discrepancy in size between the measurements with THF or DMAc as solvent can be explained by the different affinity of the polymer towards the solvents. DMAc seems to a more suitable solvent for the polymers and the polymer coil swell more compared to the polymer coils in THF. The different coil sizes diffuse differently through the SEC columns, as the smaller coil diffuses slower through the columns, compared to the larger coil. Therefore, the polymer appears to have a smaller molecular weight in the measurement with THF as a solvent.
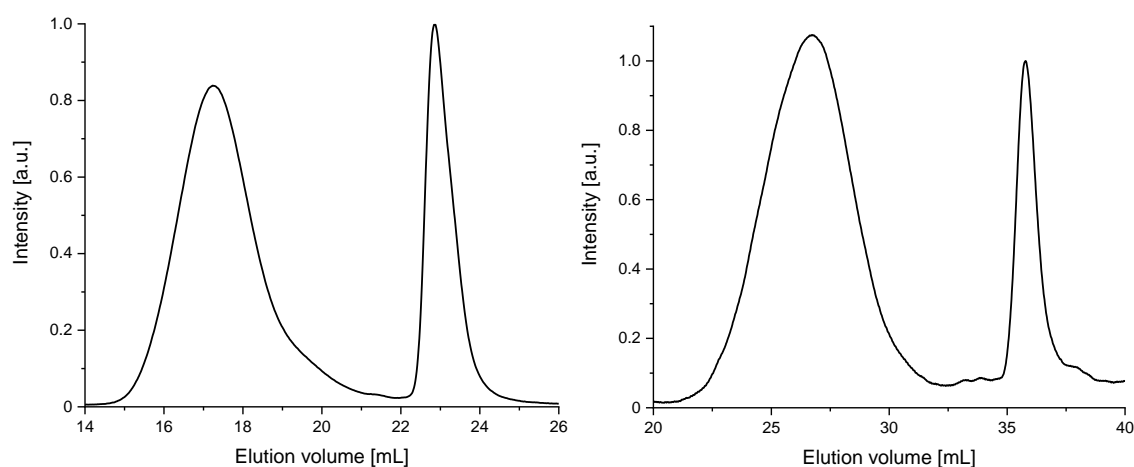
*Figure 31: SEC elugrams of polymer **9** in THF (left) and DMAc (right).*

Both signals appear to be monomodal and they have the same shape in the different SEC techniques. The yield of the polymerization is only 35%. The polymer is colorless. A typical UV/Vis spectrum is depicted in *Figure 32*.
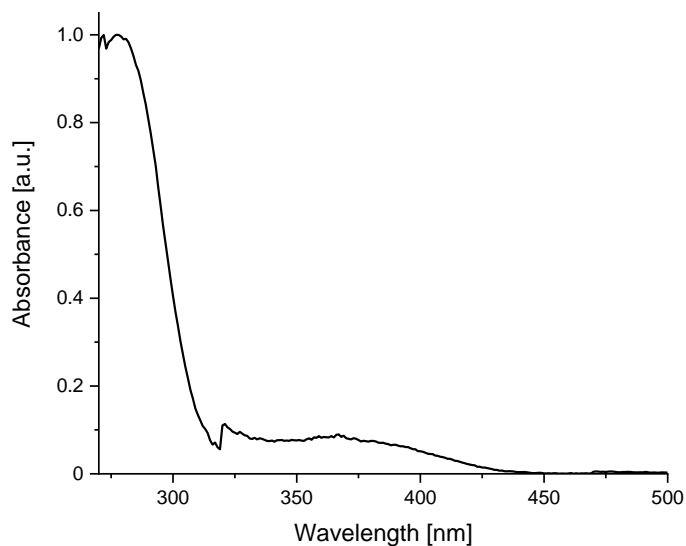
*Figure 32: UV/Vis spectrum of polymer **9**.*

The absorbance of the polymer is very low compared to the light-responsive polymers **4-7** at similar concentrations. After normalization, a relatively high noise level can be seen. A small error due to the lamp changing inside the UV/vis spectrometer can even be seen at approximately 320 nm. There is an absorbance maximum (normalized to 1) located at 277 nm and another broad signal appears between 350 – 390 nm which can still be due to the error of the lamp changing.

The second redox-responsive polymer was synthesized using monomer **11** and IPDI in a polyaddition leading to a redox-responsive polyurethane (*Scheme 44*).
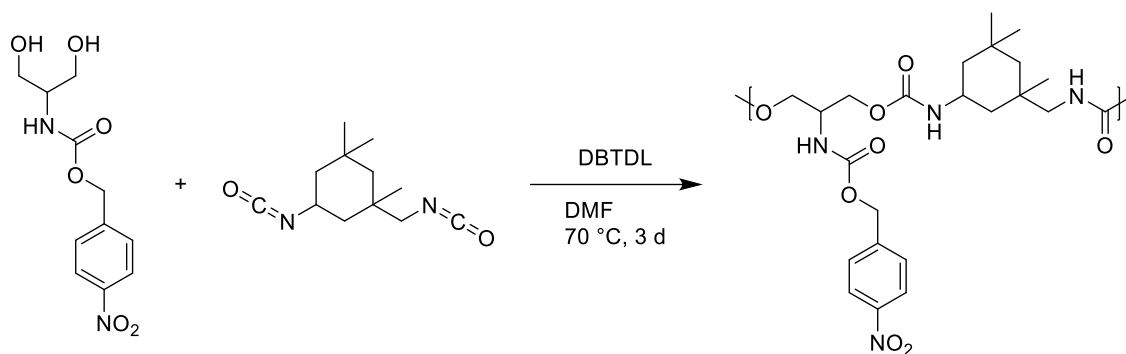
*Scheme 44: Synthesis of a redox-responsive polyurethane: DBTDL and monomer **11** were dissolved in DMF under N₂-atmosphere and IPDI was added dropwise under stirring. The reaction mixture was stirred at 70 °C for 1 d and was found to be solidified.*

The first attempts at the polyaddition were unsuccessful. The reaction mixture solidified in under 1 d and the addition of DMSO and stirring at 70 °C could not dissolve the solidified reaction mixture. No analysis of the solid mixture could be performed. Another comonomer was implemented leading to the prevention of the crosslinking. By the addition of benzene dimethanol (BDM) it was possible to synthesize a redox-responsive copolymer **15** (*Scheme 45*).
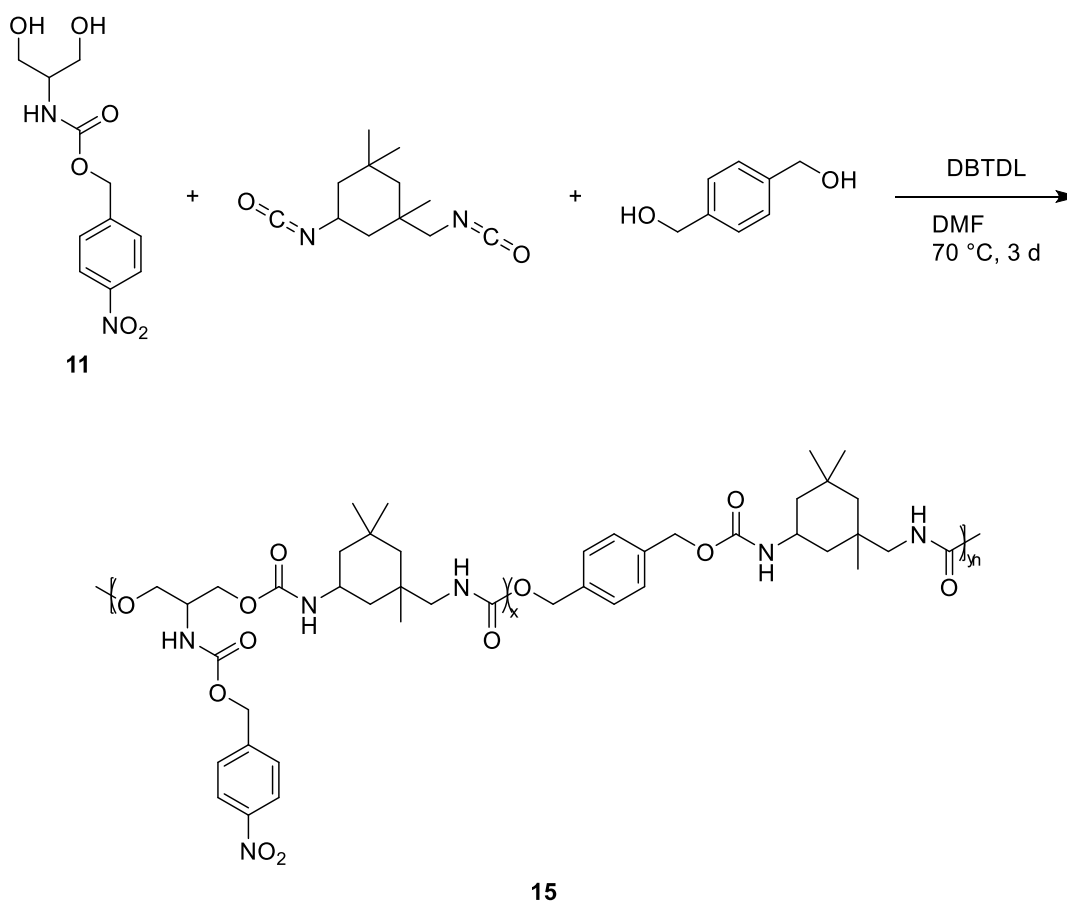
*Scheme 45: Synthesis of polymer **15**: DBTDL, BDM and monomer **11** were dissolved in DMF under N_2-atmosphere and IPDI was added dropwise under stirring. The reaction mixture was stirred at 70 °C for 3 d and precipitated from MeOH.*

This polymerization attempt was successful leading to a light-yellow colored redox-responsive polyurethane with a yield of 22%. This polymer was analyzed by SEC and NMR spectroscopy. The molar mass of the polymer was 8200 g/mol with a dispersity of 1.40 (measured in THF, *Figure 33, left*) and a M_n of 13700 g/mol with a dispersity of 2.00 (measured in DMAc with a polystyrene standard, *Figure 33, right*).
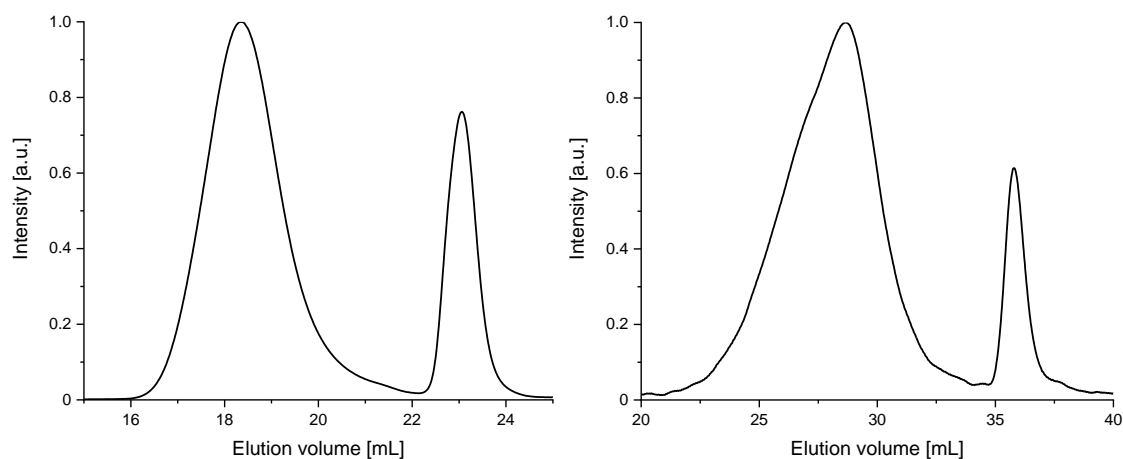
*Figure 33: SEC elugrams of polymer **15** in THF (left) and DMAc (right).*

Both signals are monomodal, but the signal in the elugram measured in DMAc seems to have a very small shoulder towards smaller elution volumes.

The third polymer was synthesized in a polyaddition reaction with monomer **14**, BDM and IPDI. The reaction mixture was heated to 70 °C and stirred for 3 d to obtain redox-responsive polyurethane **16** (*Scheme 46*).
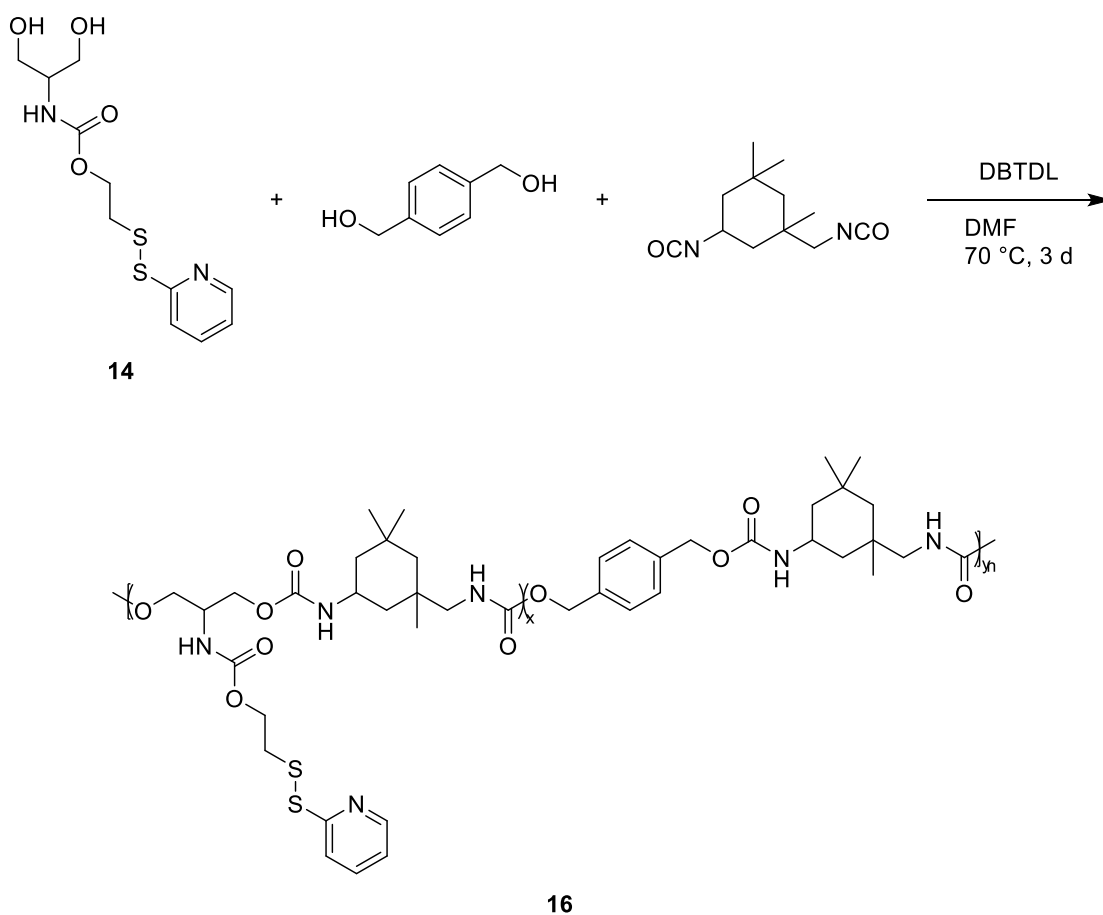
*Scheme 46: Synthesis of polymer **16**: DBTDL, BDM and monomer **14** were dissolved in DMF under N₂-atmosphere and IPDI was added dropwise under stirring. The reaction mixture was stirred at 70 °C for 2 d and precipitated from MeOH.*

This polymerization only yielded 16% of a colorless polyurethane with a ratio of 1:1.3 of monomer **14**:bdm. The molar mass of this polymer was 12400 g/mol with a dispersity of 1.25 (THF as solvent, *Figure 34, left*) and 16300 g/mol with a dispersity of 1.24 (DMAc as solvent with a polystyrene standard, *Figure 34, right*).
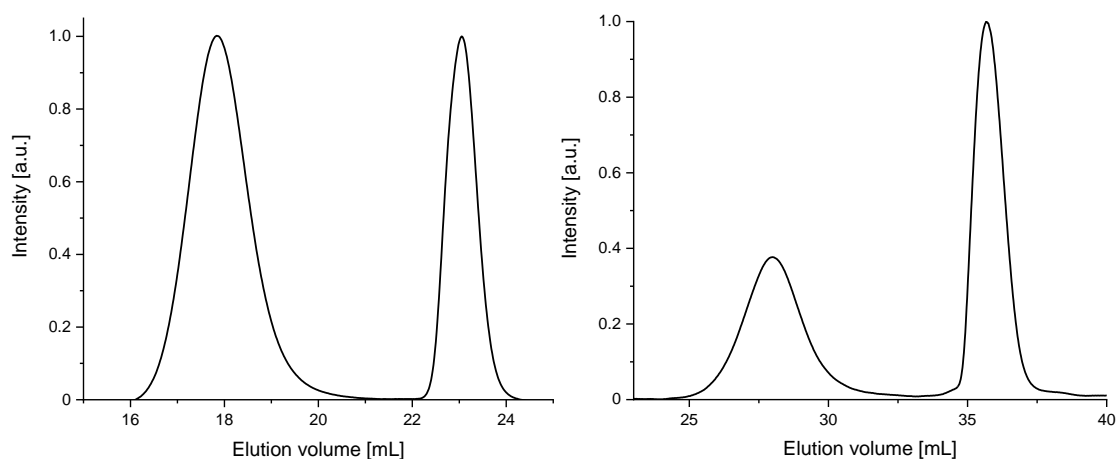
*Figure 34: SEC elugrams of polymer **16** in THF (left) and DMAc (right).*

Both SEC methods showed a monomodal polymer signal at either 16 – 20 mL (SEC with THF) or at 25 – 32 mL (SEC with DMAc). The low yield could be explained by the solubility of the polymer. MeOH was probably not suited for the precipitation of the polymer. Also, a SEC sample was taken after 24 h of reaction showing the same molar mass and dispersity. This reaction was already finished after 1 d reaction time. This polymer was analyzed by SEC, NMR and UV/Vis spectroscopy. A typical UV/vis spectrum is depicted in *Figure 35*.
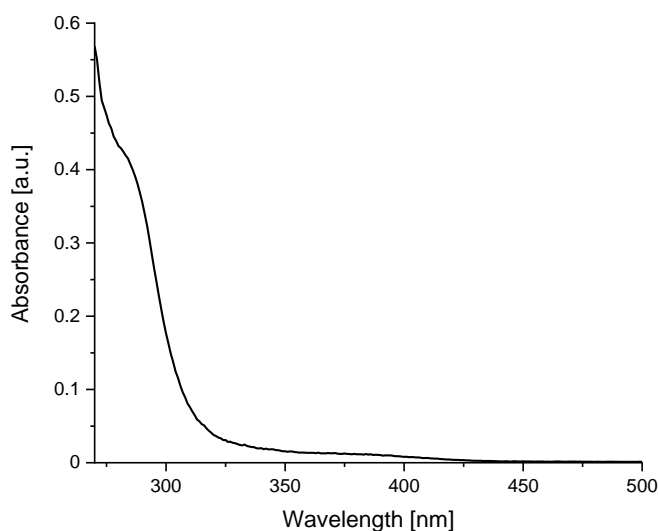
*Figure 35: UV/Vis spectrum of polymer **16**.*

As in *Figure 32*, the absorbance starts to rise at approximately 450 nm going to lower wavelengths. No maximum can be observed between 350 – 400 nm. Below 320 nm the absorbance rises drastically and would reach the maximum below the UV cutoff wavelength of DMAc.

4.2.3   Degradation studies

The most common reductive triggers are glutathione, DTT and sodium dithionite. Glutathione has two carboxylic acid functions, a thiol function and an amine function and is therefore only soluble in water and DMF (and similar polar solvents). DTT has two hydroxyl groups and two thiols and is as well only soluble in water and DMF (and similar solvents). The polymers however are only soluble in solvents like THF, DMSO and DMF. As a result of this the polymer degradation tests were performed in DMAc. The benefit of DMAc is, that SEC analysis can be performed with this solvent. The degradation of polymer **9** (RrPU) was analyzed by UV/Vis spectroscopy and SEC. The leaving group of polymer **9** is

2-mercaptopyridine (2MP). This molecule has a very strong yellow color and an UV/Vis absorbance at about 375 nm (*Figure 30*). The polymer and all other used molecules have absorbance maxima lower than 320 nm and therefore the UV/Vis analysis of the removal of the leaving group is a suitable technique. To quantify the removal of 2-mercaptopyridine, a series of 2MP in DMAc at different concentrations was made and analyzed by UV/Vis spectroscopy (*Figure 36*).
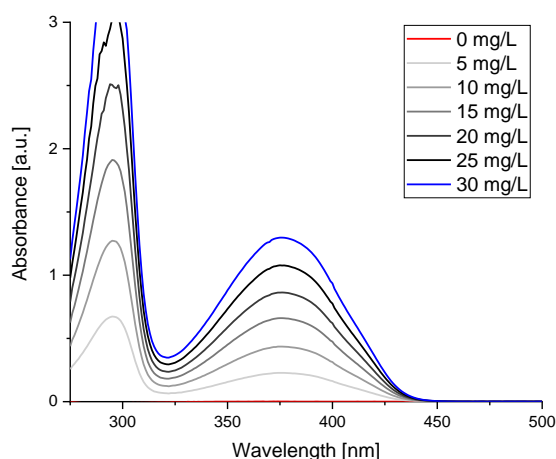
Figure 36: UV/Vis analysis of 2-mercaptopyridine in different concentrations in DMAc.

Based on this series it is possible to create a calibration line to quantify the conversion of the leaving group of the polymer. The calibration line of the absorbance at 375 nm is shown in *Figure 37*.
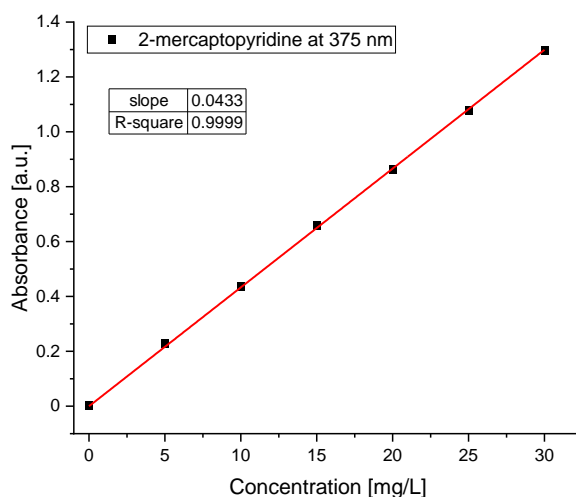
Figure 37: Calibration curve of 2-mercaptopyridine in DMAc at different concentration at 375 nm.

The calibration line is in good accordance with the data points with a coefficient of determination of above 0.9999. The calibration line has the equation

A [a.u.] = 0.0433·c [mg/L]. With this calibration it is possible to calculate the amount of 2MP that is liberated from a polymer sample. Since polymer **9** is an AB-type polymer, the total amount of 2MP that can be liberated can be calculated thanks to the repeating unit (439.6 g/mol) and weighed in amount. A degradation series was performed with the following details (*Table 5*).

Table 5: Concentrations of the degradation series of polymer 9.

Sample	$c_{r.u.}$ [mM]	c_{DTT} [mM]
1	0.057	0
2	0.057	0.001
3	0.057	0.005
4	0.057	0.01
5	0.057	0.05
6	0.057	0.16
7	0.057	0.8
8	0.057	1.6
9	0.057	8
10	0.057	16

A calculated concentration of 0.057 mM/L of polymer **9** (also the total potential concentration of 2MP) with different final concentrations of DTT were made. The samples were prepared by mixing a stock solution of the polymer and stock solutions of DTT and measured immediately after the addition and mixing of these solutions. The obtained data is shown in *Figure 38*.
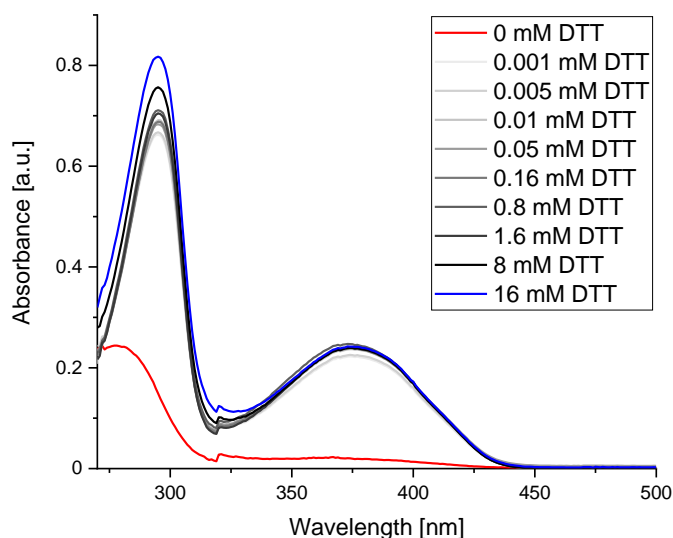
*Figure 38: UV/Vis spectrum of the degradation series of polymer **9**.*

The sample has a much higher absorbance as soon as 2MP is released. A possible linearity between absorbance and time can be seen at the maximum at 290 nm. However, no concentration related removal of the leaving group can be deduced by the absorbance maximum at 375 nm. The absorbance of this signal is varying independently of the concentration of DTT. Surprisingly, even the lowest concentration of DDT shows the same effect as the highest DTT concentration. To visualize this, the absorbance of the concentration series was plotted against the concentration of DTT (c_{DTT}) (*Figure 39*).
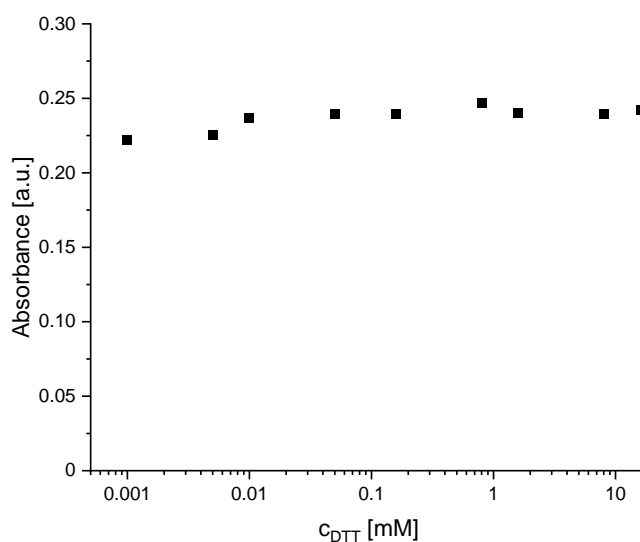
*Figure 39: UV/Vis spectrum of the absorbance at 375 nm of the degradation series of polymer **9**.*

The released concentration of 2MP is between 5.14 mg/L and 5.70 mg/L. This is equal to 0.046 mM and 0.051 mM. By comparing this to *Table 5*, a release

between 80% and 89% was achieved. However, this release is not related to the concentration of DTT that was used. A nearly 300-fold excess of DTT compared to the repeating unit leads to the same result as a nearly 60-fold excess of repeating units compared to DTT. Other experiments were conducted with 2MP instead of DTT. The 2MP concentration was 2 mg/L (0.018 mM) with an absorbance of under 0.2 to see whether 2MP is sufficient to release 2MP that is bound to the polymer (*Figure 40*).
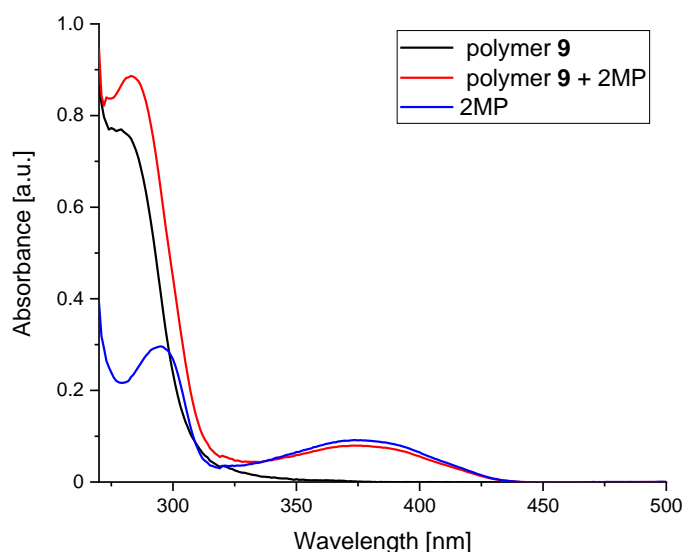
*Figure 40: UV/Vis spectrum of a polymer **9** solution, the same solution with 2MP and only a 2MP solution.*

The absorbance at 375 nm is higher after the addition of 2MP. However, the absorbance of 2MP of the same concentration without the polymer is even higher than the absorbance of a highly concentrated solution of polymer **9** (100 mg/L or 0.023 mM) with 2 mg/L 2MP. This can be due to dilution errors as the difference is insignificantly small. The polymer solution with 2 mg/L 2MP has a calculated concentration ($c_{calc, 2MP}$) of 1.83 mg/L. No elevated absorbance in the polymer **9** solution could be observed after the addition of 2MP indicating that 2MP does not induce further side-chain cleavage. It is highly unlikely that the 2MP that is liberated by small amounts of DTT can induce further side-chain cleavage. The oxidized cyclic DTT (*Scheme 8*) could also be opened by 2MP and attack the polymer subsequently leading to further liberation of 2MP which can act as a catalyst. Another explanation is, that the liberated thiol located in the polymer side-chain after the removal of 2MP could attack 2MP-protected groups in the polymer. To investigate both theories, a thiol is added to the polymer solution,

that is not as reactive as DTT and similar to the liberated thiol in the backbone. That thiol is thioglycerol, which was already used in the monomer synthesis and makes up half of the repeating unit in the backbone. To a solution of polymer **9** (25 mg/L or 0.057 mM) thioglycerol was added which results in a total concentration of 2 mg/L or 0.018 mM (*Figure 41*).
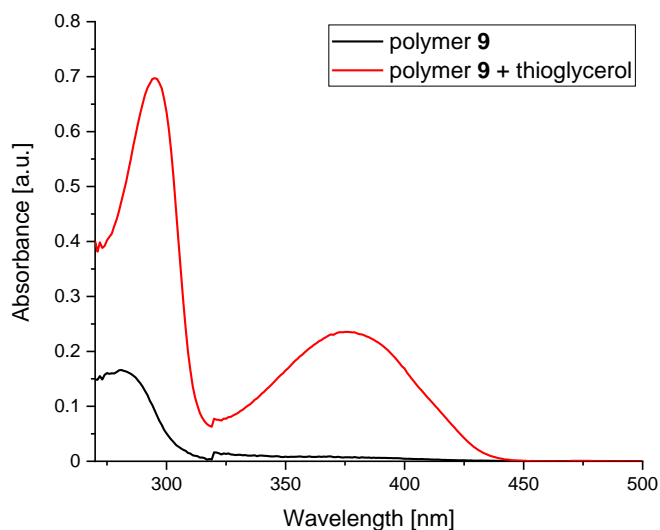
*Figure 41: UV/Vis spectrum of polymer **9** with and without the addition of thioglycerol.*

The concentration of released 2MP was 5.44 mg/l or 0.049 mM. This lies exactly in the range of the first experiment of the degradation series with DTT (*Figure 39*). The catalysis of DTT due to 2MP is disproved. However, the amount of released 2MP is still higher than the amount of added thioglycerol. This indicates that thioglycerol and the liberated thiol in the backbone can be used to remove 2MP by disulfide exchange. A large amount of 2MP is released, which indicates that crosslinking has to occur as there is not enough thioglycerol which can deprotect the polymer. No polymer degradation can occur, when the liberated thiol preferably attacks another leaving group than the backbone in a nucleophilic reaction similar to *Scheme 22*. UV/Vis spectroscopy seem to be a non-sufficient method to characterize the redox-cleavage of the redox-responsive polyurethane **9**, as the maximum cleavage occurs even under 2% (relative to repeating units) of DTT. This cannot be explained by a cascade-like reaction because the loss of a single 2MP unit from the polymer can lead to a maximal loss of another 2MP unit as proposed in *Scheme 47*.
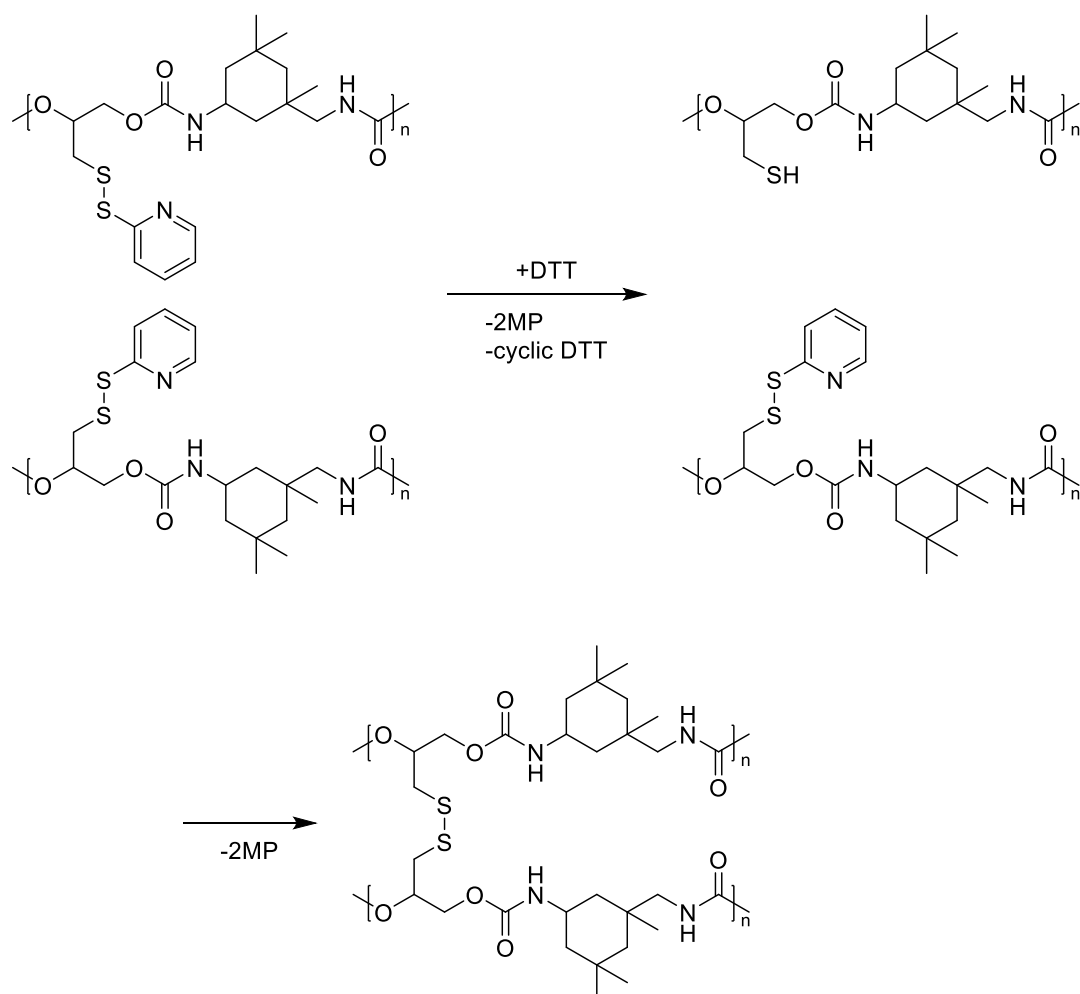
*Scheme 47: Proposed reaction of polymer **9** after losing the redox-responsive side group.*

Each DTT unit that reacts with the redox-responsive side-chain can lead to a cleavage of two 2MP units. As shown in *Figure 38*, a concentration of under 1.75% DTT with respect to the repeating units lead to the same removal as an excess of DTT. However, if the reaction takes place as proposed, a maximum of 3.5% of the repeating units should lose 2MP, which is not the case.

The same experiment was conducted for polymer **16** as this polymer bears the same protecting group as polymer **9**. The monomer ratio of monomer **14** : bdm was calculated to be 1 : 1.3. The total concentrations of the degradation series are summarized in *Table 6*.

*Table 6: Concentrations of the degradation series of polymer **16**.*

Sample	$c_{r.u.}$ [mM]	c_{DTT} [mM]
1	0.101	0
2	0.101	0.001
3	0.101	0.005
4	0.101	0.01
5	0.101	0.05
6	0.101	0.1
7	0.101	0.5
8	0.101	1
9	0.101	5
10	0.101	10

The absorbance at all wavelengths rises as soon as 2MP is released. The measurements were taken after approximately 5 min after the addition of DTT. Unlike the degradation series of polymer **9**, this degradation series seems to be dependent on c_{DTT} (*Figure 42*).
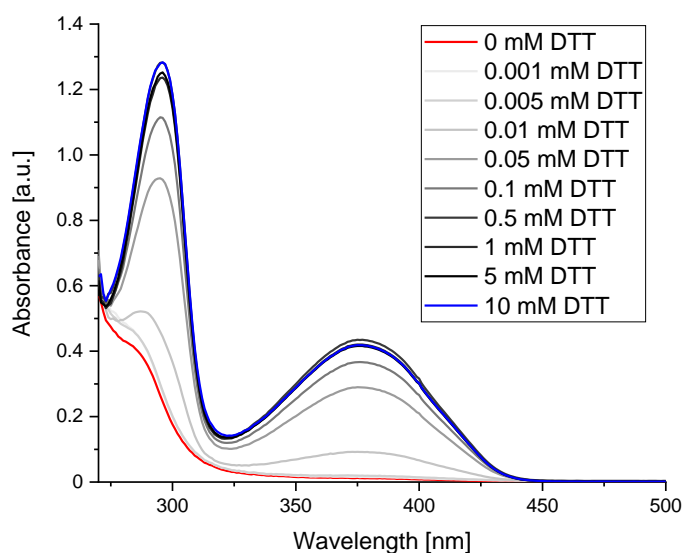
*Figure 42: UV/Vis spectrum of the degradation series of polymer **16**.*

After the addition of DTT, two maxima can clearly be observed at $\lambda_{max,1}$ = 296 nm and $\lambda_{max,2}$ = 375 nm. The absorbance at 375 nm grows as more DTT is added.

To further analyze this, the absorbance maxima at 375 nm is plotted against the corresponding concentration of DTT (c_{DTT}) to obtain *Figure 43*.
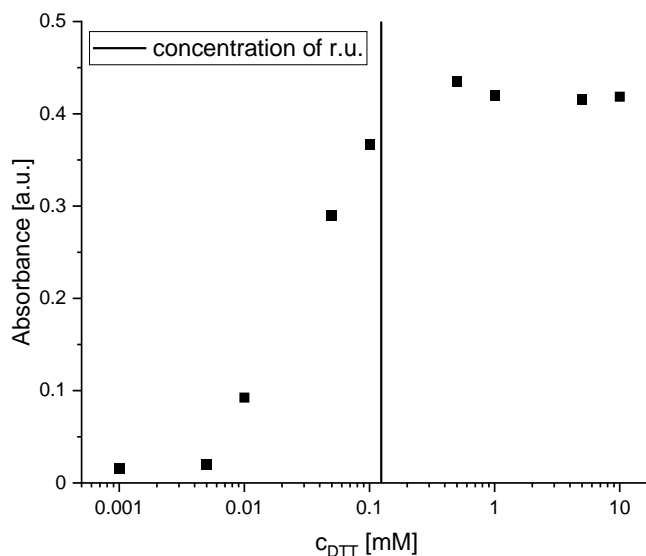
Figure 43: UV/Vis spectrum of the absorbance at 375 nm of the degradation series of polymer 16.

As already said, the absorbance seems to be concentration dependent. As soon as a concentration above the calculated concentration of repeating units ($c_{r.u.}$) is reached, the absorbance is steady. The absorbance is also steady below a c_{DTT} = 0.01 mM. The maximum 2MP concentration corresponding to *Figure 37* is 10 mg/L (0.09 mM and 89% in respect to the maximal calculated amount of 2MP). Interestingly, this polymer shows a clear DTT-concentration dependence, different from polymer **9**, where no concentration dependence could be found. Even the smallest amount of DTT lead to the complete release of 2MP in case of polymer **9**. One reason for the behavior of polymer **16** might be the longer distance of liberated thiols to 2MP groups due to the stiffer comonomer benzene dimethanol. Another reason might be the proposed backbiting of the thiol leading to a thiirane or thiocarbamate as proposed in *Scheme 25*. This reaction would proceed faster than an attack of another repeating unit. As seen in *Figure 42*, the liberated 2MP does not lead to further redox-cleavage. It was observed that this reaction is also time dependent, as the absorbance changed after the addition of DTT over the first 10 min. A suitable fit could not be applied to the data of *Figure 43*. Due to the slow reaction a direct kinetic series of the redox-cleavage of polymer **16** could be measured (*Figure 44*).
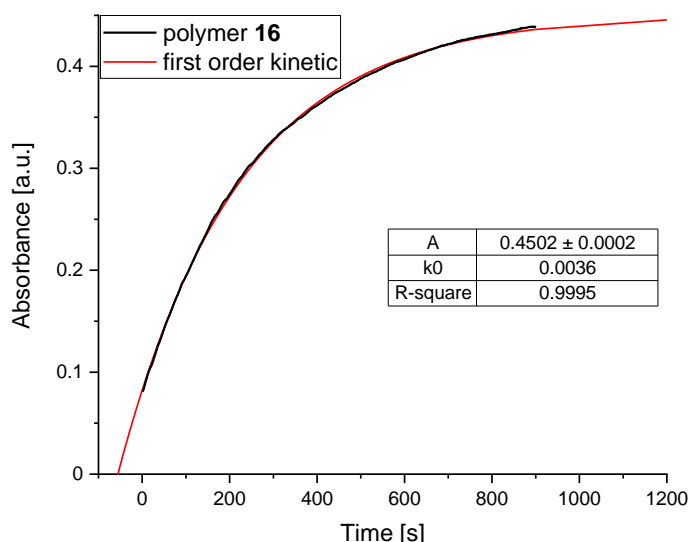
*Figure 44: UV/Vis spectrum of the kinetic measurement of polymer **16** after the addition of DTT.*

A DTT-concentration of 0.1 mM was used to trigger the redox-cleavage with a polymer concentration of 0.101 mM. The obtained data points could be fitted into first order kinetics and k_{DTT} = 0.00363 s^{-1}. This reaction is roughly 100-times slower compared to the UV-cleavage reactions previously observed (*Table 2*). Following the fit, the maximal absorbance is $A_{max,theo.}$ = 0.45 (0.093 mM of liberated 2MP) and the measured maximal measured absorbance is A = 0.439 (0.091 mM of liberated 2MP). The total conversion is therefore 92% and the measured conversion is 90% of the cleavage of the maximal calculated 2MP-groups.

The redox-cleavage of polymer **15** was not analyzed by UV/Vis spectroscopy because no difference in the maxima above 270 nm (cut-off of DMAc) was found. Instead of the UV/Vis spectroscopy, the polymers were tested by SEC, before and after addition of DTT. The analysis was started with polymer **9** with a total concentration of 10 mM DTT and a $c_{r.u.}$ = 1.36 mM. The SEC analysis of this degradation experiment could only be conducted in DMAc, because no other solvent used for SEC could dissolve DTT and the polymer. The SEC plot of the polymer with and without DTT after 1 d of stirring is depicted in *Figure 45*.
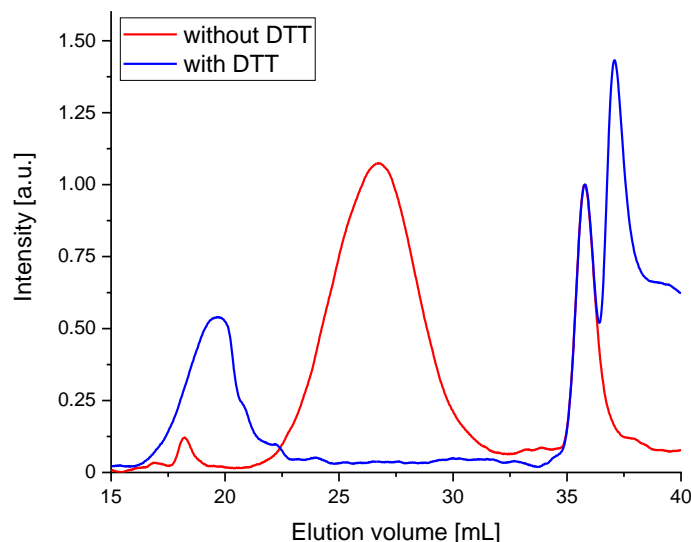
*Figure 45: SEC elugrams of polymer **9** without DTT (red) and with DTT (blue).*

The polymer sample after the addition of DTT showed a signal at 20 mL with a $M_n = 950000$ g/mol and a dispersity of 7.79 compared to the polymer analysis without DTT at 26 mL with a $M_n = 26600$ g/mol and a dispersity of 1.65. The biggest issue with this analysis is however, that the molar mass increased more than 10-fold after the addition of DTT. A big signal emerged after the addition of DTT at 37 mL after the BHT signal. This indicates that degradation indeed occurred. However, the polymer signal at 36 mL completely disappeared, but a new signal at 20 mL emerged. The polymer could have formed a loose network due to the high concentration used for this analysis technique or the polymer changed its interaction with the SEC column due to the change in polarity. Either way, degradation indeed occurred, but it led to many small molecules as well as big molecules that could even be networks.

The same analysis was conducted with polymer **15**, that has no disulfide-bond. The whole redox-cleavage mechanism is different to the disulfide-bond containing polymers **9** and **16** as depicted in *Scheme 26*. Since no change could be observed in the UV/Vis spectroscopy of polymer **15** after the addition of DTT, SEC samples of polymer **15** with and without DTT were made. The concentration of DTT was again 1 mM and $c_{r.u.} = 0.7$ mM. The SEC plot is depicted in *Figure 46*.
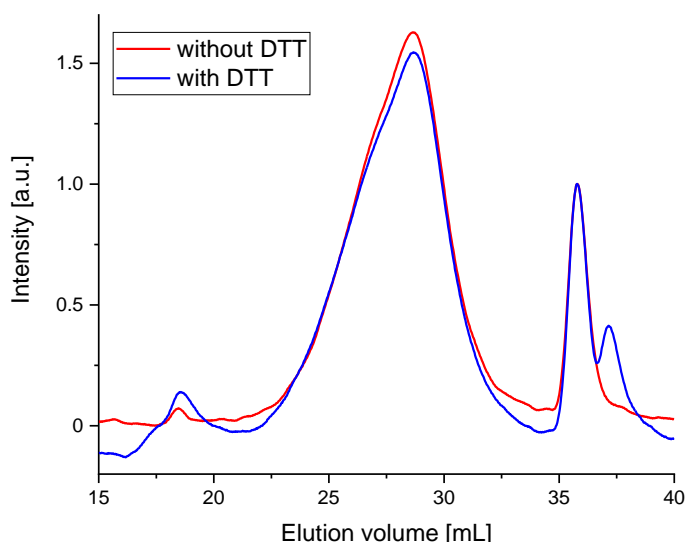
*Figure 46: SEC plot of polymer **15** with and without DTT.*

As expected, due to the lower redox-potential, DTT is too weak to reduce the nitro-group of the side-chain to induce the redox-cleavage of the amine-protecting group. As the difference between these two measurements cannot be distinguished, the results are summarized in *Table 7*.

*Table 7: Summarized molar mass and dispersity of the SEC experiment regarding the degradation of polymer **9**.*

Sample	M_n [g/mol]	Đ
polymer **15**	13700	2.00
polymer **15** with DTT	13400	2.14

The difference in these samples is insignificant with 300 g/mol and lies within the error range of the analysis technique. The dispersity however changed from 2.00 to 2.14. This change is indeed significant, but without a change in M_n no degradation can be proven. However, a small signal after the BHT signal at 37 mL emerges indicating that small UV active molecules were released from the polymer. The polymer signal decreased and another signal at 18 mL emerged. Even when no direct degradation was observed, a change definitely occurred in the polymer sample that was treated with DTT.

The last redox-responsive polymer was analyzed in the same fashion. A solution of polymer **16** ($c_{r.u.}$ = 0.101 mM) in DMAc was compared to a solution of polymer

16 with DTT (c_{DTT} = 10 mM and $c_{r.u.}$ = 0.101 mM) in DMAc. The SEC elution curves are depicted in *Figure 47*.
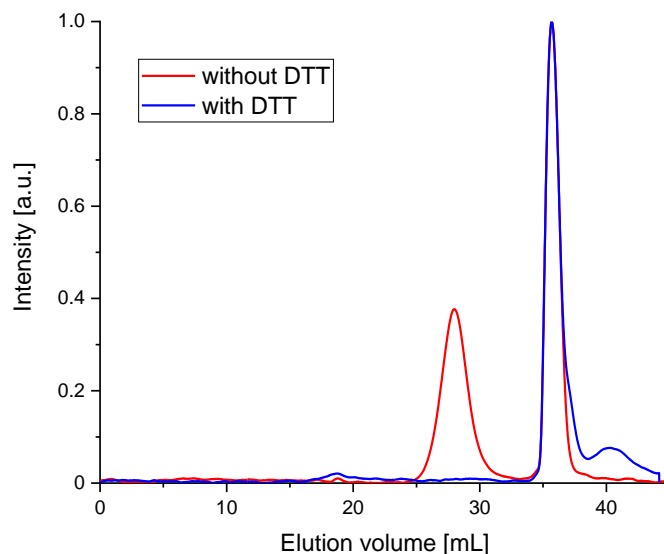
*Figure 47: SEC plot of polymer **16** with (blue) and without DTT (red).*

The polymer signal can be seen between 25 – 32 mL before adding DTT (red curve). The solution immediately changed the color from colorless to yellow upon addition of DTT due to the liberation of 2MP. The initial polymer signal disappeared, but a signal between 15 – 22 mL appeared and the liberated 2MP can be found at 38 – 44 mL (blue curve). Nearly the whole polymer degraded into small molecules except some parts, that recombined into bigger molecules or networks.

Designing polymers that respond to reductive environments is a difficult task, as the trigger is not as precise as e.g., light. From the three presented redox-responsive side groups the polymers with a DPDS-group (polymers **9** and **16**) seem to undergo an efficient cleaving. However, only polymer **16** shows a full degradation of the polymer upon addition of DTT. The side-chain cleavage of polymer **9** is successful, but the polymer does not degrade. Instead, it seems like the polymer chains undergo crosslinking resulting in high molecular polymers or polymer networks. Polymer **15** showed no significant degradation upon the addition of DTT and is no suitable base for a redox-responsive DDS.

4.3 pH-responsive self-accelerating polymers

4.3.1 Monomer synthesis

The aim was to synthesize two monomer with an acetal group that are pH-responsive. The monomers of choice were based on benzaldehyde with pentaerythritol and piperonal with pentaerythritol. Both monomers were synthesized in the same way, but small differences were made at the temperature and reaction duration. The reaction with benzaldehyde was stirred for 3 h at room temperature and recrystallized two times from toluene to obtain **17** (*Scheme 48*).
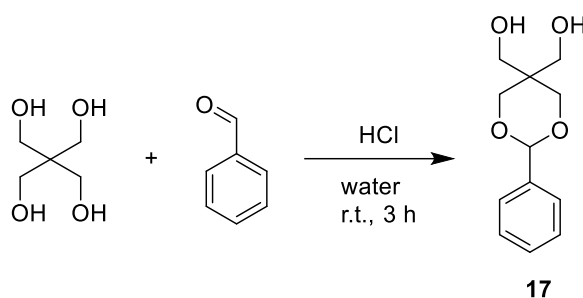
*Scheme 48: Synthesis of **17**: Pentaerythritol was dissolved in water followed by the addition of HCl and benzaldehyde. The precipitate was recrystallized twice from toluene.*

Even though the acetalization was performed in water, the reaction yielded 63% of the product. The monomer was analyzed by NMR spectroscopy and ESI-ToF-MS. The same reaction was carried out using 6-nitropiperonal and pentaerythritol. Instead stirring the reaction at room temperature for 3 h, the reaction was stirred for a much longer duration (3 d) and at 60 °C (*Scheme 49*).
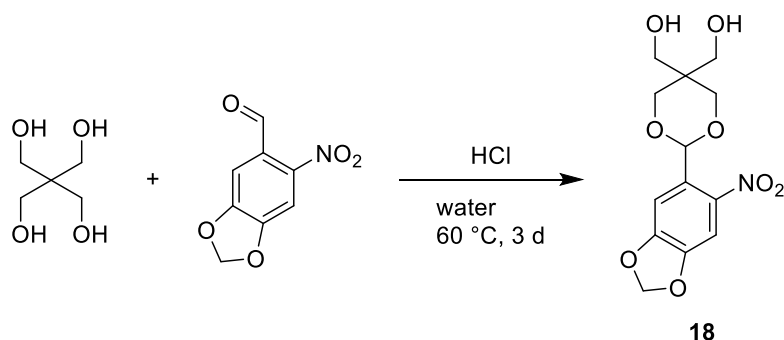
*Scheme 49: Synthesis of **18**: Pentaerythritol was dissolved in water followed by the addition of HCl and 6-nitropiperonal. The precipitate was recrystallized twice from toluene/THF (9:1).*

The yield of this reaction is again surprisingly high with 66% and even higher than in the reaction with benzaldehyde. This monomer was analyzed by NMR spectroscopy and ESI-ToF-MS.

4.3.2   Polymer synthesis

The two pH-responsive monomers **17** and **18** were used in the same polymerization methods. The first attempts involved the polyaddition of the monomers with IPDI. Only one of the two reactions is depicted in *Scheme 50*.
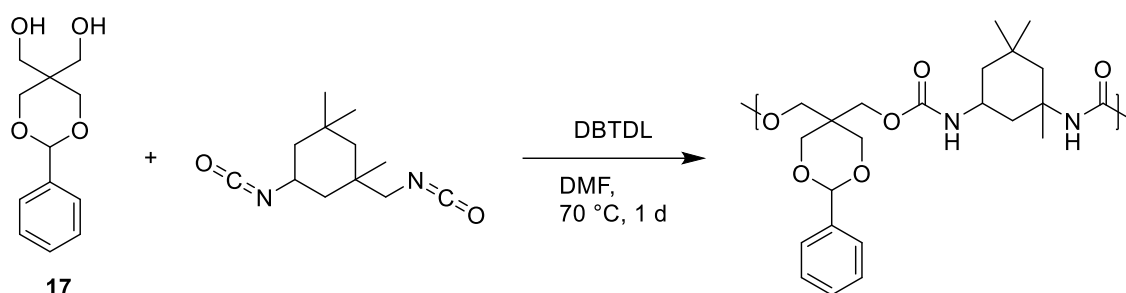
Scheme 50: Synthesis of a pH-responsive polyurethane: DBTDL and monomer 17 were dissolved in DMF under N_2-atmosphere and IPDI was added dropwise under stirring. The reaction mixture was stirred at 70 °C for 1 d and was found to be solidified.

The polymerization failed with both monomers due to the solidification of the reaction mixture after 1 d. Hence, the same approach that was described before was used. BDM was added as a comonomer to successfully prevent the solidification. Additionally, the temperature was lowered, because the addition of BDM still leads to the solidification of the polymer reaction mixture at 70 °C The first pH-responsive polymer was synthesized by the polyaddition of monomer **17**, BDM and IPDI (*Scheme 51*).
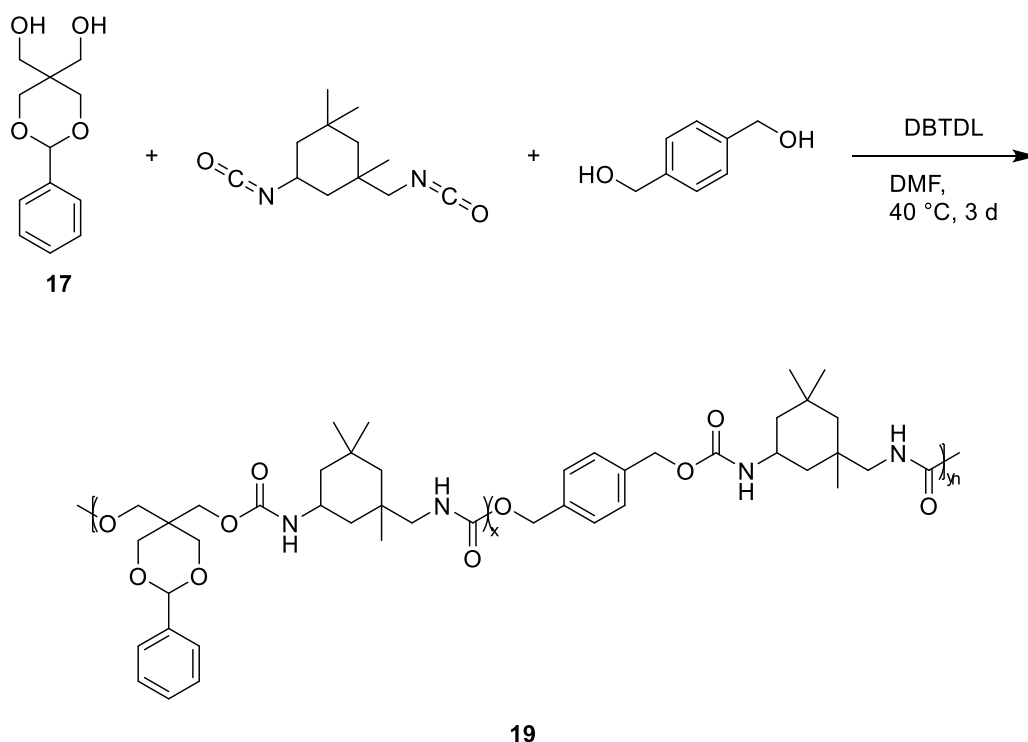
*Scheme 51: Synthesis of polymer **19**: DBTDL, BDM and monomer **17** were dissolved in DMF under N₂-atmosphere and IPDI was added dropwise under stirring. The reaction mixture was stirred at 40 °C for 3 d and precipitated from MeOH.*

The yield of 62% is relatively high. The colorless polymer **19** was obtained. This polymer was analyzed by SEC and NMR spectroscopy. The molar mass of this polymer is ranging from 15300 – 30000 g/mol with a dispersity between 1.57 – 1.85 (measured in THF with a PS standard, *Figure 47*).
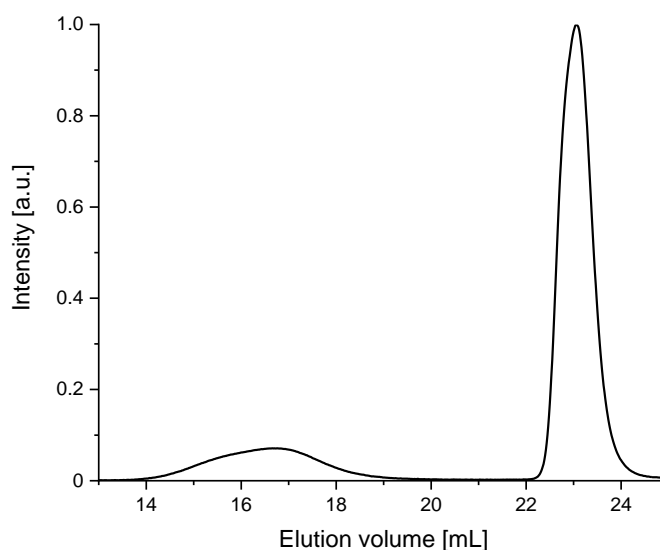
*Figure 48: SEC elugram of polymer **19** in THF.*

The SEC signal is a monomodal peak ranging from 14 mL to 19 mL. The relatively low dispersity confirms that the polymerization proceeds quite uniformly. However, for a polyaddition the dispersity is quite low. The low dispersity can be explained by the fractional precipitation of the polymer. The precipitation solvent (MeOH) might dissolve polymers with a smaller chain length and precipitates polymers with a higher chain length.

The second pH-responsive acetal-based polyurethane was synthesized by the polyaddition of monomer **18**, BDM and IPDI after unsuccessful polymerization without BDM. For that polymerization attempt, the temperature was lowered to 40 °C and the reaction time lowered to 1 d to prevent solidification of the reaction mixture (*Scheme 52*).
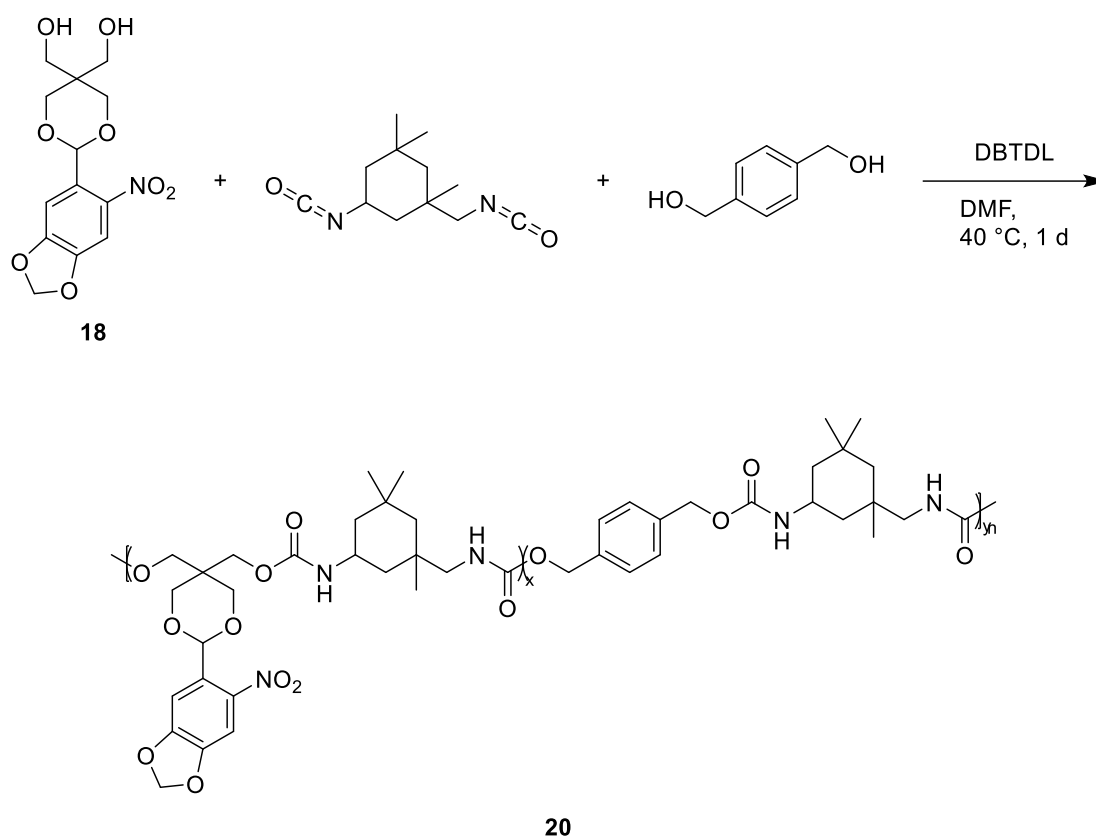
*Scheme 52: Synthesis of polymer **20**: DBTDL, BDM and monomer **18** were dissolved in DMF under N_2-atmosphere and IPDI was added dropwise under stirring. The reaction mixture was stirred at 40 °C for 1 d and precipitated from MeOH.*

Polymer **20** was obtained with a yield of 83%. This polymer was analyzed by SEC, NMR spectroscopy and UV/Vis spectroscopy. The molar mass of the polymer was ranging between 10400 – 13500 g/mol with a dispersity between 2.09-3.22 (measured in THF, *Figure 49*).
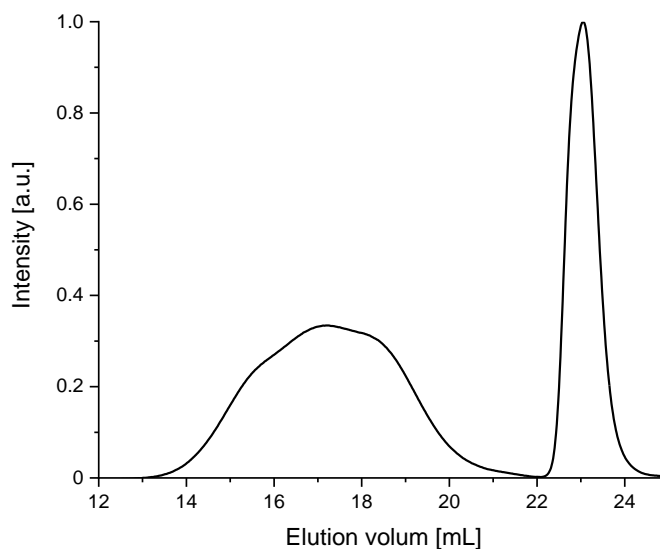
*Figure 49: SEC elugram of polymer **20** in THF.*

The SEC signal shows a multimodal (trimodal) polymer signal ranging from 13 mL to 22 mL. This broad signal is also reflected in the high dispersity. However, this polymer is still large enough to be tested for the responsivity and degradation. This polymer is based on the same aldehyde as the light-responsive polymers. This side group (6-nitropiperonal) in the light-responsive polymers had absorbance maxima ranging between 270 – 400 nm (e.g., *Figure 13*). Therefore, UV/Vis spectroscopy can be used to further characterize the polymer (*Figure 50*).
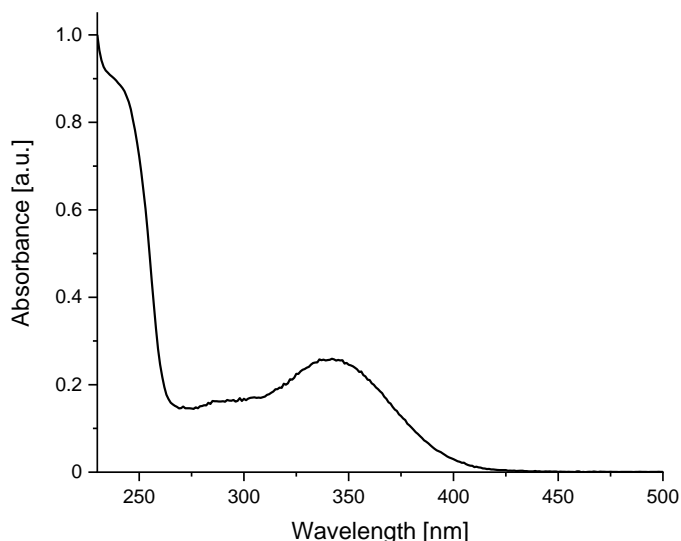
*Figure 50: UV/Vis spectrum of polymer **20**.*

This absorbance pattern is highly similar to the one of the light-responsive polymers. The three absorbance maxima are located at roughly 245 nm (no clear signal), 291 nm (no clear signal) and 342 nm and therefore in the same range as

in the light-responsive polymers. Polymer **20** could be pH-responsive and light-responsive as well and will be analyzed with regard to these two triggers.

4.3.3   Degradation studies

The first degradation test was performed with polymer **19** with respect to the pH-responsive behavior. Therefore, the polymer was dissolved in a solution of HCl in dioxane with a drop of water that is necessary for the acetal cleaving reaction (*Scheme 53*).
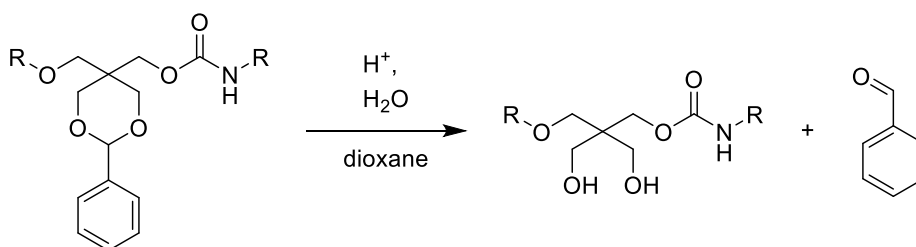
*Scheme 53: Acid cleavage of polymer **19** with HCl in dioxane with a drop of water.*

After stirring overnight, the dioxane was removed by rotary evaporation and the residue was dissolved in the solvent for the SEC analysis (THF with BHT for calibration). This was compared to the polymer before the acid cleavage (*Figure 52*).
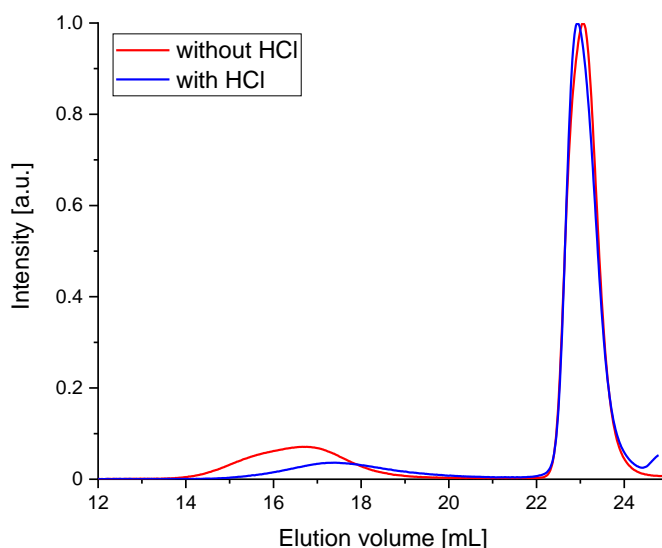
*Figure 51: SEC elugrams of polymer **19** before (red) and after stirring with dioxane and HCl (blue), measured in THF with a PS standard.*

The maximum shifted to higher elution volumes from 14 – 19 mL to 15 – 21 mL. The M_n decreased from 30000 g/mol to roughly 12000 g/mol. The intensity of the

polymer signal was lowered as well. The dispersity changed from 1.84 to 1.74. It seems that a new signal arises after the BHT after 24 mL. This signal might appear due to the liberated benzaldehyde or small molecular polymer degradation products. Polymer **19** shows an acid-responsive degradation, but the degradation only results in polymers not oligomers or small molecules. Therefore, polymer **20** is not a suitable polymer as the base for an acid-labile drug delivery system.

The same procedure was performed on polymer **20** to evaluate the acid cleavage induced polymer degradation (*Figure 52*).
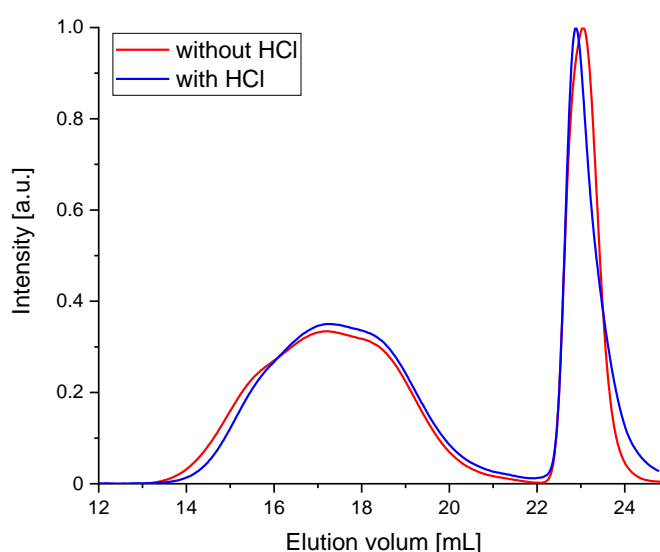
*Figure 52: SEC elugrams of polymer **20** before (red) and after stirring with dioxane and HCl (blue), measured in THF.*

No significant change in the signal intensity can be observed. These small differences can be due to the SEC sample preparation. The signal of the polymer that was treated with acid is still trimodal and shifted to minimally to higher elution volumes. The M_n decreased from 13500 g/mol to 11000 g/mol and the dispersity changed from 3.22 to 2.84. This polymer does not undergo acid triggered degradation. However, the leaving group is also light-responsive and the polymer might undergo UV light induced polymer degradation. Therefore, an irradiation series was performed similar to the irradiation series of the light-responsive polymers that was already shown. In short, polymer **20** was dissolved in DCM and irradiated for certain time units. The irradiation series of 0 – 10 s is shown in *Figure 53*.
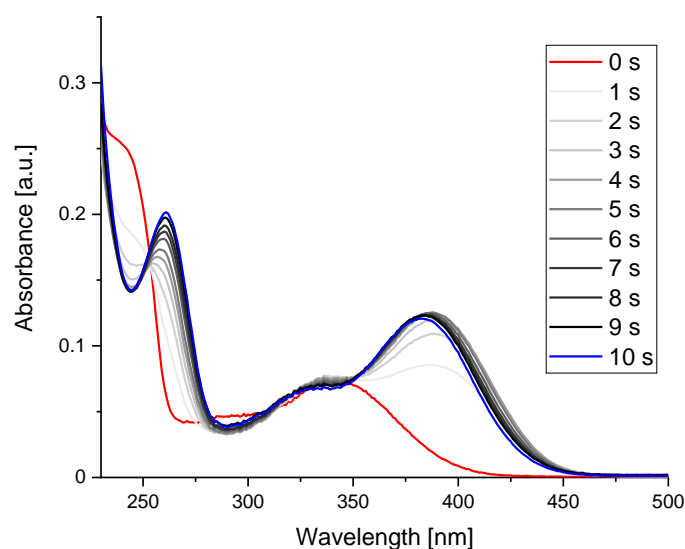
*Figure 53: UV/Vis spectrum of an irradiation series of the light-responsive polyester **20**.*

At first, the change in the absorbance looks similar to the previous one of the side group based on 6NP (e.g., *Figure 14*). However, the intensity of the absorbance changes within 10 s. After 4 s of irradiation, a maximum at 388 nm arises. This maximum however undergoes a shift to lower wavelengths until 10 s of irradiation. The new maximum has a wavelength of 383 nm. The smaller maximum shifts to roughly 336 nm after 4 s of irradiation. By irradiating the polymer for 10 s this maximum loses absorbance and shifts to roughly 330 nm. This change in both maxima is a hint to a nonuniform cleaving process of the light-responsive side group within the first 10 s of irradiation. Because of this tendency, the UV irradiation series was expanded to longer irradiation times (*Figure 54*).
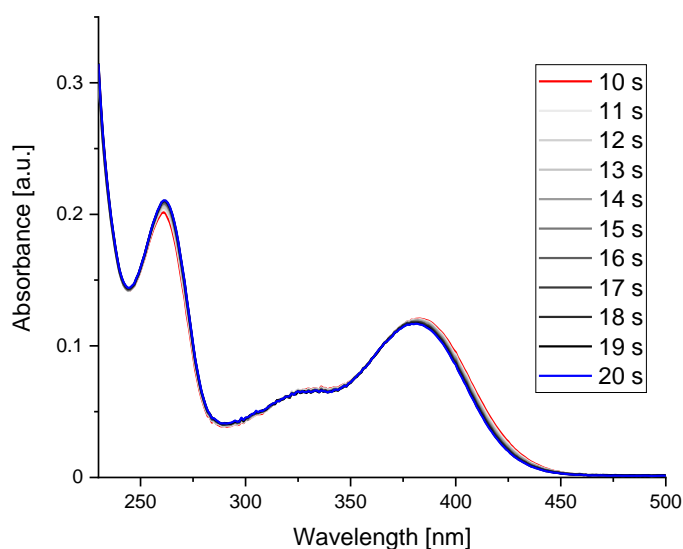
Figure 54: UV/Vis spectrum of an irradiation series of the light-responsive polyester **20**.

All in all, no significant changes could be observed between 10 s and 20 s of UV irradiation. The maximum of 383 nm shifts again to even lower wavelengths (381 nm) and the absorbance is lowered as well. The maximum at 260 nm increases in absorbance. This irradiation series was continued to 240 s to see whether any further changes occur (*Figure 55*).
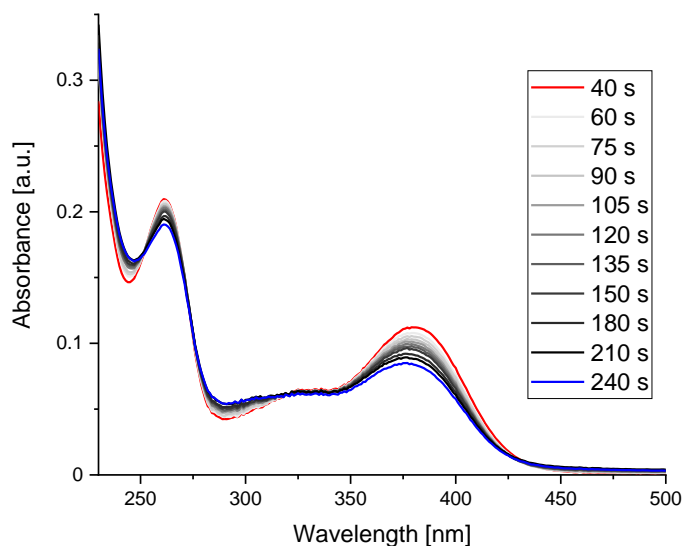
Figure 55: UV/Vis spectrum of an irradiation series of the light-responsive polyester **20**.

By irradiating the polymer sample for up to 240 s, the two previously discussed maxima change again. The maximum at 381 nm shifts to an even lower wavelength (375 nm) and the absorbance decreases significantly from 0.112 to 0.085. The absorbance of the maximum at 260 nm decreases as well from 0.21

to 0.19. Between 0 – 20 s of irradiation the absorbance increased at first and decreases after 20 s of irradiation. This UV cleavage process seems not to process as uniformly as the previous irradiation experiments with the light-responsive polymers. The absorbance of the signal at 260 nm was plotted against irradiation time to see whether a reaction constant can be derived (*Figure 56*). The other maximum cannot be used for this, as the maximum shifts to other wavelengths.
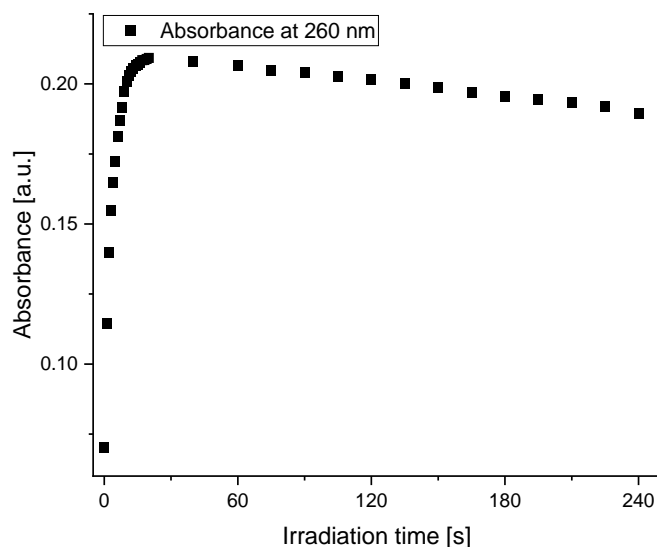
*Figure 56: UV/Vis spectrum of the absorbance at 260 nm against irradiation time of polymer **20**.*

A reaction constant cannot be calculated because the absorbance does not reach a constant value but decreases after reaching the maximum. From this data can be concluded, that the UV cleavage is not a reaction following first order kinetics. To further prove the non-uniformity of this reaction, an AD diagram is plotted (Figure 57).
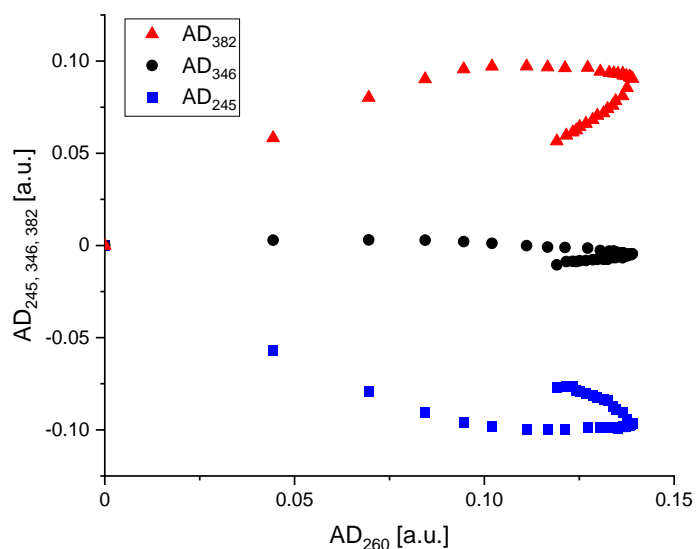
*Figure 57: AD diagrams of polymer **20** for different wavelengths.*

The data points are only linear for the first three seconds (first three points after 0). Afterwards, the curve flattens before turning directions. From this AD diagram a nonuniform reaction can be concluded. However, even with a nonuniform UV cleavage, the polymer could still be able to degrade. By assuming that the UV cleavage proceeds as previously described in *Scheme 21*, the following reaction can be formulated for the UV cleavage of polymer **20** (*Scheme 54*).
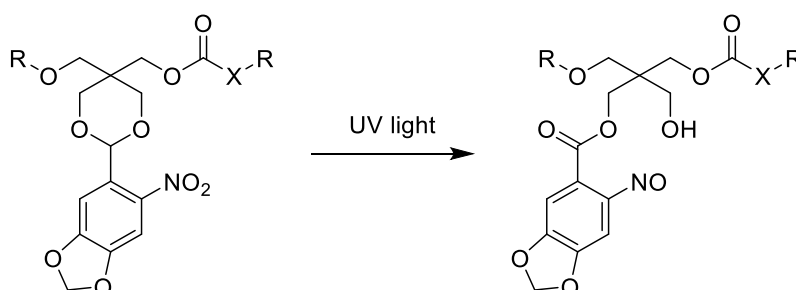
*Scheme 54: UV cleavage of the light-responsive side group of polymer **20**.*

The acetal is converted to an ester and a hydroxy group is liberated that can subsequently attack the backbone as in previous reactions. To test this degradation behavior, a stock solution of polymer **20** in DCM was prepared and distributed into five parts. These parts were irradiated for different times and analyzed by SEC after removing the solvent and redissolving the residue in the THF with BHT for calibration (*Figure 58*).
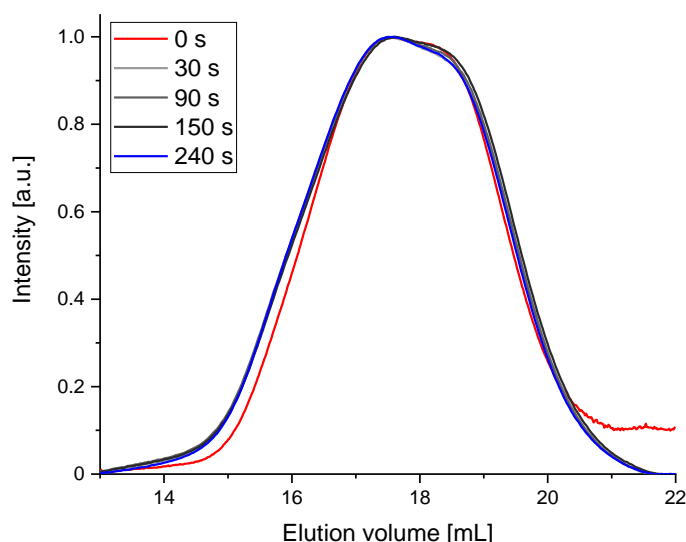
*Figure 58: SEC elugrams of polymer **20** after UV irradiation for a certain time measured in THF with a PS standard.*

As seen in the elugram of the irradiation series of polymer **20**, nearly no change can be observed. The signal of the irradiated samples is insignificantly broader compared to the non-irradiated sample. However, the signals were analyzed and the results are summarized in *Table 8*.

*Table 8: SEC data of polymer **20** after UV irradiation for a certain time measured in THF with a PS standard.*

Irradiation time [s]	M_n [g/mol]	Đ
0	10500	2.84
30	10000	2.71
90	10000	2.78
150	9700	2.80
240	10100	2.61

The M_n of the samples is ranging between 9700 – 10500 g/mol with a dispersity of 2.61 – 2.84. This change in molar mass is however not significant enough to conclude that a degradation process occurs in the polymer. Polymer **20** seems to be unsuitable as an acid-responsive or a light-responsive drug delivery system.

Both polymers are not suitable bases for functional pH-responsive drug delivery systems. Polymer **19** reacts to an acid environment, but the M_n only decreases by roughly 60%. The resulting M_n of 12000 g/mol is too high to achieve the goal

of a degradation that results in only small molecules. Polymer **20** showed changes in the UV/Vis spectroscopy upon UV light irradiation, but no degradation could be observed. The polymer also showed no degradation in acidic environment. Even when the photoreaction proceeds as proposed, a nucleophile is liberated that can attack the backbone as in previous examples. The hydroxyl group is a weaker nucleophile as an amine and is probably not able to attack the carbamate unit and cleave off the amine group of the comonomer.

5   Conclusion

In this dissertation, six monomers were synthesized and characterized that respond to either UV light, a reductive environment or a drop in pH value. Out of these monomers in total nine polymers were synthesized, whereof theoretically four respond to UV light, three respond to reductive environments and two respond to a drop of pH (whereof one should respond to UV light and a drop in pH value).

Four light-responsive polymers were synthesized out of one monomer. The polyester and two polyurethanes were used for degradation studies, as the M_n of the polycarbonate was too small. All polymers reacted upon light irradiation and showed a significant change in the UV/Vis spectrum after irradiation. After 10 s of irradiation, there was no significant change in the UV/Vis spectrum. The reaction constants of the photocleavage reaction were in the same order of magnitude. These polymers also showed a significant drop in the M_n after light irradiation that was confirmed by SEC. The light-responsive 6NP-based polyester was also used for cell tests. Nanoparticles were prepared by Timo Schoppa from the Langer group in WWU Münster and these nanoparticles underwent different studies proving the applicability of the light-responsive 6NP-based polyester as a base for a light-responsive DDS. Compared to previous groups, the 6NP-based leaving groups responds faster to the trigger and therefore improves the work on light-responsive side-chain located protecting groups.

The second addressed trigger was the reductive environment. Three polymers were synthesized out of three different responsive polymers. Two of them are serinol-based and one of them was thioglycerol-based. Both polymers that had a leaving group based on DPDS (polymer **9** and **16**) showed a reaction do DTT. However, the polymers reacted differently to DTT. Polymer **9** had an increase in M_n and polymer **16** degraded completely as analyzed by SEC. The released 4MP-group is UV-active and the cleavage was analyzed by UV/Vis spectroscopy. The cleavage of 4MP in polymer **16** was proportional to the concentration of DTT. The reaction proceeds slowly and a kinetic was measured. The 4MP-cleavage in polymer **9** however was not dependent on the concentration of DTT. Even a concentration of DTT below the concentration of calculated responsive groups lead to a nearly complete cleavage of the 4MP groups. The higher M_n and the

results of the UV/Vis spectroscopy can be explained by crosslinking reactions. The third redox-responsive polymer **15** did not react with DTT at all. The only polymer that is a suitable fit as a base for a redox-responsive DDS is polymer **16**, as the cleavage can be monitored and adjusted and the polymer degraded completely as shown by SEC.

The last addressed trigger was the change in the pH to lower values. Two polymers were synthesized out of two different responsive monomers. Both monomers consist of an aromatic aldehyde (benzaldehyde or 6NP) that was coupled *via* an acetal-bond to pentaerythritol. The degradation of the obtained polymers was tested and the benzaldehyde-based polymer **19** had a reduction of the M_n of 60%. The 6NP-based polymer **20** did not react to a reduction of the pH-value. Polymer **20** was tested for its light-responsiveness. The UV/Vis spectra showed a nonuniform photoreaction that is not finished even after 240 s. The SEC analysis showed that no degradation took place after the light irradiation up to 240 s. Both polymers are not suitable bases for pH-responsive DDS, as both polymers show either a degradation that ends up in polymers with more than 10000 g/mol or show no degradation at all.

6 Outlook

The 6NP-group of the light-responsive polymers can also be cleaved off with a two-photon absorption system as previously described in the theoretical part. By doing this, the wavelength of the light can be above 700 nm to trigger the photo removal. Light at this wavelength can penetrate deep into the tissue and gives access to a more facile therapy as no endoscopic light sources or cuts are needed for the application of a light-responsive drug delivery system.

Only one of the three presented redox-responsive polymers show a complete degradation upon the addition of DTT. Further studies on polymer **16** and the development of a redox-responsive drug delivery system is a highly interesting approach.

As the polymers **19** and **20** did not degrade in an acidic environment, two choices are left. Either the degradation tests are not suitable and need further improvement or new pH-responsive groups need to be found that show a better degradation behavior.

After having successful attempts at all chosen triggers, multi-responsive drug delivery systems can be prepared. Therefore, monomers can be used that either react to more than one trigger or a copolymer can be prepared out of two comonomers that both react to one of the triggers, respectively. Another approach is the blending of two polymers that each respond to one trigger while preparing the nanoparticles.

7   Acknowledgement

Parts of this work have already been pre-published:

T. Schoppa, D. Jung, T. Rust, D. Mulac, D. Kuckling and K. Langer, *Int. J. Pharm.*, 2021, **597**, 120326, DOI: 10.1016/j.ijpharm.2021.120326

D. Jung, T. Rust, K. Völlmecke, T. Schoppa, K. Langer and D. Kuckling, *Polym. Chem.*,
2021, DOI: 10.1039/D1PY00442E

8 Danksagung

Danksagung

Ich möchte mich auch bei allen Kommilitonen, Doktoranden und Professoren bedanken, die mein Studium in Siegen und in Adelaide begleitet und mich auf meine Promotion vorbereitet haben.

Zu guter Letzt, möchte ich allen meinen Freunden danken, die mich mein Leben lang begleitet haben und immer für die notwendige Ablenkung, Entspannung und Spaß während meiner Promotion sorgten.

9 Eidesstattliche Erklärung

Hiermit versichere ich, Dimitri Jung, die vorliegende Arbeit selbstständig, ohne Hilfe Dritter und nur mit den angegebenen Quellen und Hilfsmitteln angefertigt zu haben. Alle Stellen, die aus anderen Quellen entnommen wurden, sind als solche kenntlich gemacht worden. Diese Arbeit wurde in gleicher oder ähnlicher Form noch keiner Prüfungsbehörde vorgelegt.

Paderborn, den

_____   _____
Dimitri Jung   Ort, Datum

10   Anerkennung der Promotionsordnung

Hiermit erkenne ich, Dimitri Jung, die Promotionsordnung der Fakultät für Naturwissenschaften der Universität Paderborn, welche am 12. November 2012 von der Universität erlassen wurde und durch die Satzung vom 20. Februar 2020 zuletzt geändert wurde, an. Bisher wurde weder an der Universität Paderborn noch an einer anderen Hochschule im In- oder Ausland ein Promotionsversuch angenommen.

Paderborn, den

_____   _____
Dimitri Jung   Ort, Datum

11 Appendix

11.1 Abbreviation

Table 9: Abbreviations

2MP	2-Mercaptopyridine
5-FU	5-Fluorouracil
6NP	6-Nitropiperonal
a.u.	Arbitrary unit
AD	Absorbance differences
AFM	Atomic force microscopy
ATRP	Atom transfer radical polymerization
BDM	1,4-Benzenedimethanol
BHT	Butylated hydroxytoluene
Boc	tert-Butyloxycarbonyl protecting group
BSA	Bovine serum albumin
CCK-8	Cell counting kit – 8
CHO-PCL-CHO	Aldehyde-terminated polycaprolactone
CLSM	Confocal laser scanning microscopy
CMC	Critical micelle concentration
conc.	Concentrated
CRP	Controlled radical polymerization
Đ	Dispersity
DAD	Diode array detector
DBTDL	Dibutyltin dilaurate
DCM	Dichloromethane
DDS	Drug delivery system
DiI	1,1-Dioctadecyl-3,3,3,3-tetramethylindocarbocyanine perchlorate
DIPEA	Diisopropyl ethylamine
DLS	Dynamic light scattering
DMAc	Dimethylacetamide

DMAP	4-Dimethylaminopyridine
DMEM	Dulbecco's Modified Eagle Medium
DMF	*N,N'*-Dimethylformamide
DOX	Doxorubicin
DPDS	2,2′-Dipyridyl disulfide
DSDA	Disulfide-based diacrylate
DTT	Dithiothreitol
EC_{50}	Half maximal effective concentration
EDTA	Ethylenediaminetetraacetic acid
EPR	Enhanced permeability and retention
Eq.	Equvalents
ESI	Electrospray ionization
EtOAc	Ethyl acetate
EtOH	Ethanol
FDA	Food and Drug Administration from USA
FLD	Fluorescence detector
gly	Glycine
GSH	Glutathione
HDI	Hexamethylene diisocyanate
HPLC	High performance liquig chromatography
HRMS	High-resolution mass spectrometry
IPDI	Isophorone diisocyanate
*i*PrOH	*Iso*-Propanol
LCST	Lower critical solution temperature
LrPC	Light-responsive polycarbonate
LrPE	Light-responsive polyester
LrPU	Light-responsive polyurethane
MCF-7	Michigan cancer foundation - 7
MeCN	Acetonitrile
MeOH	Methanol

MMA	Methyl methacrylate
M_n	Number average molecular weight
MPDL	2-Methylene-4-phenyl-1,3-dioxolane
mPEG	Poly(ethylene glycol) monomethylether
MS	Mass spectrometry
*m*THPC	5,10,15,20-Tetrakis(*m*-hydroxyphenyl)chlorine
MTT	3-(4,5-Dimethylthiazol-2-yl)-2,5-diphenyltetrazolium bromide
NMP	Nitroxide-mediated radical polymerization
NMR	Nuclear magnetic resonance
NP	Nanoparticle
OEGMA	Oligoethylene glycol methacrylate
*o*NB	*ortho*-nitrobenzyl aclohols
OPCL	Oxime-linked polycaprolactone
*p*ABA	*para*-Aminobenzyl alcohol
PBH	*O,O'*-1,3-Propanediylbishydroxylamine
PBS	Phosphate-buffered saline
PCS	Photon correlation spectroscopy
PDI	Polydispersity index
PDSC	Pyridyldisulfide-carbonate
PDT	Photodynamic therapy
PEG	Poly(ethylene glycol)
PEG-CHO	Aldehyde-terminated poly(ethylene glycol)
*p*HBA	*para*-Hydroxybenzyl alcohol
PLA	Polylactic acid
PLGA	Polylactic-*co*-glycolic acid
*p*NBA	*para*-Nitrobenzyl alcohol
PNIPAAm	Poly(*N*-isopropylacrylamide)
*p*NPCF	*Para*-Nitrophenyl chloroformate
POEA	Poly(ortho ester amide)
PS	Polystyrene

PTX	Paclitaxel
PVA	Poly(vinyl alcohol)
PVAS	Poly(vinyl acetate-alt-sulfur dioxide)
PVCL	Poly(*N*-vinyl caprolactam)
PVME	Poly(vinyl methyl ether)
r.t.	Room temperature
r.u.	Repeating unit
RAFT	Reversible addition-fragmentation chain transfer
R_f	Retardation factor
ROP	Ring-opening polymerization
ROS	Reactive oxygen-species
SEC	Size exclusion chromatography
SEM	Scanning electron microscopy
TBAF	Tetrabutyl ammonium fluoride
TEA	Triethylamine
THF	Tetrahydrofuran
TLC	Thin layer chromatography
T_m	Melting point
ToF	Time-of-flight
UCST	Upper critical solution temperature
USA	United states of America
UV	Ultraviolet
UV/Vis	Wavelength range of ultraviolet/visible
WST-1	Water soluble tetrazolium
λ_{max}	Wavelength at maximum absorbance

12 References

1 Global health estimates: Leading causes of death, https://www.who.int/data/gho/data/themes/mortality-and-global-health-estimates/ghe-leading-causes-of-death, (accessed 8 March 2021).

2 H. Sung, J. Ferlay, R. L. Siegel, M. Laversanne, I. Soerjomataram, A. Jemal and F. Bray, *CA Cancer J. Clin.*, 2021.

3 L. A. Torre, F. Bray, R. L. Siegel, J. Ferlay, J. Lortet-Tieulent and A. Jemal, *CA Cancer J. Clin.*, 2015, **65**, 87–108.

4 D. M. Parkin, F. Bray, J. Ferlay and P. Pisani, *CA Cancer J. Clin.*, 2005, **55**, 74–108.

5 D. M. Parkin, P. Pisani and J. Ferlay, *CA Cancer J. Clin.*, 1999, **49**, 33-64, 1.

6 E. Silverberg and R. N. Grant, *CA Cancer J. Clin.*, 1970, **20**, 10–23.

7 R. Baskar, K. A. Lee, R. Yeo and K.-W. Yeoh, *Int. J. Med. Sci.*, 2012, **9**, 193–199.

8 I. Tannock, *Cancer Treat. Rep.*, 1978, **62**, 1117–1133.

9 C. C. Koning, S. J. Wouterse, J. G. Daams, L. L. Uitterhoeve, M. M. van den Heuvel and J. S. Belderbos, *Clin. Lung Cancer*, 2013, **14**, 481–487.

10 M. Loos, P. Quentmeier, T. Schuster, U. Nitsche, R. Gertler, A. Keerl, T. Kocher, H. Friess and R. Rosenberg, *Ann Surg Oncol*, 2013, **20**, 1816–1828.

11 Z. Huang, *Technol. Cancer Res. Treat.*, 2005, **4**, 283–293.

12 T. J. Dougherty, *J. Clin. Laser Med. Surg.*, 2002, **20**, 3–7.

13 K. Esfahani, L. Roudaia, N. Buhlaiga, S. V. Del Rincon, N. Papneja and W. H. Miller, *Curr. Oncol.*, 2020, **27**, S87-S97.

14 L. B. Kennedy and A. K. S. Salama, *CA Cancer J. Clin.*, 2020, **70**, 86–104.

15 S. J. Oiseth and M. S. Aziz, *JCMT*, 2017, **3**, 250.

16 S. Dawood, L. Austin and M. Cristofanilli, *Oncology (Williston Park)*, 2014, **28**, 1101-7, 1110.

17 B. Feng and L. Chen, *Cancer Biother. Radiopharm.*, 2009, **24**, 717–721.

18 E. Cukierman and D. R. Khan, *Biochem. Pharmacol.*, 2010, **80**, 762–770.

19 L. P. Ganipineni, F. Danhier and V. Préat, *J. Control. Release*, 2018, **281**, 42–57.

20 J. Zugazagoitia, C. Guedes, S. Ponce, I. Ferrer, S. Molina-Pinelo and L. Paz-Ares, *Clin. Ther.*, 2016, **38**, 1551–1566.

References

21 C. Barbé, J. Bartlett, L. Kong, K. Finnie, H. Q. Lin, M. Larkin, S. Calleja, A. Bush and G. Calleja, *Adv. Mater.*, 2004, **16**, 1959–1966.

22 F. Danhier, O. Feron and V. Préat, *J. Control. Release*, 2010, **148**, 135–146.

23 S. Bamrungsap, Z. Zhao, T. Chen, L. Wang, C. Li, T. Fu and W. Tan, *Nanomedicine (Lond)*, 2012, **7**, 1253–1271.

24 J. H. Doroshow, *N. Engl. J. Med.*, 1991, **324**, 843–845.

25 R. Injac and B. Strukelj, *Technol. Cancer Res. Treat.*, 2008, **7**, 497–516.

26 A. Pugazhendhi, Edison, Thomas Nesakumar Jebakumar Immanuel, B. K. Velmurugan, J. A. Jacob and I. Karuppusamy, *Life Sci.*, 2018, **200**, 26–30.

27 K. Park, *J. Control. Release*, 2007, **120**, 1–3.

28 M.-X. Zhao, E.-Z. Zeng and B.-J. Zhu, *ChemNanoMat*, 2015, **1**, 82–91.

29 F. Wang, C. Li, J. Cheng and Z. Yuan, *Int. J. Environ. Res. Public Health*, 2016, **13**, 1182.

30 A. Das, P. Mukherjee, S. K. Singla, P. Guturu, M. C. Frost, D. Mukhopadhyay, V. H. Shah and C. R. Patra, *Nanotechnology*, 2010, **21**, 305102.

31 X. Feng, F. Lv, L. Liu, H. Tang, C. Xing, Q. Yang and S. Wang, *ACS Appl. Mater. Interfaces*, 2010, **2**, 2429–2435.

32 X.-Y. Lu, D.-C. Wu, Z.-J. Li and G.-Q. Chen, in *Progress in Molecular Biology and Translational Science : Nanoparticles in Translational Science and Medicine*, ed. A. Villaverde, Academic Press, 2011, pp. 299–323.

33 S. Sur, A. Rathore, V. Dave, K. R. Reddy, R. S. Chouhan and V. Sadhu, *Nano-Structures & Nano-Objects*, 2019, **20**, 100397.

34 B. Balachandran and Y. Yuana, *Cogent Med.*, 2019, **6**, 1635806.

35 S. Jain, V. Jain and S. C. Mahajan, *Advances in Pharmaceutics*, 2014, **2014**, 1–12.

36 S. Talegaonkar, P. R. Mishra, R. K. Khar and S. S. Biju, *Indian J. Pharm. Sci.*, 2006, **68**, 141.

37 J. Gong, M. Chen, Y. Zheng, S. Wang and Y. Wang, *J. Control. Release*, 2012, **159**, 312–323.

38 H. M. Aliabadi and A. Lavasanifar, *Expert Opin. Drug Deliv.*, 2006, **3**, 139–162.

39 S. R. Croy and G. S. Kwon, *Polymeric micelles for drug delivery*, Bentham Science Publishers, 2006.

40 J. K. Oh, R. Drumright, D. J. Siegwart and K. Matyjaszewski, *Prog. Polym. Sci.*, 2008, **33**, 448–477.

41 M. Malmsten, H. Bysell and P. Hansson, *Curr. Opin. Colloid Interface Sci.*, 2010, **15**, 435–444.

42 J. K. Oh, D. I. Lee and J. M. Park, *Prog. Polym. Sci.*, 2009, **34**, 1261–1282.

43 Y. Jiang, J. Chen, C. Deng, E. J. Suuronen and Z. Zhong, *Biomaterials*, 2014, **35**, 4969–4985.

44 G. K. Balendiran, R. Dabur and D. Fraser, *Cell Biochem. Funct.*, 2004, **22**, 343–352.

45 J. M. Estrela, A. Ortega and E. Obrador, *Crit. Rev. Clin. Lab. Sci.*, 2006, **43**, 143–181.

46 S. Tavakol, *Med. Hypotheses*, 2014, **83**, 668–672.

47 E. S. Lee, Z. Gao and Y. H. Bae, *J. Control. Release*, 2008, **132**, 164–170.

48 W. Gao, J. M. Chan and O. C. Farokhzad, *Mol. Pharm.*, 2010, **7**, 1913–1920.

49 Gaurav Tiwari, Ruchi Tiwari, Birendra Sriwastawa, L Bhati, S Pandey, P Pandey and Saurabh K Bannerjee, *Int. J. Pharm. Investig.*, 2012, **2**, 2–11.

50 K. K. Jain, ed., *Drug Delivery Systems*, Springer New York; Imprint; Humana, New York, NY, 3rd edn., 2020, vol. 2059.

51 R. Langer, *Science*, 1990, **249**, 1527–1533.

52 D. Liu, F. Yang, F. Xiong and N. Gu, *Theranostics*, 2016, **6**, 1306–1323.

53 O. Pillai and R. Panchagnula, *Curr. Opin. Chem. Biol.*, 2001, **5**, 447–451.

54 S. Hajebi, N. Rabiee, M. Bagherzadeh, S. Ahmadi, M. Rabiee, H. Roghani-Mamaqani, M. Tahriri, L. Tayebi and M. R. Hamblin, *Acta Biomater.*, 2019, **92**, 1–18.

55 C. Alvarez-Lorenzo and A. Concheiro, *Chem. Commun.*, 2014, **50**, 7743–7765.

56 J. Li, C. Fan, H. Pei, J. Shi and Q. Huang, *Advanced Materials*, 2013, **25**, 4386–4396.

57 I. Galaev, *Trends Biotechnol.*, 1999, **17**, 335–340.

58 Y.-J. Zhu and F. Chen, *Chemistry – An Asian Journal*, 2015, **10**, 284–305.

59 H. Zheng, L. Xing, Y. Cao and S. Che, *Coord. Chem. Rev.*, 2013, **257**, 1933–1944.

60 A. Popat, J. Liu, G. Q. Lu and S. Z. Qiao, *J. Mater. Chem.*, 2012, **22**, 11173.

References

61 X. Guo, Y. Cheng, X. Zhao, Y. Luo, J. Chen and W.-E. Yuan, *J Nanobiotechnol*, 2018, **16**, 74.

62 M. A. Gauthier, *Antioxid. Redox Signal.*, 2014, **21**, 705–706.

63 R. Li, F. Peng, J. Cai, D. Yang and P. Zhang, *Asian J. Pharm. Sci.*, 2020, **15**, 311–325.

64 M. Nakayama, T. Okano, T. Miyazaki, F. Kohori, K. Sakai and M. Yokoyama, *J. Control. Release*, 2006, **115**, 46–56.

65 X. Gu, J. Wang, X. Liu, D. Zhao, Y. Wang, H. Gao and G. Wu, *Soft Matter*, 2013, **9**, 7267.

66 M. Bikram and J. L. West, *Expert Opin. Drug Deliv.*, 2008, **5**, 1077–1091.

67 N. Ž. Knežević, B. G. Trewyn and V. S.-Y. Lin, *Chem. Commun.*, 2011, **47**, 2817–2819.

68 H. Wang, W. Miao, F. Wang and Y. Cheng, *Biomacromolecules*, 2018, **19**, 2194–2201.

69 C. S. Linsley and B. M. Wu, *Ther. Deliv.*, 2017, **8**, 89–107.

70 P. R. Chandran and N. Sandhyarani, *RSC Adv.*, 2014, **4**, 44922–44929.

71 S. Murdan, *J. Control. Release*, 2003, **92**, 1–17.

72 J. Ge, E. Neofytou, T. J. Cahill, R. E. Beygui and R. N. Zare, *ACS Nano*, 2012, **6**, 227–233.

73 M. S. Aw, J. Addai-Mensah and D. Losic, *J. Mater. Chem.*, 2012, **22**, 6561.

74 J. Estelrich, E. Escribano, J. Queralt and M. A. Busquets, *Int. J. Mol. Sci.*, 2015, **16**, 8070–8101.

75 K. Hayashi, K. Ono, H. Suzuki, M. Sawada, M. Moriya, W. Sakamoto and T. Yogo, *ACS Appl. Mater. Interfaces*, 2010, **2**, 1903–1911.

76 J. L. Paris, M. V. Cabañas, M. Manzano and M. Vallet-Regí, *ACS Nano*, 2015, **9**, 11023–11033.

77 Y. Uesugi, H. Kawata, J. Jo, Y. Saito and Y. Tabata, *J. Control. Release*, 2010, **147**, 269–277.

78 X. Cai, Y. Jiang, M. Lin, J. Zhang, H. Guo, F. Yang, W. Leung and C. Xu, *Front. Pharmacol.*, 2019, **10**, 1650.

79 W. B. Liechty, D. R. Kryscio, B. V. Slaughter and N. A. Peppas, *Annu. Rev. Chem. Biomol. Eng.*, 2010, **1**, 149–173.

80 W.-W. Yang and E. Pierstorff, *J. Lab. Autom.*, 2012, **17**, 50–58.

81 T. M. Allen and P. R. Cullis, *Science*, 2004, **303**, 1818–1822.

82 A. Gaitanis and S. Staal, *Methods Mol. Biol.*, 2010, **624**, 385–392.

83 L. Sercombe, T. Veerati, F. Moheimani, S. Y. Wu, A. K. Sood and S. Hua, *Front. Pharmacol.*, 2015, **6**, 286.

84 S. Walker, S. Busatto, A. Pham, M. Tian, A. Suh, K. Carson, A. Quintero, M. Lafrence, H. Malik, M. X. Santana and J. Wolfram, *Theranostics*, 2019, **9**, 8001–8017.

85 J. P. K. Armstrong and M. M. Stevens, *Adv. Drug Deliv. Rev.*, 2018, **130**, 12–16.

86 K. Kataoka, A. Harada and Y. Nagasaki, *Adv. Drug Deliv. Rev.*, 2012, **64**, 37–48.

87 K. Kazunori, K. Glenn S., Y. Masayuki, O. Teruo and S. Yasuhisa, *J. Control. Release*, 1993, **24**, 119–132.

88 A. Kumari, S. K. Yadav and S. C. Yadav, *Colloids Surf. B Biointerfaces*, 2010, **75**, 1–18.

89 K. S. Soppimath, T. M. Aminabhavi, A. R. Kulkarni and W. E. Rudzinski, *J. Control. Release*, 2001, **70**, 1–20.

90 H. Ragelle, F. Danhier, V. Préat, R. Langer and D. G. Anderson, *Expert Opin. Drug Deliv.*, 2017, **14**, 851–864.

91 A. C. Anselmo and S. Mitragotri, *J. Control. Release*, 2014, **190**, 15–28.

92 G. Pillai, *SOJ Pharm. Pharm. Sci.*, 2014, **1**.

93 P. Schattling, F. D. Jochum and P. Theato, *Polym. Chem.*, 2014, **5**, 25–36.

94 F. Liu and M. W. Urban, *Prog. Polym. Sci.*, 2010, **35**, 3–23.

95 D. Crespy and R. M. Rossi, *Polymer International*, 2007, **56**, 1461–1468.

96 P. Wust, B. Hildebrandt, G. Sreenivasa, B. Rau, J. Gellermann, H. Riess, R. Felix and P. M. Schlag, *Lancet Oncol.*, 2002, **3**, 487–497.

97 T. Kobayashi, *Biotechnol. J.*, 2011, **6**, 1342–1347.

98 M. Nakayama and T. Okano, *React. Funct. Polym.*, 2011, **71**, 235–244.

99 S. R. Abulateefeh, S. G. Spain, J. W. Aylott, W. C. Chan, M. C. Garnett and C. Alexander, *Macromol. Biosci.*, 2011, **11**, 1722–1734.

100 M. Huo, J. Yuan, L. Tao and Y. Wei, *Polym. Chem.*, 2014, **5**, 1519–1528.

101 A. Iturmendi, U. Monkowius and I. Teasdale, *ACS Macro Lett.*, 2017, **6**, 150–154.

102 K. Kumar and A. P. Goodwin, *ACS Macro Lett.*, 2015, **4**, 907–911.

References

103   M. G. Olah, J. S. Robbins, M. S. Baker and S. T. Phillips, *Macromolecules*, 2013, **46**, 5924–5928.

104   H. Wang, G. Liu, H. Gao and Y. Wang, *Polym. Chem.*, 2015, **6**, 4715–4718.

105   Y. Zhang, J. Yu, H. N. Bomba, Y. Zhu and Z. Gu, *Chem. Rev.*, 2016, **116**, 12536–12563.

106   W. Zhao, Y. Zhao, Q. Wang, T. Liu, J. Sun and R. Zhang, *Small*, 2019, **15**, e1903060.

107   H. Yim, M. S. Kent, S. Mendez, S. S. Balamurugan, S. Balamurugan, G. P. Lopez and S. Satija, *Macromolecules*, 2004, **37**, 1994–1997.

108   P. Klán, T. Šolomek, C. G. Bochet, A. Blanc, R. Givens, M. Rubina, V. Popik, A. Kostikov and J. Wirz, *Chem. Rev.*, 2013, **113**, 119–191.

109   V. Torchilin, *Adv. Drug Deliv. Rev.*, 2011, **63**, 131–135.

110   T. Alfrey and G. Goldfinger, *J. Chem. Phys.*, 1944, **12**, 205–209.

111   F. R. Mayo and C. Walling, *Chem. Rev.*, 1950, **46**, 191–287.

112   T. Yokozawa and A. Yokoyama, *Prog. Polym. Sci.*, 2007, **32**, 147–172.

113   J. K. Stille, *J. Chem. Educ.*, 1981, **58**, 862.

114   K. Matyjaszewski, *Handbook of Radical Polymerization*, s.n, s.l., 1st edn., 2002.

115   O. W. Webster, *Science*, 1991, **251**, 887–893.

116   O. Nuyken and S. Pask, *Polymers (Basel)*, 2013, **5**, 361–403.

117   Marcel Van Beylen, Stanley Bywater, Georges Smets, Michael Szwarc and Denis J. Worsfold, in *Polysiloxane Copolymers/Anionic Polymerization*, Springer, Berlin, Heidelberg, 1988, pp. 87–143.

118   D. A. Shipp, *Polym. Rev. (Phila Pa)*, 2011, **51**, 99–103.

119   K. Matyjaszewski, *Macromolecules*, 2012, **45**, 4015–4039.

120   T. D. Michl, D. Jung, A. Pertoldi, A. Schulte, P. Mocny, H.-A. Klok, H. Schönherr, C. Giles, H. J. Griesser and B. R. Coad, *Macromol. Chem. Phys.*, 2018, **219**, 1800182.

121   J. Nicolas, Y. Guillaneuf, C. Lefay, D. Bertin, D. Gigmes and B. Charleux, *Prog. Polym. Sci.*, 2013, **38**, 63–235.

122   Y. Guillaneuf, D. Gigmes, S. R. A. Marque, P. Astolfi, L. Greci, P. Tordo and D. Bertin, *Macromolecules*, 2007, **40**, 3108–3114.

123   D. Seifert, M. Kipping, H.-J. P. Adler and D. Kuckling, *Macromolecular Symposia*, 2007, **254**, 386–391.

124   G. Moad, E. Rizzardo and S. H. Thang, *Chemistry – An Asian Journal*, 2013, **8**, 1634–1644.

125   Kajsa M. Stridsberg, Maria Ryner and Ann-Christine Albertsson, in *Degradable Aliphatic Polyesters*, Springer, Berlin, Heidelberg, 2002, pp. 41–65.

126   F. Sanda and T. Endo, *Journal of Polymer Science Part A: Polymer Chemistry*, 2001, **39**, 265–276.

127   A. M. DiLauro, J. S. Robbins and S. T. Phillips, *Macromolecules*, 2013, **46**, 2963–2968.

128   J. Sun, W. Birnbaum, J. Anderski, M.-T. Picker, D. Mulac, K. Langer and D. Kuckling, *Biomacromolecules*, 2018, **19**, 4677–4690.

129   J. Sun, D. Jung, T. Schoppa, J. Anderski, M.-T. Picker, Y. Ren, D. Mulac, N. Stein, K. Langer and D. Kuckling, *ACS Appl. Bio Mater.*, 2019, **2**, 3038–3051.

130   J. Sun, T. Rust and D. Kuckling, *Macromol. Rapid Commun.*, 2019, **40**, e1900348.

131   A.-K. Müller, D. Jung, J. Sun and D. Kuckling, *Polym. Chem.*, 2020, **11**, 721–733.

132   L. Mahlert, J. Anderski, T. Schoppa, D. Mulac, J. Sun, D. Kuckling and K. Langer, *Int. J. Pharm.*, 2019, **565**, 199–208.

133   Y. Xia, N. Wang, Z. Qin, J. Wu, F. Wang, L. Zhang, X. Xia, J. Li and Y. Lu, *J. Mater. Chem. B*, 2018, **6**, 3348–3357.

134   W. Chen, Y. Zou, J. Jia, F. Meng, R. Cheng, C. Deng, J. Feijen and Z. Zhong, *Macromolecules*, 2013, **46**, 699–707.

135   D. Li, Y. Bu, L. Zhang, X. Wang, Y. Yang, Y. Zhuang, F. Yang, H. Shen and D. Wu, *Biomacromolecules*, 2016, **17**, 291–300.

136   C.-H. Whang, K. S. Kim, J. Bae, J. Chen, H.-W. Jun and S. Jo, *Macromol. Rapid Commun.*, 2017, **38**.

137   S. Santra, M. A. Sk, A. Mondal and M. R. Molla, *Langmuir*, 2020, **36**, 8282–8289.

138   X. Duan, T. Bai, J. Du and J. Kong, *J. Mater. Chem. B*, 2018, **6**, 39–43.

References

139   B. Yu, A. B. Lowe and K. Ishihara, *Biomacromolecules*, 2009, **10**, 950–958.

140   Y. Mitsukami, A. Hashidzume, S. Yusa, Y. Morishima, A. B. Lowe and C. L. McCormick, *Polymer*, 2006, **47**, 4333–4340.

141   Z. Song, K. Wang, C. Gao, S. Wang and W. Zhang, *Macromolecules*, 2016, **49**, 162–171.

142   J. Cui, Y. Yan, Y. Wang and F. Caruso, *Adv. Funct. Mater.*, 2012, **22**, 4718–4723.

143   Y. H. Kim, J. H. Park, M. Lee, Y.-H. Kim, T. G. Park and S. W. Kim, *J. Control. Release*, 2005, **103**, 209–219.

144   C.-C. Song, R. Ji, F.-S. Du, D.-H. Liang and Z.-C. Li, *ACS Macro Lett.*, 2013, **2**, 273–277.

145   L. Feng, Z. Dong, D. Tao, Y. Zhang and Z. Liu, *Natl. Sci. Rev.*, 2018, **5**, 269–286.

146   G. Kocak, C. Tuncer and V. Bütün, *Polym. Chem.*, 2017, **8**, 144–176.

147   B. Wei, Y. Tao, X. Wang, R. Tang, J. Wang, R. Wang and L. Qiu, *ACS Appl. Mater. Interfaces*, 2015, **7**, 10436–10445.

148   Y. Jin, L. Song, Y. Su, L. Zhu, Y. Pang, F. Qiu, G. Tong, D. Yan, B. Zhu and X. Zhu, *Biomacromolecules*, 2011, **12**, 3460–3468.

149   E. Guégain, J.-P. Michel, T. Boissenot and J. Nicolas, *Macromolecules*, 2018, **51**, 724–736.

150   L. Fu, X. Sui, A. E. Crolais and W. R. Gutekunst, *Angew. Chem. Int. Ed Engl.*, 2019, **58**, 15726–15730.

151   C. P. Reis, R. J. Neufeld, A. J. Ribeiro and F. Veiga, *Nanomedicine*, 2006, **2**, 8–21.

152   J. Y. Jun, H. H. Nguyen, S.-Y.-R. Paik, H. S. Chun, B.-C. Kang and S. Ko, *Food Chem.*, 2011, **127**, 1892–1898.

153   K. Krishnamoorthy and M. Mahalingam, *Adv. Pharm. Bull.*, 2015, **5**, 57–67.

154   H. Fessi, F. Puisieux, J. Devissaguet, N. Ammoury and S. Benita, *Int. J. Pharm.*, 1989, **55**, R1-R4.

155   S. Hornig, T. Heinze, C. R. Becer and U. S. Schubert, *J. Mater. Chem.*, 2009, **19**, 3838.

156   S. Schubert, J. J. T. Delaney and U. S. Schubert, *Soft Matter*, 2011, **7**, 1581–1588.

157   M. Lee, Y. W. Cho, J. H. Park, H. Chung, S. Y. Jeong, K. Choi, D. H. Moon, S. Y. Kim, I.-S. Kim and I. C. Kwon, *Colloid Polym. Sci.*, 2006, **284**, 506–512.

158   M. G. Nava-Arzaluz, E. Piñón-Segundo, A. Ganem-Rondero and D. Lechuga-Ballesteros, *Recent Pat. Drug Deliv. Formul.*, 2012, **6**, 209–223.

159   Y.-P. Sun, M. J. Meziani, P. Pathak and L. Qu, *Chemistry*, 2005, **11**, 1366–1373.

160   S.-D. Yeo and E. Kiran, *J. Supercrit. Fluids*, 2005, **34**, 287–308.

161   B. A. Magill, X. Guo, C. L. Peck, R. L. Reyes, E. M. See, W. L. Santos and H. D. Robinson, *Photochem. Photobiol. Sci.*, 2019, **18**, 30–44.

162   C. Daengngam, S. B. Thorpe, X. Guo, S. V. Stoianov, W. L. Santos, J. R. Morris and H. D. Robinson, *J. Phys. Chem. C Nanomater. Interfaces*, 2013, **117**, 14165–14175.

163   R. M. LoPachin and T. Gavin, *Chem. Res. Toxicol.*, 2014, **27**, 1081–1091.

164   I. Altinbasak, M. Arslan, R. Sanyal and A. Sanyal, *Polym. Chem.*, 2020, **11**, 7603–7624.

165   R. Bej, J. Sarkar and S. Ghosh, *J. Polym. Sci. A Polym. Chem.*, 2018, **56**, 194–202.

166   T. Suma, J. Cui, M. Müllner, S. Fu, J. Tran, K. F. Noi, Y. Ju and F. Caruso, *J. Am. Chem. Soc.*, 2017, **139**, 4009–4018.

167   C. Batisse, E. Dransart, R. Ait Sarkouh, L. Brulle, S.-K. Bai, S. Godefroy, L. Johannes and F. Schmidt, *Eur. J. Med. Chem.*, 2015, **95**, 483–491.

168   M. Lapeyre, J. Leprince, M. Massonneau, H. Oulyadi, P.-Y. Renard, A. Romieu, G. Turcatti and H. Vaudry, *Chemistry*, 2006, **12**, 3655–3671.

169   K. Mizoguchi, T. Higashihara and M. Ueda, *Macromolecules*, 2009, **42**, 3780–3787.

170   M. Du, Q. Guo, H. Feng, G. Lu and X. Huang, *Chin. J. Chem.*, 2014, **32**, 448–453.

171   M. Hesse, H. Meier and B. Zeeh, *Spektroskopische Methoden in der organischen Chemie. 102 Tabellen*, Thieme, Stuttgart, 7th edn., 2005.

References

172   T. Schoppa, D. Jung, T. Rust, D. Mulac, D. Kuckling and K. Langer, *Int. J. Pharm.*, 2021, **597**, 120326.

173   D. Manzanares and V. Ceña, *Pharmaceutics*, 2020, **12**, 371.

174   A. Sakakura, K. Kawajiri, T. Ohkubo, Y. Kosugi and K. Ishihara, *J. Am. Chem. Soc.*, 2007, **129**, 14775–14779.

175   P. Wu, Z. Xiao, J. Zhang, J. Hao, J. Chen, P. Yin and Y. Wei, *Chem. Commun.*, 2011, **47**, 5557–5559.